

**THE ROLE AND REGULATION OF OSTEOPONTIN IN HYPERTENSION  
RELATED REMODELING AND INFLAMMATION OF THE AORTA**

A Dissertation  
Presented to  
The Academic Faculty

by

Christa Caesar

In Partial Fulfillment  
of the Requirements for the Degree  
Doctor of Philosophy in Biomedical Engineering

Georgia Institute of Technology  
May 2016

**COPYRIGHT © 2016 BY CHRISTA CAESAR**

**THE ROLE AND REGULATION OF OSTEOPONTIN IN HYPERTENSION  
RELATED REMODELING AND INFLAMMATION OF THE AORTA**

Approved by:

Dr. W. Robert Taylor, Advisor  
Division of Cardiology  
*Emory University & Georgia Institute of  
Technology*

Dr. Hanjoong Jo  
Department of Biomedical Engineering  
*Georgia Institute of Technology*

Dr. Roy Sutliff  
Division of Pulmonary Medicine  
*Emory University*

Dr. Rudolph L Gleason  
Department of Mechanical Engineering  
*Georgia Institute of Technology*

Dr. Michael Davis  
Department of Biomedical Engineering  
*Georgia Institute of Technology*

Date Approved: January 6th, 2016

## ACKNOWLEDGEMENTS

This work would not have happened had it not been for the wonderful people I have had the privilege and honor of working with. Every figure and paragraph has made its way into this dissertation because of the immense support, guidance, training, and encouragement I have generously received from my mentor, Dr. Taylor, thesis committee, mentors, fellow lab mates, friends, and family.

First and foremost, I have to thank my mentor and advisor, Dr. Bob Taylor, for taking me under his wing and giving me the opportunity to be part of the wonderful Taylor Lab Family. From designing and troubleshooting experiments in lab, deciding which conferences to present my work at, reviewing grant applications, or finding an internship in industry - Bob has been my best advocate and guide. Bob has always given me sound advice and has always had my best interest at heart – all reasons for which I consider myself to be one of the luckiest graduate students at Georgia Tech.

In addition, I have thoroughly enjoyed listening to the numerous stories Bob has shared with us about life and science, and have learnt by his example that it is possible to successfully balance work and family, albeit with a lot of patience and hard work! Bob is one of the most generous people I know, and has always encouraged his trainees to give back to the community and everyone around them as well. I will fondly cherish memories of being part of the Toy Drive during the holiday season these past five years. During this time each year, our lab led by Bob, has come together to raise money for over a 100 children in the Fulton County Court system, shopped, assembled, and gift wrapped truck-loads of toys, and personally delivered each of these toys with much love and joy. These are all experiences that have played an integral role in making me the person that I am today – and for which I will forever be indebted to Bob.

Next, I have to thank my thesis committee – Dr. Hanjoong Jo, Dr. Roy Sutliff, Dr. Michael Davis, and Dr. Rudy Gleason – for how generous they have been with their time, guidance, and support of this project. I would like to thank Dr. Jo for all his advice and guidance in helping me better understand the progression of atherosclerosis in large arteries and help with the design of experiments. Some of the best courses I have taken in graduate school have been with Dr. Jo – from systems physiology, pathophysiology, to the cardiovascular seminar course where I learnt to carefully read, scrutinize, and interpret data from journal articles in the field. I am grateful to Dr. Sutliff for his expertise in helping me accurately interpret our data, his guidance on troubleshooting experiments, and invaluable feedback on this dissertation. Dr. Davis has been instrumental in helping us understand and think about the role of the extracellular matrix in regulating the response of cells of the aorta to mechanical forces in the setting of hypertension. Some of the best friends I have made in graduate school have been from the Davis lab and I will always cherish memories that the Taylor and Davis labs have created together – right from our Fall outing and Bocce-ball tournament at Stone Mountain, to the Whirly ball tournament, and celebration of friends’ weddings. Finally, I am most grateful to Dr. Gleason, who first introduced me to the world of cardiovascular research as a young and naive undergraduate. I have thoroughly enjoyed and greatly learnt from all the courses I have taken with Dr. Gleason – beginning with Statics as an undergraduate to Tissue Mechanics in graduate school. Finally, I am immensely grateful to Dr. Gleason for generously opening up his lab and equipment to allow me to complete all the biomechanics experiments detailed in aim 3 of this dissertation.

My graduate school experience would have been incomplete and this work impossible if not for my dear friends of the Taylor Lab. Over the past 5 years, my colleagues have become more family and less colleagues. My first mentor and friend in the Taylor Lab was Dr. Alicia Lyle. Ali

– I wish I had the words to thank you enough – but here’s an attempt. Thank you for being my most awesome coach and friend – for showing me the ropes in the exciting world of experimental biology. Thank you for helping me take those first baby steps and showing me the near perfect way of doing a Western Blot, PCR, growing cells, designing, and analyzing experiments. I will always admire you for so beautifully juggling your many roles as a scientist, mother, wife, sister, daughter, mentor, and friend.

I would also like to thank Dr. Daiana Weiss for becoming one of my closest friends in the Taylor Lab. Daiana has played an important role in teaching me how to properly design and execute experiments using animal models. Daiana has played a pivotal part in helping me successfully complete all my experiments for both aims 2 and 3 – on time – so a big thank you goes out to Dr. Weiss! In addition to all the science we’ve done together, I have thoroughly enjoyed all our long conversations about our families, cultures, food, and life – and will truly miss them when I leave graduate school.

I am immensely grateful to another wonderful expert of the Taylor Lab – Giji Joseph, without whom, we would not have all the beautiful histology images in this dissertation. In addition to being a mother-figure to me in lab, I was surprised to find out when I first joined lab that Giji and I were from the same part of India - Kerala, spoke the same language - Malayalam, and shared the same faith - in Christ. Giji Aunty (as I fondly call her), I will always cherish your motherly affection, guidance, support, and encouragement – thank you!

Another important Taylor Lab member that I would like to thank immensely is Dr. Laura Hansen. It was great when Laura was my graduate mentor in the Gleason lab and Teaching Assistant in my first physiology lab course during my undergraduate years at Georgia Tech, but I was ecstatic to have her mentor me again when she decided to join the Taylor Lab for her post-

doctoral fellowship. Thank you, Laura, for being such an amazing mentor and friend. You know, I would have not completed my final aim were it not for your guidance in teaching me the trickiest microsurgical techniques needed to complete the mechanical testing of the tiny mouse aortas – so a big thank you goes out to you!

Finally, I would like to thank my dear friends – both current and past members of the Taylor Lab - Kiyoko Takemiya, Yanbo Liu, Anita Saraf, Jane Titterington, Rebecca Levit, Lizz Iffrig, John Wilson, Ebony Washington, Ian Campbell, Ioannis Parastatidis, Alex Smolensky, and Sarah Knight – for making the Taylor Lab such a multi-cultural melting pot and wonderful place to work in. I especially want to thank Kiyoko for becoming such a great friend and role-model to me. I truly admire your professionalism, hard-work, humility, and dedication to science. I will miss getting to enjoy your delicious baked goods and wonderful smile. I would also like to thank my dear friend Yanbo Liu for being a great companion and making work so much fun in room 312. I have thoroughly enjoyed all our long conversations, lunch breaks watching funny YouTube videos, and I will truly miss your curiosity, positive-spirit, open-mindedness, and enthusiasm for life!

It would be amiss to not thank Drs. Anastassia Pokutta and Alex Caulk of the Gleason lab for all their support for aim 3 as well. Thank you for showing me how to use your equipment and for so graciously sharing your lab with me. Anastassia - it was so great to have you around to see me through to the finish line.

Finally, I am also immensely grateful to all my dear colleagues and friends from the Division of Cardiology – the administrative staff, Dr. Lu Hilenski of the Imaging Core, members of the Griendling, Lyle, Levit, San-Martin, Davis, and Jo labs. I will miss all the fun times and smiles we have shared together through the yearly Chili cook-offs, BBQs, zip-lining and pontoon

boating experiences, and of course the weekly seminars, divisional meetings, annual conferences, coffee and lunch breaks ☺.

I am grateful to my dear friends from both graduate and undergraduate years for their faith and belief in me. I am thankful to my extended family – grandparents, aunts, uncles, and cousins for being role-models and always showering me with kindness and encouragement. My in-laws Bijy and George, have pampered me with copious amounts of delicious home-cooked meals, love, and encouragement – since our wedding, which was just six months prior to my defense.

Most importantly, I would like to thank my dear parents – Sheela and Caesar, and sister - Sarah - for their unfailing love, unyielding support, and encouragement. My mother, as a teacher of Physics and father as helicopter pilot, have been the earliest to encourage my curiosity and love for science. They have inspired and motivated me to chase my dreams, but always reminded me that it is more important to be kind than smart. Finally, I owe this dissertation and the fact that I made it thus far, to my sweet, most loving husband, and best friend – Nishant. I can't imagine my life without you – from the earliest days of our undergraduate life back in 2006 to the busy last experiments of graduate school in 2015 – you have been with me through the thick and thin of it all. Thank you for being my shoulder to cry on, cheer-leader in chief, company in lab for all those late-night experiments, chef and chauffer in charge, voice of sanity, and best friend! This dissertation is a reflection of all the love you have so selflessly poured on me and I am so excited that I get to do all future projects with you by my side.

## TABLE OF CONTENTS

	Page
ACKNOWLEDGEMENTS	iii
LIST OF FIGURES	xii
LIST OF SYMBOLS & ABBREVIATIONS	xv
SUMMARY	xviii
CHAPTER 1 - SPECIFIC AIMS	1
Specific Aim 1	2
Specific Aim 2	2
Specific Aim 3	3
Significance and Innovation	4
CHAPTER 2 – BACKGROUND & LITERATURE REVIEW	5
Blood Vessels of the Human Body	5
Aorta: Structure, Function, and Mechanics	5
Hypertension Epidemiology	7
Hypertension Pathology	8
Effects of Hypertension on the Aorta	9
Humoral Effects of Hypertension: RAAS and Norepinephrine	10
Mechanical Effects: Arterial Remodeling	13
Reactive Oxygen Species: Overview	14
Reactive Oxygen Species and Hypertension	16
Antioxidants and the Enzyme Catalase	18

Sources of ROS and Hypertension	18
Osteopontin (OPN): Structure, Function, and Role	21
Osteopontin in Vascular Pathophysiology and Regulation	23
<b>CHAPTER 3 – REGULATION OF OSTEOPONTIN BY CYCLIC STRAIN IN-VITRO</b>	<b>25</b>
Introduction	25
Methods	27
Cell Culture and Materials	27
Cyclic Strain of Vascular Smooth Muscle Cells	27
Western Blot Analysis	28
ELISA	28
RNA Isolation and Quantitative Real-time Polymerase Chain Reaction	30
Detection of ROS	30
Statistics	30
Results	31
Cyclic Strain Increases OPN Expression	31
OPN Expression with Varying Degrees of Strain	35
Cyclic Strain Increases ROS	37
NADPH Oxidases May Play a Role in Mediating Cyclic Strain-induced OPN	40
Discussion	43
<b>CHAPTER 4 – HYPERTENSION UPREGULATES OSTEOPONTIN VIA H<sub>2</sub>O<sub>2</sub></b>	<b>48</b>
Introduction	48
Methods	50
Animals	50

Osmotic Mini-Pump Implantation	50
Measurement of Systolic Blood Pressure	51
Immunohistochemistry	51
Protein Analysis	51
RNA Isolation and Quantitative Real-time Polymerase Chain Reaction	52
Statistics	53
Results	54
Angiotensin-II (AngII) & Norepinephrine (NE) Increase Systolic Blood Pressure	54
AngII and NE Increase OPN mRNA and Protein	56
OPN is Primarily Localized to the Medial Layer with Hypertension	60
Catalase Blunts Hypertension-induced Increase in OPN	62
Discussion	65
CHAPTER 5 – EXPLORING THE ROLE OF OPN IN AORTIC BIOMECHANICS	73
Introduction	73
Methods	75
Animals	75
Osmotic Mini-pump Implantation	75
Measurement of Systolic Blood Pressure	75
Measurement of Aortic In-Vivo Length, Aorta Isolation, and Preparation	75
Mechanical Testing of Aortas	77
Pressure-Diameter (PD) Curves and Compliance Analysis	77
Histological Analysis	78

Statistics	78
Results	79
Systolic Blood Pressure is Increased in Both WT and OPN KO Mice	79
In-Vivo Length is Not Altered with AngII Treatment in OPN KO Mice	81
AngII Increases Aortic Diameter, but Does Not Alter Aortic Compliance	83
AngII Increases Medial Thickness	86
Aortic Diameter and Compliance is Altered in OPN KO Mice	89
OPN KO Aortas Have Altered Microstructural Features and are Protected Against Inflammatory Infiltration in Hypertension	92
Discussion	99
CHAPTER 6 – SUMMARY, LIMITATIONS, and FUTURE DIRECTIONS	104
Summary	104
Limitations and Future Considerations	106
Implications	113
Conclusion	115
APPENDIX	116
REFERENCES	118

## LIST OF FIGURES

Figure 2.1: Layers of the Healthy Aorta	6
Figure 2.2: Definition and Factors Influencing Blood Pressure	8
Figure 2.3: Renin-Angiotensin-Aldosterone (RAAS) Pathway	11
Figure 2.4: Differences in Aortic Compliance with Age and Disease	14
Figure 2.5: Chemical Reactions Governing ROS Production in the Vasculature	16
Figure 2.6: Structure of the NADPH Oxidase Enzyme	20
Fig 3.1: Suggested Mechanism of Mechanical Strain Induced OPN Expression	26
Fig 3.2: Schematic of Application of Biaxial Strain on a Single Well of Cultured Vascular Smooth Muscle Cells	28
Fig 3.3: Phenotype of Rat Aortic Smooth Muscle Cells 24h post Strain	29
Fig 3.4: 24 hours of Cyclic Strain Increases OPN mRNA Expression	32
Fig 3.5: 24 hours of Cyclic Strain Increases Cellular OPN Protein Expression	33
Fig 3.6: Cyclic Strain Increases Secreted OPN Protein Expression	34
Fig 3.7: Varying Magnitudes of Cyclic Strain Increases OPN Protein Expression	36
Fig 3.8: Cyclic Strain for 4 hours Increases Superoxide ( $O_2^{\bullet}$ )	38
Fig 3.9: Cyclic Strain Significantly Increases $H_2O_2$	39
Fig 3.10: Strain-Induced Increase in OPN Expression was Blunted in the Presence of DPI	41
Fig 3.11: Strain-Induced Increase in OPN Expression was Blunted in the Presence of Apocynin	42
Figure 4.1: Continuous Infusion of AngII or NE for 7 days Significantly Increase Systolic Blood Pressure	55
Figure 4.2: OPN mRNA expression is upregulated in aortas of mice treated with AngII for 7 days	57
Figure 4.3: 7 day AngII Infusion Increases OPN Protein Expression in the Aorta	58

Figure 4.4: 7 day NE Infusion Increases OPN Protein Expression in the Aorta	59
Figure 4.5: OPN expression was Increased with Hypertension and Localized Primarily to the Media	61
Figure 4.6: Systolic Blood Pressure is Increased in both WT and Transgenic Catalase Overexpressing Mice in both models of hypertension	63
Figure 4.7: Hypertensive Smooth Muscle Cell Catalase overexpressing mice (Tg <sup>SMC-Cat</sup> ) showed attenuated OPN levels	64
Figure 5.1: Systolic Blood Pressure is Significantly Increased in both WT and OPN KO mice with AngII infusion	80
Figure 5.2: <i>In-Vivo</i> Length of WT and OPN KO Aortas is not Altered with AngII Treatment	82
Figure 5.3: AngII-induced Hypertension Increases Aortic Diameter	84
Figure 5.4: Pressure-Dependent Local Compliance is not Altered in murine WT aortas with AngII Treatment at 3, 7 or 14 days	85
Figure 5.5: Medial Thickness is Increased with 3, 7, or 14 day AngII infusion	87
Figure 5.6: Medial Thickness of Aorta Increases with AngII Treatment	88
Figure 5.7: OPN KO Aortas Have Dramatically Higher Aortic Diameter with and without AngII treatment	90
Figure 5.8: OPN KO aortas have Higher Maximal Compliance than WT aortas	91
Figure 5.9: Hypertensive OPN KO mice are Protected against Adventitial Inflammation	93
Figure 5.10: AngII Infusion Induces Medial Thickening in Both WT and OPN KO aortas	94
Figure 5.11: OPN KO Aortas Have Altered Elastin Organization	95
Figure 5.12: OPN KO Aortas Have Increased Elastin Interlamellar Gaps	96
Figure 5.13: Hypertensive OPN KO have Reduced Adventitial Collagen and Adventitial Thickening	97
Figure 5.14: Hypertensive OPN KO have Reduced Inflammation	98
Figure 6.1: Different regions of the flexible membrane well experience different strain profiles	107

Fig A.1: Cyclic Strain-induced Increase in OPN was not Affected with 24 hours PEG-Catalase Treatment	116
Fig A.2: Catalase Activity in Cell Culture Medium Drops Within 6 hours	116
Fig A.3: Updated Experimental Design to Account for Reduced Catalase Activity	117
Fig A.4: PEG-Catalase May Blunt Strained-induced cellular OPN at Higher Concentrations	117

## LIST OF SYMBOLS & ABBREVIATIONS

AAA	Abdominal Aortic Aneurysm
ACE	Angiotensin Converting Enzyme
AHA	American Heart Association
ANGI	Angiotensin I
ANGII	Angiotensin II
ANOVA	Analysis of Variance
AP-1	Activator Protein - 1
BSA	Bovine Serum Albumin
CHD	Coronary Heart Disease
CRP	C-Reactive Protein
CVD	Cardiovascular Disease
CVS	Cardiovascular System
DCF-DA	5-(and-6)-carboxy-2',7'-dichlorofluorescein diacetate
DMEM	Dulbecco's Modified Eagle's Medium
DHE	Dihydroethidium
DNA	Deoxyribonucleic Acid
DPI	Diphenyleneiodonium
ECM	Extra Cellular Matrix
ELISA	Enzyme-Linked Immunosorbent Assay
eNOS	Endothelial Nitric Oxide Synthase
ET-1	Endothelin-1
FEA	Finite Element Analysis

GPx	Glutathione Peroxidase
H <sub>2</sub> O <sub>2</sub>	Hydrogen Peroxide
ICAM-1	Intercellular Adhesion Molecule - 1
IL-6	Interleukin-6
KO	Knockout
MCP-1	Monocyte Chemotactic Protein - 1
MI	Myocardial Infarction
MMP	Matrix Metalloproteinases
mRNA	Messenger Ribonucleic Acid
NADPH	Nicotinamide Adenine Dinucleotide Phosphate
NE	Norepinephrine
NF-κB	Nuclear Factor Kappa B
NO	Nitric Oxide
NOX	NADPH Oxidase
O <sub>2</sub> <sup>•-</sup>	Superoxide Radical
ONOO <sup>•-</sup>	Peroxynitrite
OPN	Osteopontin
PAI-1	Plasminogen Activator Inhibitor-1
PBS	Phosphate Buffer Solution
PD	Pressure-Diameter
PECAM	Platelet Endothelial Cell Adhesion Molecule
PEG-Catalase	Polyethylene Glycol Catalase
PEG-SOD	Polyethylene Glycol Superoxide Dismutase

PTSD	Post Traumatic Stress Disorder
RT-PCR	Reverse Transcription Polymerase Chain Reaction
RAAS	Renin-Angiotensin-Aldosterone System
RGD	Arginine-Glycine-Aspartate
ROS	Reactive Oxygen Species
SBP	Systolic Blood Pressure
siRNA	Small Interfering Ribonucleic Acid
SMCs	Smooth Muscle Cells
Tg <sup>SMC-Cat</sup>	Transgenic Smooth Muscle Cell Catalase Overexpressing
TNF- $\alpha$	Tumor Necrosis Factor Alpha
WT	Wild Type
XDH	Xanthine Dehydrogenase
XO	Xanthine Oxidase

## SUMMARY

With an impact on nearly 1 billion individuals worldwide and 70 million Americans currently, hypertension is one of the most readily identifiable risk factors for myocardial infarction (MI), heart failure, stroke, aortic aneurysms, dissections, and peripheral vascular disease. Furthermore, with rapidly aging populations around the world and ever increasing obesity rates, the burden of hypertension is estimated to affect a staggering 1.5 billion individuals globally by the year 2025 [1]. Hypertension is known to accelerate vascular inflammation – a hallmark of several cardiovascular disease pathologies – although the exact mechanism by which this happens still remains largely unknown.

The primary objective of this thesis was, therefore, to (a) explore the mechanisms by which elevated cyclic strain in the setting of hypertension leads to inflammation of the aorta and (b) to better identify the role of the potent pro-inflammatory protein osteopontin (OPN) and its role in regulating vascular inflammation and remodeling. We hypothesized that (a) elevated cyclic vascular wall strain acts through ROS to increase the expression of OPN and that (b) this increased OPN expression leads to a decrease in aortic compliance in the setting of hypertension. We used a cell culture (*in-vitro*) approach, two reproducible murine (*in-vivo*) models of hypertension, and performed mechanical testing of isolated murine aortas (*ex-vivo*) to test these hypotheses.

We found that OPN is upregulated with cyclic strain in culture smooth muscle cells and in the aortas of hypertensive mice. We have further identified that cyclic strain increases levels of ROS like superoxide ( $O_2^{\bullet}$ ) and hydrogen peroxide ( $H_2O_2$ ) in vascular smooth muscle cells. We also observed that transgenic mice that overexpress human catalase (a  $H_2O_2$  scavenger), specifically in their smooth muscle cells ( $Tg^{SMC-Cat}$ ) are protected against an increase in the expression of hypertension-induced OPN. These observations strongly suggest a prominent role

of ROS, in mediating the translation of mechanical cues such as elevated vascular wall strain in the setting of hypertension, into increased expression of pro-inflammatory products such as OPN. Our *in-vitro* findings also suggest a potential role for NADPH oxidases (which are major sources of ROS), in mediating mechanical strain-induced OPN production. In conclusion, these *in-vitro* and *in-vivo* studies suggest that elevated mechanical strain in the setting of hypertension may have an independent effect on upregulating critical mediators of inflammation, in our case OPN, and that this increase is regulated via ROS such as H<sub>2</sub>O<sub>2</sub>.

Finally, we have observed that OPN plays a role in mediating the mechanical properties of the aorta. Our *ex-vivo* mechanical tests have revealed that OPN KO aortas have increased pressure-dependent diameters under both baseline and hypertensive conditions as compared to their WT counterparts.

In conclusion, this thesis shows that (1) the arterial wall is sensitive to changes in its mechanical environment, and that (2) it responds to these mechanical changes via ROS dependent pathways by (3) increasing expression of pro-inflammatory proteins like OPN which (4) ultimately leads to vascular remodeling and inflammation. Overall these results deepen our understanding of the underlying mechanisms leading to vascular inflammation, and could have significant implications in facilitating our design of future therapies and strategies against the consequences of hypertension

## **CHAPTER 1:**

### **SPECIFIC AIMS**

Hypertension is a multifactorial inflammatory disease that imparts a myriad of humoral and mechanical signals to the vascular wall [2, 3]. *Humoral* signals are complex and variable. The renin-angiotensin system, comprised of molecules such as angiotensin-II (AngII), is one example of a humoral mechanism [3]. *Mechanical* stimuli impacting the arterial wall *in-vivo* are simplistically divided into three components – 1) frictional wall shear stress caused by flow across the endothelial layer, 2) circumferential and axial stress by wall deformation due to pulsatile blood flow and longitudinal tractions respectively, and finally 3) compressive stress due to the hydrostatic pressure of blood [4].

While the specific role and relative importance of humoral and mechanical signals in the ultimate development of vascular pathologies is not completely understood, a growing body of evidence has established that a combination of these signals leads to vascular inflammation [2]. This process involves accumulation of cells such as macrophages and leukocytes in the arterial wall [3]. Studies from many other labs and our own suggest that increased reactive oxygen species (ROS), such as superoxide ( $O_2^{\bullet-}$ ) and hydrogen peroxide ( $H_2O_2$ ), play a vital role in modulating the inflammatory response in hypertension by stimulating increased pro-inflammatory gene products [3, 5].

It has been shown that vascular inflammation is mediated by a plethora of pro-inflammatory gene products including osteopontin (OPN). Evidence from our lab has suggested that OPN plays a role in mediating AngII induced vascular hypertrophy [6] and that OPN is regulated by  $H_2O_2$  [7].

While several studies suggest a potential causal link between elevated mechanical cyclic strain in the setting of hypertension and pro-inflammatory proteins, very few have actually proven that such a relationship in fact exists. *We, therefore, hypothesized that mechanical changes due to hypertension increase ROS, which in turn enhance OPN expression, and that this ultimately leads to altered blood vessel biomechanics.*

### **SPECIFIC AIM 1**

*Establish if mechanical stretch in-vitro increases osteopontin expression*

Our first objective was to determine if mechanical strain applied to isolated vascular smooth muscle cells (SMCs) in culture would induce an increase in OPN expression and to determine if this increase was ROS dependent. We used a computer controlled bioreactor that applied uniform, reproducible biaxial strain to SMCs. Following treatment, the media surrounding these SMCs and the cells themselves were harvested and analyzed for H<sub>2</sub>O<sub>2</sub>, protein, and mRNA levels using molecular techniques including amplex red assay, Western Blotting, ELISA, and quantitative real time PCR (qRT-PCR). We hypothesized that mechanical strain of SMCs would induce a H<sub>2</sub>O<sub>2</sub>-dependent increase of OPN expression.

### **SPECIFIC AIM 2**

*To determine if osteopontin expression is increased in a murine model of hypertension and if this increase is H<sub>2</sub>O<sub>2</sub>-dependent*

In this aim, we assessed the role of H<sub>2</sub>O<sub>2</sub> in the regulation of OPN *in-vivo* using two murine models of hypertension. The reason why we utilized two independent murine models of

hypertension by infusing two humoral agents, namely, AngII and norepinephrine (NE), was in order to delineate the effects of humoral versus mechanical factors. We also used a strain of transgenic mice that specifically overexpresses catalase in smooth muscle to determine if H<sub>2</sub>O<sub>2</sub> is responsible for modulating OPN expression in hypertension. Following treatment, murine aortas were harvested and analyzed for OPN mRNA and protein levels using qRT-PCR, immunohistochemistry, and Western Blotting. We hypothesized that hypertension would increase OPN expression in the murine aorta, via a H<sub>2</sub>O<sub>2</sub>-dependent pathway.

### **SPECIFIC AIM 3**

*To determine the contribution of osteopontin to the mechanical properties of the aorta at baseline and in the setting of hypertension.*

In this aim, differences in the biomechanical properties of the aorta in OPN knock-out (KO) mice and wild type (WT) mice - under baseline and hypertensive conditions - were studied. Murine aortas were excised, cleaned of excess fat, and loaded onto a vessel isolation chamber and transmural pressures within the aorta was varied at fixed intervals. The outer diameter of the aorta was continuously recorded. Pressure-diameter curves, local compliance, and histology of the aorta was analyzed for the different groups that ultimately shed light on differences in vessel mechanical properties due to the presence or absence of OPN. OPN is believed to mediate vascular hypertrophy in the setting of hypertension, leading to aortic stiffness, and therefore, we hypothesized that hypertensive OPN KO mice would have more compliant aortas compared to their hypertensive WT counterparts.

## **Significance and Innovation**

Hypertension is one of the leading risk factors for cardiovascular morbidity and mortality [8]. Nearly one third (~29%) of all US adults over the age of 18 are hypertensive [9]. However, hypertension is not a single disease entity, but rather a clinical presentation of different underlying diseases that leads to elevated blood pressure [4]. With this premise in mind, it is surprising that these varied etiologies cause a uniform response on the arterial wall which includes thickening of the vessel wall (hypertrophy) and early atherosclerotic lesions [3]. A possible explanation for this uniform effect may be attributed to the common stimulus in hypertension – which is the increased mechanical strain on the arterial wall as a result of elevated blood pressure. While several studies have explored the role of humoral signals on the vascular wall, very few have studied the effects of mechanical stimuli on smooth muscle cells.

Moreover, the effects of hypertension on the vascular wall are so varied and numerous that its pathological consequences affect almost every single organ system, especially the cardiovascular system. Therefore, it is imperative to fully understand the effects of hypertension on large arteries. The results of this study will allow us to understand whether the increase in pro-inflammatory protein, osteopontin (OPN), under hypertensive conditions is modulated by ROS and for the first time, we will also be able to determine the role OPN plays in modulating the biomechanical properties of large arteries under both healthy and diseased conditions.

## **CHAPTER 2: BACKGROUND AND LITERATURE REVIEW**

### **Blood Vessels of the Human Body – Arteries and Veins**

The cardiovascular system (CVS) comprises of the heart and blood vessels that are responsible for the transportation of blood. This is essential for the delivery of vital nutrients and hormones, and removal of waste products to and from different organs, tissues, and cells of the body [10]. Arteries and veins are the two major types of blood vessels of the CVS. Arteries are thick-walled, elastic, muscular conduits whose main function is to transport oxygenated blood from the heart to the rest of the body, while veins collect deoxygenated blood from all the tissues and organs of the body, and transports it back to the heart, which then pumps it to the lungs for oxygenation [10].

#### **Aorta: Structure, Function, and Mechanics**

The aorta is the largest artery of the body, running from the aortic valve to the iliac bifurcation [11]. Its most important function is to distribute oxygenated blood from the heart to the rest of the body and to convert the intermittent inflow of blood it receives during systole, into a steady outflow at the smaller arteries and capillaries, during diastole – also referred to as the *Windkessel* effect [11, 12].

The aorta comprises of three main layers broadly classified as the (a) intima, (b) media, and (c) adventitia (Fig 2.1). The intima is the innermost layer of the aorta which is lined by a single cell layer of endothelial cells, serving as the primary interface with flowing blood. The media is the middle layer of the aorta comprising of smooth muscle cells and elastic fibers that allows for the contraction and expansion of aorta with each heartbeat. The media is the thickest layer of the aorta comprising around 80% of the thickness [11]. The adventitia is the outermost layer of the

aorta and consists mostly of collagen and a network of blood vessels called the vasa vasorum that nourishes the outer half of the aorta [11].

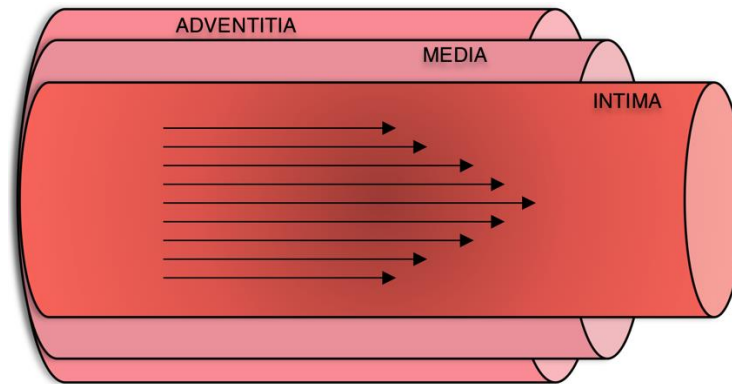


**Figure 2.1: Layers of the Healthy Aorta** The aorta comprises of three main layers – the intima, media, and adventitia. The intima comprises of a single layer of endothelial cells that is exposed to a shear stress from flowing blood, the media comprises of alternating layers of vascular smooth muscle cells, elastin, and collagen. The outer adventitial layer comprises of collagen and fibroblast cells.

There are numerous structural proteins and cell types that support the function of the aorta that include collagen and elastic fibers, endothelial cells, and smooth muscle cells (SMCs) as previously mentioned [13]. These structural proteins and cell types are normally under tension as reflected by the contraction of the aortic diameter by 20% and length by 40% when it is isolated from the body [14]. The pressure due to blood further induces a strain within the aorta, ranging from around 10% to 20% [15].

The aorta is constantly exposed to several mechanical forces due to blood flow and the pressure generated by the heart with every heartbeat. The major forces acting on the aorta include (a) wall shear stress which is primarily experienced by the intimal endothelial layer due to the parallel flow of blood (b) circumferential stress generated from blood flow during the systolic and diastolic phases of the beating heart, and finally (c) compressive forces due to the hydrostatic pressure on the aorta [16].

## **Hypertension Epidemiology**

Hypertension or high blood pressure is defined as the state wherein the mean systolic blood pressure is higher than 140 mmHg and mean diastolic blood pressure is higher than 90mm Hg [9, 17, 18]. Hypertension was the primary or leading cause of death in about 360,000 Americans in 2008 or an estimated 1000 deaths per day [9].

About 30% of the US population aged 18 to 65 suffers from hypertension – that’s a total of about 70 million individuals or about 1 in every 3 adults [9]. Furthermore, another 29% of US adults are pre-hypertensive – which is defined as a systolic blood pressure ranging from 120-139 mmHg or 80-89 mmHg of diastolic blood pressure – which further increases their risk of developing hypertension [9]. It is also discouraging to note that roughly only 52% of hypertensive patients have their blood pressure under control [9].

The prevalence of hypertension increases with age to more than 50% in the population aged 60 to 69, and to 70% in populations aged 70 years or older [17]. It is also important to note differences in the prevalence of hypertension among different population groups. The prevalence is much higher in the non-Hispanic black population (42.1%) than in the non-Hispanic White (28%), non-Hispanic Asian (24.7%), or Hispanic populations (26%) [17, 19]. Hypertension is also slightly more prevalent among men (29.7%) than women (28.5%) [19].

There is a very strong correlation between the incidence of hypertension and the risk of developing coronary heart disease (CHD) and stroke [17]. Furthermore, hypertension is a leading predictor for the development of end-stage kidney and heart failure [17]. Overall, hypertension poses a major global public health challenge and therefore, a deeper understanding of its etiology, progression, and myriad consequences are imperative to reduce hypertension associated morbidity and mortality.



A major consequence of elevated blood pressure is the onset of vascular inflammation within and around the tissues surrounding arteries such as the aorta [3, 21], and it is recognized as one of the most critical processes leading to the development of several other cardiovascular disease pathologies such as atherosclerosis [2], abdominal aortic aneurysms [22], dissections [23], strokes [24, 25], myocardial ischemia [25], and infarction [25]. Several clinical studies have highlighted a direct correlation between increasing blood pressure and plasma levels of inflammatory and adhesion markers such as C-reactive protein (CRP), interleukin-6 (IL-6), vascular cell adhesion molecule (VCAM-1), platelet endothelial cell adhesion molecule (PECAM), and intercellular cell adhesion molecule (ICAM-1) [26-29]. Anti-fibrinolytic proteins such as plasminogen activator protein (PAI-1) and chemokines such as monocyte chemoattractant factor (MCP-1) have also been shown to be upregulated with hypertension. Finally, transcription factors that mediate levels of the aforementioned inflammatory proteins, such as nuclear factor- $\kappa$ B (NF- $\kappa$ B) and activator protein-1 (AP-1) have been shown to increase within vascular tissue obtained from hypertensive animals [30, 31].

### **Effects of Hypertension on the Aorta**

The healthy aortic wall is a carefully regulated and balanced, but dynamic system, constantly interacting with a plethora of local and global environmental cues. On the one hand it is exposed to several humoral stimuli such as growth factors, contractile agonists, and differentiation factors; while on the other, it is constantly stimulated by mechanical forces that include active stresses and strains, hemodynamic forces, and passive stretch [32, 33]. With the onset of hypertension, there is an imbalance in these forces – the most prominent being a uniform increase in circumferential strain as a result of elevated blood pressure applied on the aortic wall.

The cells of the aorta are thus primed to adapt to this elevated strain, leading ultimately to adaptive or maladaptive responses. Adaptive responses lead to vascular hypertrophy and normalization of arterial wall stress [3, 4], while maladaptive responses lead to changes in the vascular wall that directly or indirectly cause secondary vascular pathologies, such as atherosclerosis, dissections, and aneurysms [22, 23, 34, 35]

Currently there is considerable debate over the specific role and relative importance of the numerous humoral and mechanical stimuli in the progression of these adaptive or maladaptive changes in response to hypertension. In reality, the net effect of hypertension is likely a “synthesis of multiple input stimuli from both categories” – humoral and mechanical [4]. There is, however, a definite need for future studies to further elucidate the specific mechanisms that control hypertension related vascular inflammation and clearer identification of potential therapeutic targets.

### **Humoral Effects of Hypertension:**

#### **Renin-Angiotensin-Aldosterone System (RAAS) and Norepinephrine (NE)**

The renin-angiotensin-aldosterone (RAAS) system is a critical modulator of blood pressure in the body (Fig 2.3). The juxtaglomerular cells of the kidney synthesize and release the enzyme renin, which catalyzes the conversion of angiotensinogen into angiotensin-I (AngI) [36, 37]. The final step of this pathway is the conversion of angiotensin-I (AngI) into angiotensin-II (AngII) in the presence of angiotensin converting enzyme (ACE) and other proteases such as chymase [38]. The most important physiologic and pathophysiologic outcomes of the RAAS pathway are in fact regulated by AngII. These AngII mediated processes range from vasoconstriction of arteries,

aldosterone production and release, sodium reabsorption, stimulation of thirst, and a heightened sympathetic response [20].

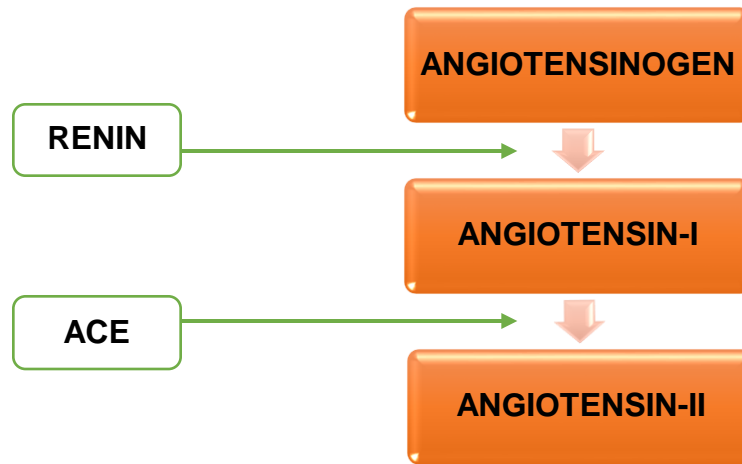


**Figure 2.3: Renin-Angiotensin-Aldosterone (RAAS) Pathway** AngII is the final product of the Renin-Angiotensin-Aldosterone pathway that plays a critical role in the regulation of blood pressure in the body and is typically upregulated at the onset of hypertension.

In the setting of hypertension, AngII plays a potent role in mediating pathophysiologic vascular change by modulating cytokine production and oxidative stress, which in turn leads to adhesion molecule expression, vascular wall inflammation, extracellular matrix (ECM) deposition, hypertrophy, and proliferation of vascular smooth muscle cells (SMCs) [39-42]. AngII, in the context of hypertension, is also a potent stimulator of PAI-1 and activator of matrix metalloproteinases (MMPs) which may promote plaque rupture and a pro-thrombotic environment within an atherosclerotic lesion [43, 44]. Finally, AngII activates the enzyme nicotinamide adenine dinucleotide phosphate oxidase (NADPH oxidase) which is a major source of reactive oxygen species (ROS) such as superoxide ( $O_2^{\bullet-}$ ) and hydrogen peroxide ( $H_2O_2$ ) [39, 45]. In the healthy aorta, these ROS act as important second messengers in vascular smooth muscle cells and in modulating vascular tone and structure [39, 46], but with hypertension these ROS induce vascular remodeling through hypertrophy and accelerated proliferation of vascular smooth muscle cells

(SMCs) and collagen deposition [21, 47, 48]. AngII further stimulates the expression of adhesion proteins such as ICAM-1 and MCP-1 through the activation of NADPH oxidases, which in turn attract a host of inflammatory cells such as macrophages which leads to a pro-inflammatory environment conducive to vascular injury and dysfunction [49].

Aldosterone is a byproduct of the RAAS pathway that is synthesized in the zona glomerulosa of the adrenal cortex [50]. It is a steroid hormone that regulates salt and water balance in the body, by promoting unidirectional sodium transport and consequentially the retention of water [51]. Animal studies have shown that a diet high in sodium in the presence of excess aldosterone causes organ damage characterized by perivascular inflammation and necrosis [52].

Norepinephrine (NE) is a catecholamine or stress hormone that has a direct effect on blood pressure [53]. It is part of the sympathetic nervous system. Some of its most profound effects include (a) rapid increase in blood pressure (b) shunting blood towards the skeletal muscle system, heart, and brain, and away from the gastrointestinal system (c) increase of heart rate and contraction (d) elevated respiration and bronchodilation (e) increased lipid breakdown in adipocytes (f) and increased production of glucose and glycolysis in the liver [53]. Typically, the presence of NE is necessary in the short term for an individual's survival. However, elevated levels of this circulating catecholamine over long periods of time may lead to development of pathological conditions that range from cardiac hypertrophy, hypertension, and post-traumatic stress disorder (PTSD) [53]. Catecholamines can further induce cell proliferation on vascular smooth muscle cells independent of its effect on blood pressure [54].

## **Mechanical Effects: Arterial Remodeling**

Understanding the mechanical effects of hypertension on large arteries has become a critical area of investigation in cardiovascular research and biomechanics, especially since it is known that large arteries associated with hypertension have a tendency to develop early atherosclerotic lesions, aneurysms, and dissections [55]. Some of the well recorded effects of hypertension on arteries include vascular hypertrophy [47] and decreased arterial compliance (Fig 2.4) [55].

Early studies by Burton et al. have highlighted that increasing luminal pressure within arteries causes an increase in arterial radius, which then leads to increased arterial wall tension [56]. The effect of acutely elevated vascular wall tension with hypertension would then lead to vascular hypertrophy, increased wall thickness, and therefore reduced wall stress [3, 4, 41, 56]. Other modeling and observational studies have also shown that increased pulsatile arterial pressure induces wall stress at certain sites along the aorta (such as bifurcations), which in addition to a high fat diet leads to development of atherosclerotic lesions at these locations [34].

Another study looking into the direct effects of mechanical pressure on the aortic wall was conducted by Ollerenshaw et al, where an aortic coarctation model of hypertension was used and demonstrated the presence of significantly higher vascular hypertrophy in the region above the coarctation, where the blood pressure was elevated, as opposed to the region below the coarctation, where blood pressure was normal [57]. This study further highlighted that even though the region above and below the coarctation was exposed to the same humoral milieu; the differences in mechanical pressure seemed to have a greater effect on vascular hypertrophy [57]. However, there is still a significant need for future studies to highlight the role of mechanical forces within the

blood vessel and better elucidate how they contribute to the progression and development of disease pathologies such as atherosclerosis.

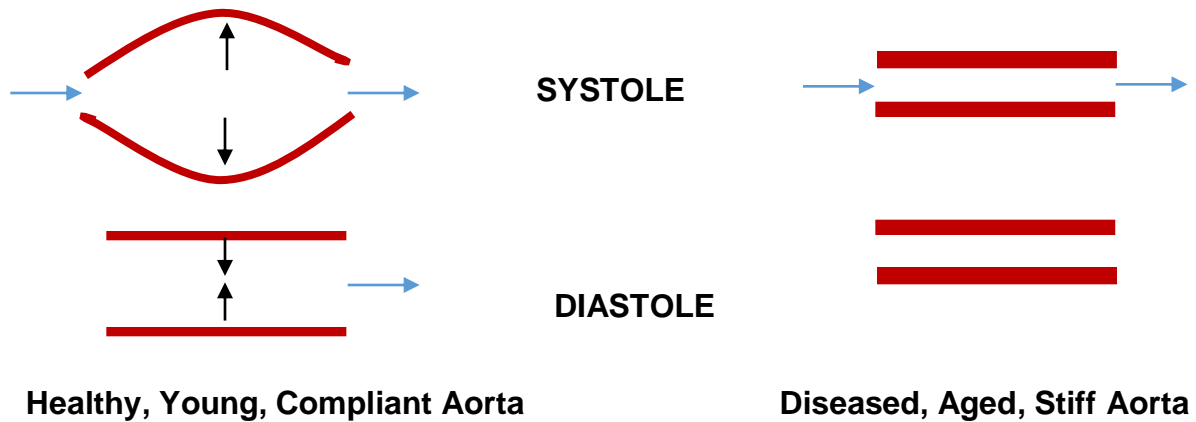


**Figure 2.4: Differences in Aortic Compliance with Age & Disease** The healthy aorta is typically compliant among younger age groups, but stiffens with age. This stiffness may be attributed to increased collagen deposition and a loss of elastin within the aortic walls and hypertension related vascular inflammation.

### Reactive Oxygen Species: Overview

ROS are oxygen-based molecules and sometimes contain an unpaired free electron. The summed effect of these ROS in living systems is commonly referred to as oxidative stress. The most important ROS in the vasculature include superoxide ( $O_2^{\bullet-}$ ), nitric oxide ( $NO^{\bullet}$ ), peroxynitrite ( $ONOO^{\bullet-}$ ), and hydrogen peroxide ( $H_2O_2$ ), which play important roles as signaling molecules that regulate cellular functions when produced in small amounts. Numerous sources of ROS have been identified in literature such as xanthine-xanthine oxidases, NADPH oxidases, mitochondrial respiration, cyclooxygenases, lipoxygenases, and uncoupled nitric oxide synthases [58].

*Nitric Oxide* - Under healthy conditions  $NO^{\bullet}$  is produced by endothelial nitric oxide synthase (eNOS) in blood vessels, however, under inflammatory states,  $NO^{\bullet}$  may be produced by inducible NOS in macrophages and smooth muscle cells [59, 60].  $NO^{\bullet}$  is a very critical mediator

of endothelium-dependent vasodilation. It is also known to maintain balance between growth and differentiation of smooth muscle cells and modulate platelet aggregation [61, 62].

*Peroxynitrite* - When  $O_2^{\bullet-}$  and  $NO^{\bullet}$  are produced simultaneously they react rapidly to form another highly reactive molecule peroxynitrite ( $ONOO^{\bullet-}$ ), which is responsible for lipid peroxidation, protein nitration, and is highly proatherogenic [63-65].

*Superoxide ( $O_2^{\bullet-}$ )* – These molecules are highly unstable and are therefore rapidly dismutated by the enzyme superoxide dismutase (SOD) into the more stable molecule,  $H_2O_2$ , which is further degraded by either catalase or glutathione peroxidase into water (Fig 2.5) [66-68].  $O_2^{\bullet-}$  molecules have a short half-life and are membrane impermeable [69]. They can act as signaling molecules altering the function of critical proteins such as enzymes, structural proteins, small GTPases, ion channels, phosphatases, and kinases [70]. More importantly they are important precursors to other ROS such as  $H_2O_2$  and highly reactive peroxynitrites. Finally, they serve as oxidants and react with DNA, the cell membrane, or biologic macromolecules to further prolong the oxidative state of target cells or tissues [58, 65].

*Hydrogen Peroxide ( $H_2O_2$ )* - is one of the most stable ROS produced in the vasculature that is freely diffusible across the cell membrane, making it an ideal candidate for a signaling molecule [71]. It is capable of reacting with a plethora of other molecules. For example, it is able to induce a change in the cell state by reacting with thiol residues which results in sulfur oxidation [71].



as atherosclerosis, strokes, aneurysms, myocardial infarction, and hypertension [75]. In arterial disease pathologies such as atherosclerosis and hypertension related inflammation, ROS have also been implicated in the breakdown of the extracellular matrix (ECM) [72, 76-78].

ROS produced by NADPH oxidases have been shown to increase ECM degradation by increased MMP activation [78, 79]. Since a balance of proteins such as elastin, collagen, and other ECM proteins, plays a critical role in the maintenance of an intact artery, oxidative disturbance of the ECM can lead to endothelial dysfunction and SMC remodeling and reorganization. This breakdown can in turn attract inflammatory cells such as monocytes and macrophages, which then propagates the secretion of ECM destroying enzymes such as interleukins, MMPS, and cathepsins, leading to a vicious inflammatory cascade and further breakdown of healthy tissue [76, 77].

It has been also shown that in hypertension, ROS are produced from multiple organs systems and cell types that range from neuronal, renal, vascular, and cardiac origin [58], but we focus on increased ROS within the vasculature for the purpose of our discussion. Clinical studies show that plasma levels of ROS and related large quantities of peroxidation and DNA oxidation byproducts significantly increase in the presence hypertension [80]. The role of H<sub>2</sub>O<sub>2</sub> has been also elucidated in animal models such as the catalase overexpressing transgenic mouse model, wherein increased catalase levels in the vascular smooth muscle, leads to lower H<sub>2</sub>O<sub>2</sub> levels in the medial, which ultimately protects the vasculature against AngII induced hypertrophy [81]. Other studies using a high salt-intake rat model of hypertension shows that superoxide interacting with NO, along with L-buthionine sulfoximine treatments, induces vascular dysfunction [82]. Another study demonstrated that potential inhibition of Nox-1 induced ROS using atorvastatin would reverse AngII induced arterial contractions [83].

## **Antioxidants**

The body has several defense mechanisms to protect itself against excess ROS, which are a natural byproduct of metabolism. Most of the molecules and enzymes that work together to breakdown these ROS are termed antioxidants. In fact, several studies involving antioxidants have shown a critical link between oxidative stress and vascular pathologies. For example, there have been studies that show that animals treated with the antioxidant Vitamin E have a lower incidence of AAA formation [84]. Additionally, there was a smaller influx of macrophages in the media of these Vitamin E treated animals [84]. Conversely, there are clinical studies that have shown that hypertensive subjects have lower levels and activity of physiologic antioxidants such as superoxide dismutase, catalase, and glutathione peroxidase [68].

Catalase is an important antioxidant enzyme that converts  $H_2O_2$  into water and molecular oxygen. The work described in this thesis involves the use of the transgenic mouse that overexpresses the human catalase gene specifically in vascular smooth muscle cells ( $Tg^{SMC-Cat}$ ) [81]. These mice have increased activity of catalase in the SMC and therefore lower  $H_2O_2$  levels in the media of the aorta. As previously mentioned, studies with these mice show that  $H_2O_2$  within the medial layer of the aorta promotes SMC hypertrophy in the setting of AngII infused hypertension [81].

## **Sources of ROS and Hypertension**

There are several sources of ROS in the vasculature that include (a) NADPH oxidases, (b) xanthine oxidase, (c) the mitochondrial electron transport chain, and finally (d) the endothelial nitric oxide synthase.

*NADPH oxidases* are membrane bound receptor enzyme complexes that generate superoxide and H<sub>2</sub>O<sub>2</sub>, especially when stimulated by AngII [45]. They are comprised of multiple units that include a catalytic subunit, membrane bound, and NOX domain (Fig 2.6) [85]. They are the most common and best studied source of ROS in the vasculature. Compared with NADPH oxidases found in phagocytes, vascular NADPH oxidases generate much lower levels of superoxide (less than 1%) [86]. Vascular NADPH oxidases also generate superoxide that play a vital role in cell signaling as opposed to playing a cytotoxic role which it does in phagocytes. There are several kinds of NADPH oxidase homologues expressed in vascular cells of the body ranging from NADPH oxidase 1-7 (NOX 1-7). NOX 1, 2, 4 and 5 – are the most commonly found NOXes within the vasculature [71, 87]. It is known that endothelial cells express high levels of the NOX 2 and NOX 4 homologues and low levels of NOX 1 and NOX 5 [71, 87]. Vascular NADPH is also regulated by numerous humoral factors such as growth factors, cytokines, and vasoactive molecules, and several physical factors such as shear stress, cyclic strain, and stretch [88].

Several animal studies have shown that NADPH oxidase activity and expression is upregulated in the setting of hypertension. Animal studies involving spontaneously hypertensive rats (SHR) have shown increased NADPH oxidase dependent superoxide production in large arteries such as the aorta [89-91]. Another important discovery is that several polymorphisms in the promoter region of the p22<sup>phox</sup> gene (note that p22<sup>phox</sup> is a subunit of the NADPH oxidase complex) have been observed in the animal model of SHR [92]. This discovery has major implications because other clinical studies have shown that in patients suffering from hypertension, there is a strong link between a p22<sup>phox</sup> gene polymorphism and NADPH oxidase dependent superoxide production [92]

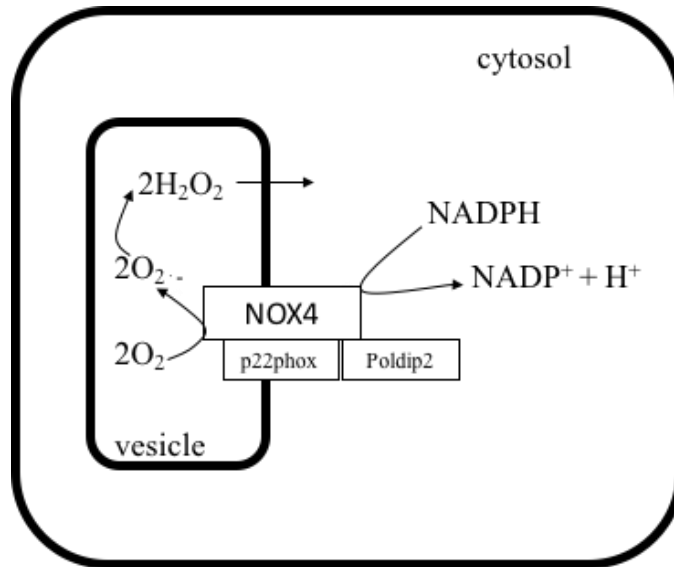


**Figure 2.6: Structure of the NADPH Oxidase 4 Enzyme** ROS are generated by the conversion of molecular oxygen into superoxide and then rapidly into hydrogen peroxide by enzymes such as NADPH oxidase as shown above. This enzyme comprises of multiple subunits (such as NOX4, p22phox, and Poldip2) across different cellular components (vesicle, cytosol). Adapted from [74]

*Xanthine oxidases* - These enzymes are another important source of superoxide. The ROS producing form of xanthine oxidoreductase comprises of XO which uses oxygen as an electron acceptor [70, 93]. There is another non-ROS producing form of xanthine oxidase also referred to as XDH [70, 93]. The XDH to XO ratio determines the oxidative state of the cell. A transition in this ratio from XDH to XO can occur via inflammatory cytokine stimulation and by cysteine residue oxidation by ROS such as peroxynitrites. Activation of NADPH oxidases can also further trigger the balance of XDH to XO, in favor of XO further inducing oxidative stress [70, 93].

*Mitochondrial electron transport chain* is another major contributor of ROS in the vasculature [70]. The mitochondrial electron transport chain works through a series of complexes (1-4), that pass an electron from one complex to the next. The final transfer of this electron to an oxygen molecule is what generates superoxide.

*Endothelial Nitric Oxide Synthase (eNOS)* – In the healthy vasculature, this enzyme is highly expressed and is thereby responsible for the synthesis of the atheroprotective molecule NO. This enzyme typically comprises of two subunits. Under conditions of oxidative stress, however, these subunits uncouple and they generate ROS [70, 93, 94]. As the vascular cells further shift into an oxidative state, some of the eNOS continues to remain coupled, and produce NO, which in turn reacts with superoxide generated by the uncoupled eNOS, resulting in a plethora of undesired ROS, ultimately leading to a pro-inflammatory state and vascular dysfunction [70, 93, 94].

### **Osteopontin: Structure, Function, and Role**

Osteopontin (OPN) is a multifunctional, non-collagenous ECM protein [95]. It is commonly categorized as a matricellular protein. These proteins are found in the extracellular space, but unlike ECM proteins do not play any structural or mechanical role within tissues they are expressed in [96]. OPN is found abundantly in the matrix of several mineralized tissue such as the bone, where it was first discovered in the late 1970s [97]. Within cells, OPN is first synthesized as a 34-kDa protein and then undergoes several post-translational modifications that include phosphorylation and glycosylation, depending on its site of expression [97]. OPN is known to bind to hydroxyapatite and to calcium because of its negative charge and acidic nature [95]. Early research surrounding OPN focused on its role within bones, but it was soon discovered that OPN played an important role in tissues undergoing active remodeling, inflammation, wound repair, metastasis, tumor formation, cell migration, adhesion, and mineralization [95]. OPN can respond to and interact extremely efficiently with surrounding cells and proteins because it contains an RGD sequence known to bind to integrins, thrombin cleavage site, and additional sequences known to bind to the CD44 (hyaluronic acid) receptors [95].

Integrin mediated signaling is a critical link between cells and their external environments, and even more relevant in the setting of hypertension, because of the need for vascular cells to be able to respond to changing physical forces (such as elevated blood pressure) [98]. OPN is able to successfully interact with integrin receptors, thereby not only allowing cells to adhere to their ECM, but also mechanotransduce external signals into the nucleus, alter gene expression and their overall response [98]. The family of integrin receptors that are currently known to interact with OPN include  $\alpha_v\beta_1$ ,  $\alpha_v\beta_3$ ,  $\alpha_v\beta_5$ ,  $\alpha_4\beta_1$ ,  $\alpha_5\beta_1$ ,  $\alpha_8\beta_1$ , and  $\alpha_9\beta_1$ . OPN is able to interact with most integrins through its RGD motif, except for  $\alpha_4\beta_1$  and  $\alpha_9\beta_1$  which interacts with a novel amino acid binding sequence – SVVYGLR [95, 98-102]. OPN has a thrombin cleavage site which is believed to increase the access of numerous cell receptors to their binding domains and allow for better enhanced cellular effects of OPN [103]. The other important OPN receptor CD44, is a glycoprotein and allows for cell migration and adhesion [104]. The principal ligand for CD44 is hyaluronic acid, but it binds to other proteins such as OPN and other ECM proteins like fibronectin, laminin, and collagen [105].

OPN affects cell migration, chemotaxis, and adhesion through its several binding domains and therefore, its role in several disease pathologies that involve wound repair, tumor growth, metastasis, and inflammation has been well defined and studied. OPN plays an important role in immune cell migration and in mediating the overall inflammatory response of tissues to injury [95, 106]. OPN is known to mediate immune response to bacterial and viral infections and act as a potent chemoattract for macrophages at sites of inflammation [107]. These effects of OPN on immune cell migration and activation provide strong evidence in support of the hypothesis that OPN plays an important role in wound repair and tissue remodeling. These effects are also supported by the early observations made of the OPN KO mice generated by Liaw et al. that

demonstrate reduced macrophage infiltration and matrix organization in response to skin injury [108]. Studies have shown that OPN is also highly expressed in the blood and in tumors that are in advanced stages and undergoing active metastasis [109].

### **Osteopontin in Vascular Pathophysiology & Regulation**

In the vasculature, it is established that OPN is present only in small amounts in the uninjured arteries, however, its expression increases several fold in endothelial, smooth muscle, and activated inflammatory cells in injured arteries [5, 95, 110]. The functional role of OPN in this inflammatory setting has been attributed to its role as a chemo attractant for endothelial cells and smooth muscle cells, inhibitor of calcification, and activator of inflammatory cells [5, 102, 111]. Furthermore, it has been observed that OPN protein and mRNA are expressed in higher levels at sites of dystrophic calcification, atherosclerotic plaques, and in macrophages present in calcified aortic valves [5, 110, 112]. OPN has also been implicated to play a critical role in wound healing, collateral vessel formation, vascular remodeling, and development of atherosclerosis [110].

Several studies from our lab have shown that OPN plays a critical role in neovascularization within the hind limb [113, 114]. Studies by Duvall et al provide early evidence that OPN plays a critical role in ischemic limb revascularization and suggest that this maybe driven by macrophage and monocyte inflammation at the site of injury, which was impaired in OPN KO mice with hind-limb ischemia [113]. Furthermore, *in-vitro* and *in-vivo* studies by Lyle et al demonstrate that OPN is regulated by ROS such as hydrogen peroxide [7]. Animal studies of hind limb ischemia in transgenic mice that overexpress catalase in vascular smooth muscle cells (Tg<sup>SMC-Cat</sup>) animals demonstrate that hydrogen peroxide plays an important role in mediating OPN expression in response to hind limb ischemia [114]. *In-vitro* studies by Lyle et al further elucidates

the specific cellular mechanisms by which hydrogen peroxide regulated OPN expression via activation of transcriptional and translational pathways [7].

Finally, several clinical studies have shown that there are elevated levels of OPN detected in plasma of hypertensive individuals [115]. However, it is unknown why OPN is upregulated and its specific functional role in the setting of hypertension is also unclear. As previously mentioned OPN is a matricellular protein that acts to translate mechanical cues into cellular signaling within the vascular wall [116], but its expression in response to mechanical strain from the vascular wall in response to hypertension has not been explored before. It is therefore critical to study its response to increased cyclic stretch in a controlled *in-vitro* and *in-vivo* setting, and is therefore, the primary objective of this thesis.

## CHAPTER 3

### REGULATION OF OSTEOPONTIN IN-VITRO BY CYCLIC STRAIN IN AORTIC SMOOTH MUSCLE

#### *SPECIFIC AIM 1:*

*Establish if mechanical strain in-vitro increases osteopontin expression*

#### **Introduction**

Uncontrolled high blood pressure is a major risk factor for a plethora of cardiovascular pathologies that range from atherosclerosis, aneurysms, dissections, strokes, heart failure, and myocardial infarctions (MI). There are numerous factors that are dysregulated with the onset of hypertension and these can be broadly classified into two categories – humoral and mechanical. Humoral factors include higher levels of circulating agonists such as AngII and NE, while mechanical factors include increased circumferential vascular wall strain as a result of elevated blood pressure. The current body of literature reflects a much greater emphasis placed upon the study of the effects of humoral factors on the vasculature [3, 36, 41, 53, 83] both *in-vivo* and *in-vitro*, but little is known about the effects of increased mechanical strain on the arteries [3, 4]. In reality, however, the progression of arterial inflammation is *likely* due to a combination of *both* these factors and not just one.

Our first objective, therefore, was to determine the effect of mechanical strain on the expression of the pro-inflammatory protein, OPN, in isolated vascular smooth muscle cells in culture, and to study if this was a redox sensitive mechanism (Fig 3.1). We used a computer controlled bioreactor that applied uniform, reproducible biaxial strain to SMCs. Following treatment, the media surrounding these SMCs and the cells themselves were harvested and

analyzed for H<sub>2</sub>O<sub>2</sub>, protein, and mRNA levels using techniques including Amplex Red Assay, Western blot analysis, ELISA, immunohistochemistry, and quantitative real time PCR (qRT-PCR).

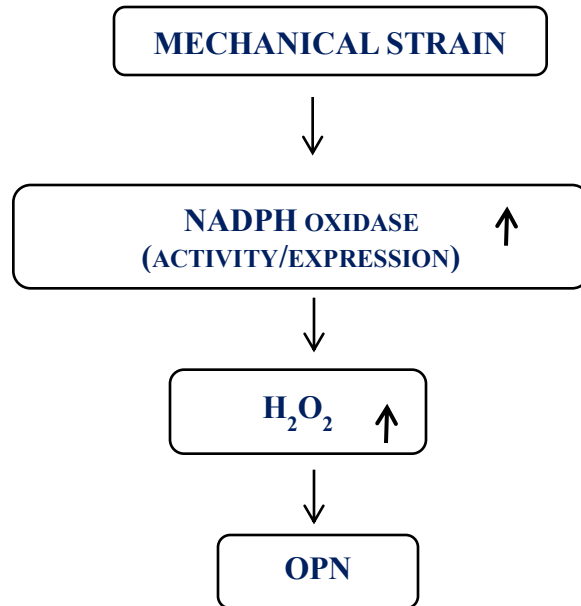


**Figure 3.1: Suggested Mechanism of Mechanical Strain Induced OPN Expression** We hypothesize that OPN expression is increased when smooth muscle cells experience cyclic mechanical strain, and that this happens via increases in hydrogen peroxide and an NADPH oxidase dependent mechanism.

## **Methods**

### **Cell Culture & Materials**

Vascular Smooth Muscle Cells (SMCs) were harvested by enzymatic elastase/collagenase digestion from rat thoracic aorta, as previously described [117]. SMCs between passage 6 and 14 were cultured on silicone membrane 6-well plates that had been coated with collagen type - I (Bioflex © Culture Plates, Flexcell International) and grown in DMEM (Sigma Aldrich, St Louis, MO) which was supplemented with 10% calf serum (Invitrogen), 2mmol of L-glutamine, 100U/mL of penicillin, 100ug/mL of streptomycin, and 1M of HEPES solution. SMCs were then quiesced by serum starvation in 0% calf serum containing DMEM for 48 hours. Note that media was changed every 24 hours during the period of quiescence. Polyethylene-glycol catalase (PEG-Catalase), Polyethylene-glycol superoxide dismutase (PEG-SOD), Apocynin (200ug/mL), and Diphenyliodonium (DPI, 10uM) were all obtained from Sigma Aldrich.

### **Cyclic Strain of Vascular Smooth Muscle Cells**

After quiescing SMCs, cells were stretched at 10% cyclic strain on the computer controlled Flexcell® FX-5000 Tension System in all experiments unless stated otherwise. This system uses a patented, computer controlled, pressurized device that applies a reproducible, user defined cyclic tension. In this device, cells cultured in a monolayer on elastomeric, flexible bottom culture plates experience equibiaxial strain when the plate is deformed using a regulated vacuum pressure (Fig 3.2 and Fig 3.3). Cells of the control group were seeded in an identical manner on identical flexible bottom culture plates, but did not experience any cyclic strain, and were kept on another stationary chamber within the same incubator containing the biaxial strain, loading platform.

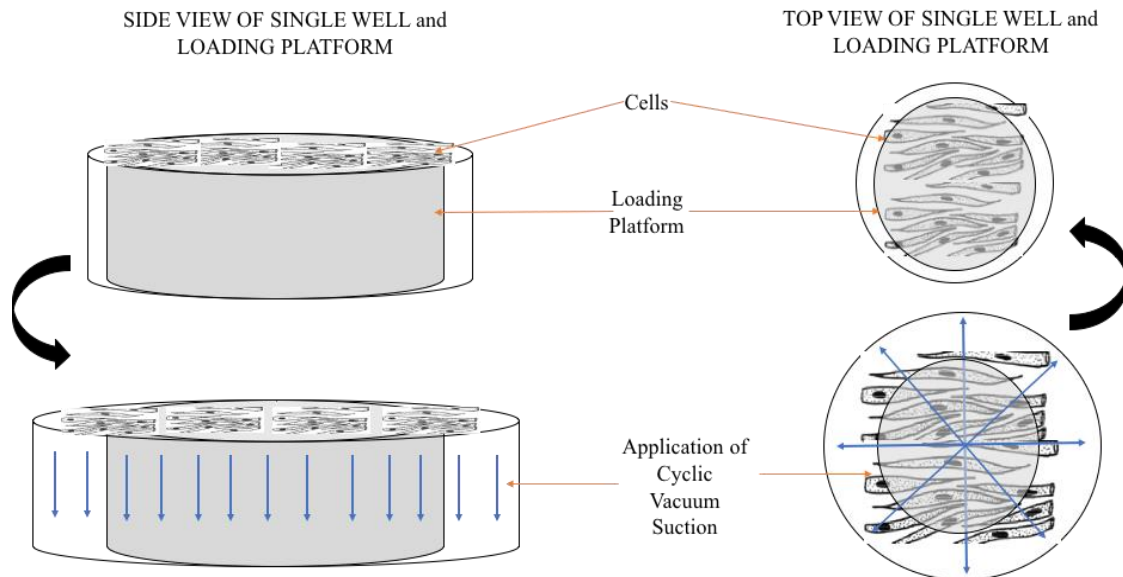


**Figure 3.2: Schematic of Application of Biaxial Strain on a Single Well of Cultured Vascular Smooth Muscle Cells.** SMCs are cultured on flexible membrane Collagen-I coated 6-well plates that are then mounted over a loading platform controlled by the FX-5000 Tension System. This system utilizes a computer controlled, pressure operated mechanism to apply reproducible, equibiaxial strain on cells that are located directly over the loading platform. Application of a uniform cyclic vacuum pressure (bottom two images) pulls the membrane with cells over the loading platform to generate the desired magnitude of strain, thereby straining cells.

### Western Blot Analysis

SMCs were lysed in Hunter's Buffer, as previously described [118]. Cells were sonicated using a sonic dismembrator at 10W for 10 x 1 sec pulses. Whole cell lysates were then boiled and subsequently used for immunoblotting. Band intensity was quantified by densitometry analysis and normalized to  $\beta$ -Actin. The OPN antibody was purchased from R&D systems (Cat#: AF808). The  $\beta$ -Actin antibody was from Cell Signaling (Cat# 13E5).

### ELISA

Secreted OPN expression was measured using a rodent OPN ELISA kit obtained from Enzo Life Sciences and manufacturer's instructions were strictly followed. DMEM from cyclically strained SMCs was harvested and stored with protease inhibitor cocktail (PIC) from Sigma.

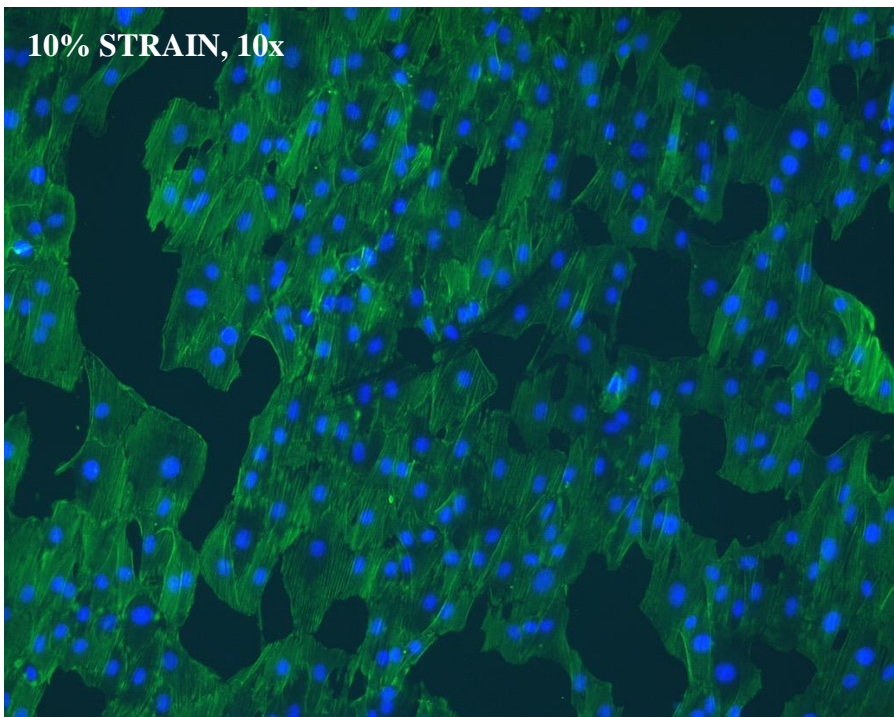
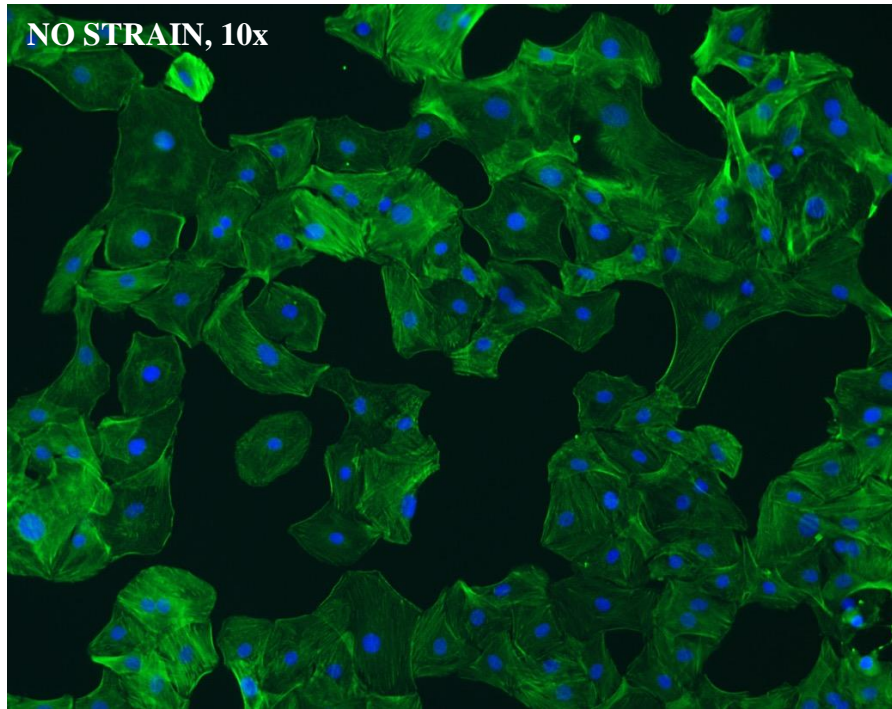


**Figure 3.3: Phenotype of Rat Aortic Smooth Muscle Cells 24h post Strain** Rat aortic smooth muscle cells were stained for Phalloidin (green) and DAPI (blue). Cells located near the circumference of the Collagen-I coated flexible membrane plates are observed to align tangentially in response to cyclic strain. Images courtesy of Dr. Alejandra San Martin.

## **RNA Isolation and Quantitative Real-time Polymerase Chain Reaction**

RNA was harvested from aortas or cultured SMCs in RLT Buffer and processed for mRNA using the RNEasy kit from Qiagen. OPN mRNA levels were then measured by amplification of cDNA using an Applied Biosystems thermocycler, primers specific for mouse or rat OPN (QuantiTect Primers, Qiagen), and SYBR green dye. Copy numbers were calculated by the instrument software from standard curves of genuine templates. OPN copy numbers were then normalized to a million copies of the housekeeping gene 18s.

## **Detection of ROS**

The production of superoxide ( $O_2^{\cdot-}$ ) was measured via immunocytochemistry using 50 $\mu$ M of hydrocyanine-3 fluorescent probe (ROSstar 550 Probe).  $H_2O_2$  production was measured using the Amplex Red Assay Kit (Invitrogen) as previously described [67].

## **Statistics**

All results are presented as mean  $\pm$  SEM and analyzed using ANOVA or t-test using GraphPad <sup>TM</sup> Prism Software (GraphPad Prism), followed by Bonferroni or Tukey multiple comparisons test. A p-value  $< 0.05$  was considered significant.

## Results

### Cyclic Strain Increases Osteopontin Expression in Cultured SMCs

At the onset of hypertension, it is well established that the vessel wall experiences increased levels of cyclic mechanical forces such as elevated circumferential vascular wall strain. We wanted to study the independent effect of elevated cyclic strain on OPN expression and therefore first conducted a time-course study where rat SMCs were strained at 10% elongation for 2, 4, 8, and 24 hours. Following strain, SMCs were harvested and analyzed for OPN levels. We observed a significant increase in OPN mRNA in the SMCs strained for 24 hours compared to the non-strained control cells (Fig 3.4). We did not observe any significant increase in OPN mRNA at any of the earlier time points (2, 4, or 8 hours). OPN protein expression was also measured using Western blot analysis (Fig 3.5) after straining SMCs at the time points previously mentioned and we observed a significant increase at the 24-hour time point. We did not observe any significant change in cellular OPN levels at the earlier 2, 4, or 8-hour time points, similar to what was observed with OPN mRNA.

Finally, it is known that OPN is a secreted protein, and therefore, we measured secreted levels of OPN (from the media surrounding the strained cells) using an ELISA (Fig 3.6) and found that SMCs strained for 24 hours secreted ~4 fold-higher levels of OPN compared to the non-strained controls. Combined, these results demonstrate that osteopontin is indeed a mechanosensitive gene that is up-regulated with cyclic strain in vascular smooth muscle cells.

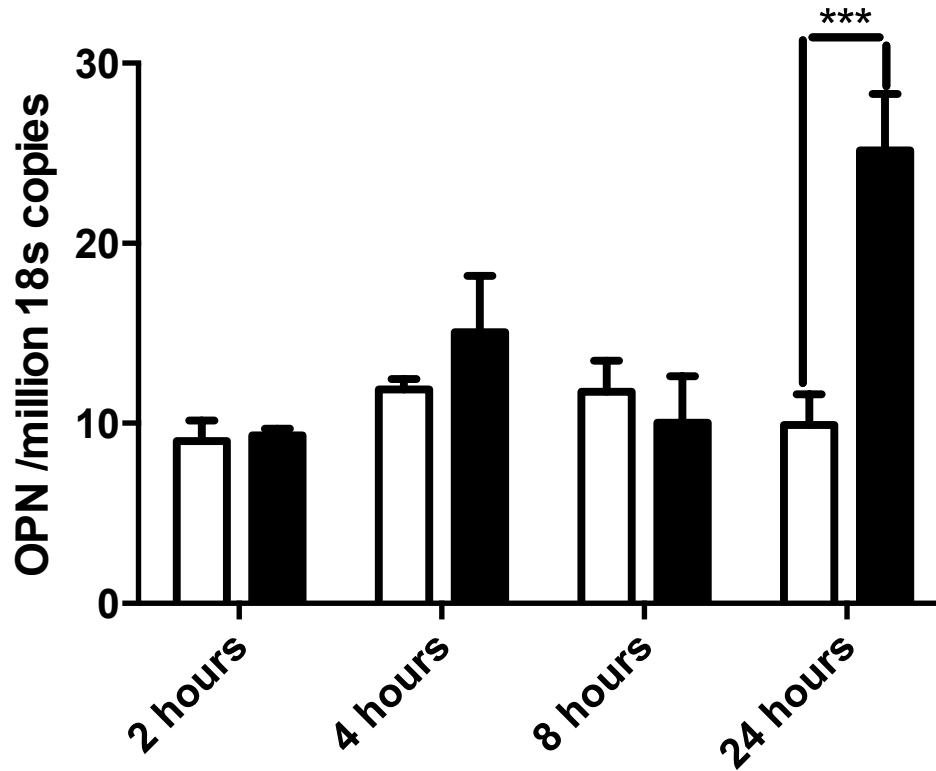


**Figure 3.4: 24 hours of Cyclic Strain Increases OPN mRNA Expression** SMCs were cyclicly strained for 2, 4, 8, and 24 hours and then harvested for analysis. Quantitative real-time PCR was used to measure levels of OPN mRNA that were normalized to a million copies of the 18s housekeeping gene. Samples were obtained by straining RASMs for 24hrs at 10% elongation. \* $p < 0.05$  for  $N=3$ . Black bars represent the SMCs strained at 10%, while the white bars represent the control, non-strained SMCs. We observed a significant increase in OPN mRNA expression with cyclic strain at 24 hours, but not at 2, 4, or 8 hours.

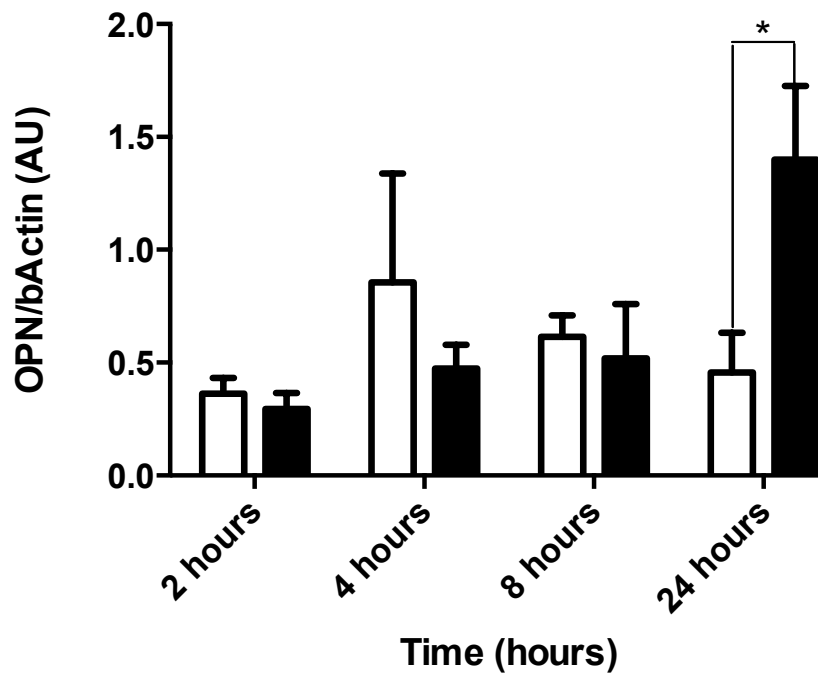
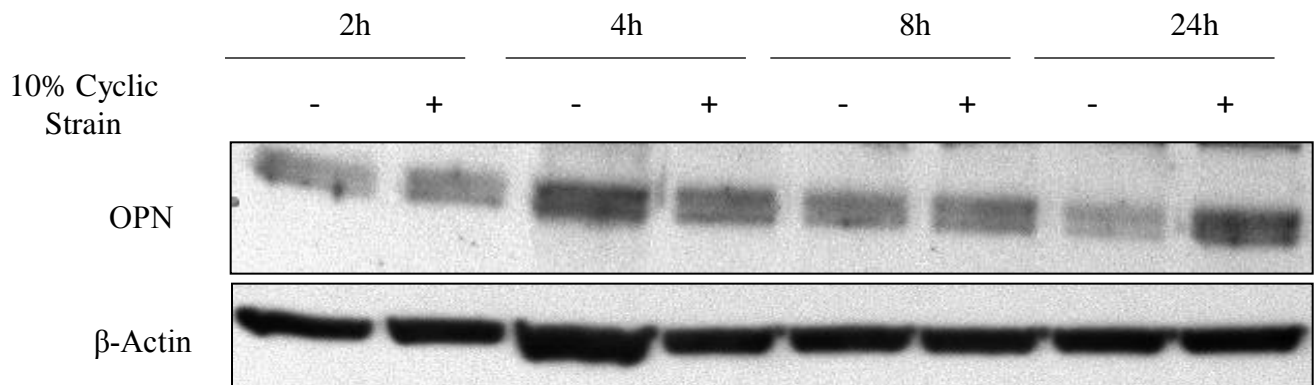


**Figure 3.5: 24 hours of Cyclic Strain Increases Cellular OPN Protein Expression** OPN protein expression was measured SMCs via Western Blot analysis after 2, 4, 8, and 24 hours of cyclic strain. Protein expression was quantified via protein densitometry and is represented in arbitrary units normalized to  $\beta$ -Actin expression \* $p < 0.05$ ,  $N = 4$ . Black bars represent the SMCs strained at 10%, while the white bars represent the control, non-strained SMCs. We observed a significant increase in cellular OPN in SMCs strained for 24 hours, but not at 2, 4, and 8 hours of strain.

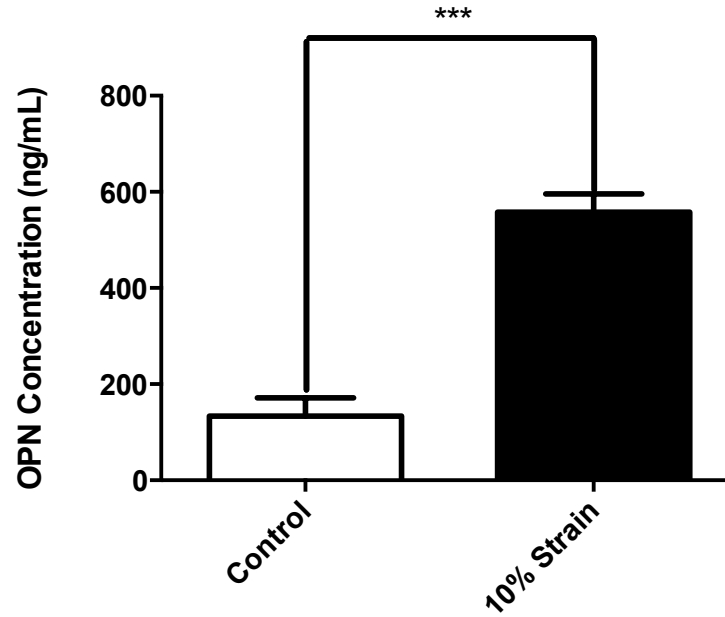


**Figure 3.6: Cyclic Strain Increases Secreted OPN Protein Expression** Secreted OPN protein expression was measured in conditioned media using an ELISA after SMCs were strained at 10% for 24 hours \*\*\* $p < 0.001$ ,  $N=3$ . Secreted OPN expression in SMCs was increased significantly by ~3 fold with cyclic strain for 24 hours.

## **Osteopontin Expression Increases with Varying Degrees of Strain, but is not Dependent on Strain Magnitude**

The cells of the aorta experience average circumferential cyclic strains that range from around 5 to 25% or more [119], depending on the physiologic state of the organism. Furthermore, these strain levels chronically change from a healthy to diseased state, and specifically in the setting of hypertension, this circumferential strain is increased [119]. For this study, we wanted to identify the effect of varying degrees of cyclic strain on the expression of OPN. We, therefore, strained SMCs at 5, 10, 15, and 20% cyclic strain for 24 hours and harvested the cells for protein and analyzed cellular OPN levels via Western blot analysis. We hypothesized that the increase in OPN would be proportional to the degree of strain that the SMCs were experiencing. We observed that OPN had a trending increase at all levels of cyclic strain, with the most significant change (~6-fold increase) observed with 10% cyclic strain for 24 hours (Fig 3.7). There was a trend towards a 2 to 4-fold increase in OPN expression observed at the other strain magnitudes of 5, 15, and 20%, but these were not statistically significant, for an N=3. These results suggest that OPN is indeed mechanosensitive and is upregulated with varying levels of cyclic strain, however, this increase is not strain magnitude dependent.

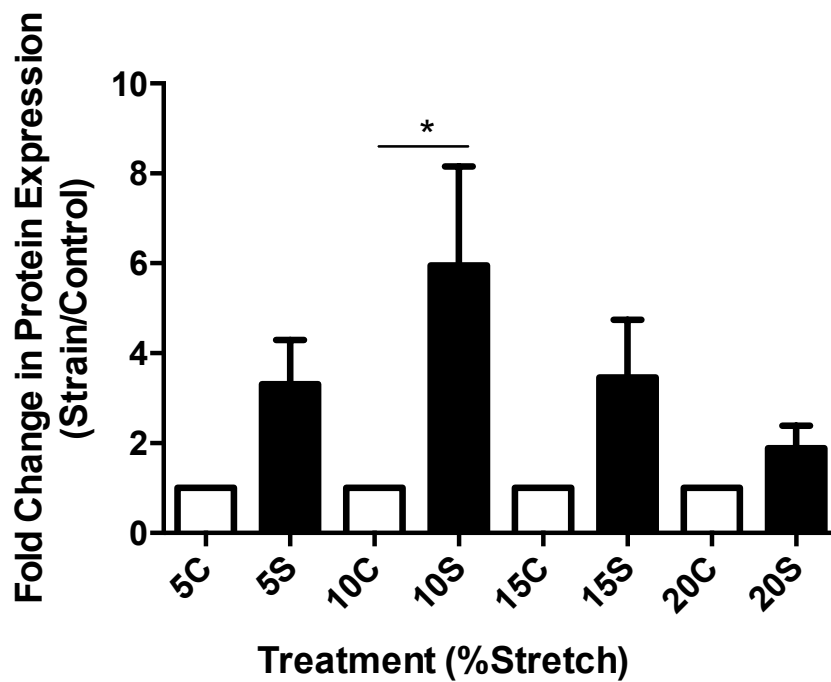
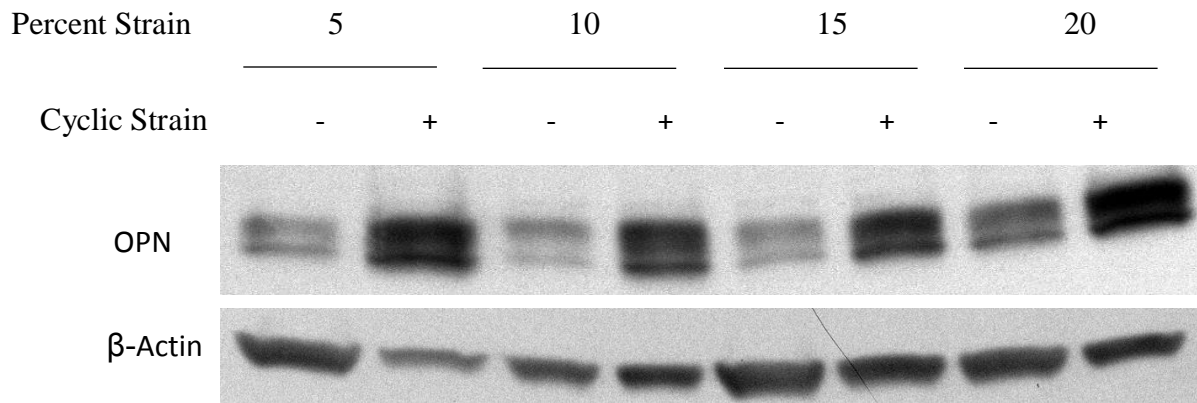


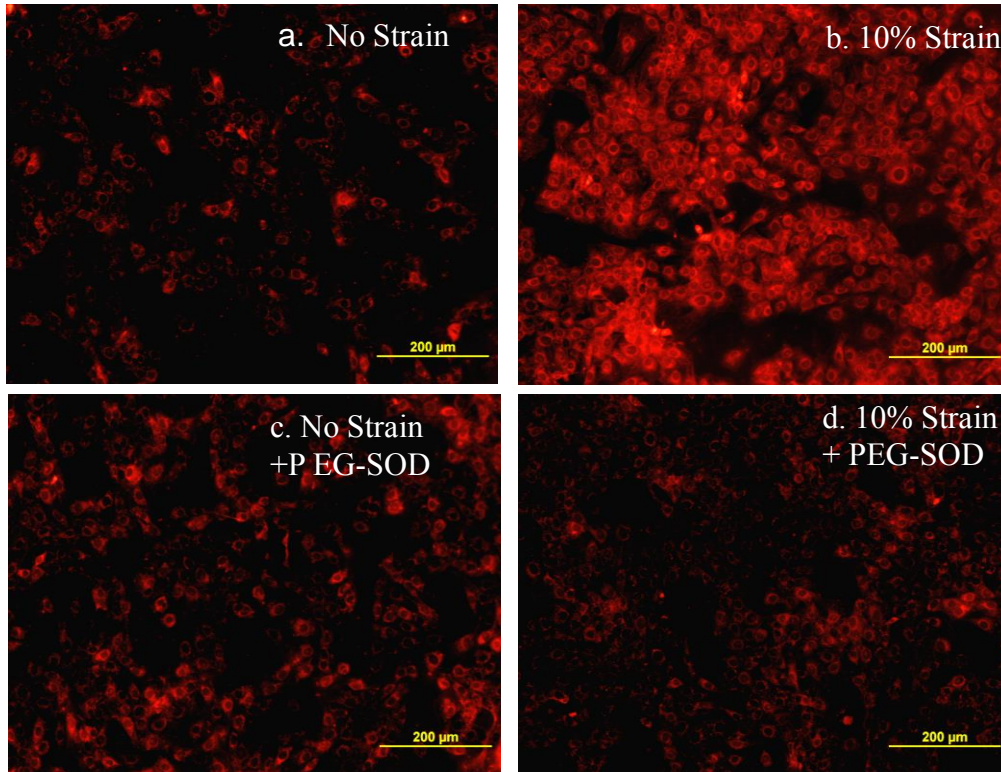
**Figure 3.7: Varying Magnitudes of Cyclic Strain Increases OPN Protein Expression** OPN protein expression was measured in SMCs via Western Blot analysis after cyclic strain at 5, 10, 15, and 20% Strain. Protein expression was quantified via protein densitometry and is represented in arbitrary units normalized to  $\beta$ -Actin expression \*\*\* $p < 0.001$ , N=3. OPN expression is observed to go up with all strain magnitudes, but most significantly at 10% strain.

## **Cyclic Strain Increases Reactive Oxygen Species (ROS) in SMC in Culture**

Several human clinical and animal studies of hypertension show compelling evidence of the role of ROS in cardiovascular disease progression [39]. ROS play an important role as second messengers and in signal transduction, especially in cardiovascular pathophysiology. In this study, we measured levels of ROS in SMCs following cyclic strain using the fluorescent hydrocyanine-3 dye. We found that cyclic strain of SMCs after 4 hours increased levels of superoxide ( $O_2^{\cdot -}$ ) compared to non-strained SMCs. Representative images from a set of three independent experiments is shown in Figure 3.8 and quantified below. Superoxide Dismutase (SOD) is an enzyme that converts the superoxide molecule into hydrogen peroxide. In order to determine if the signal observed using the hydrocyanine-3 dye was specific to increases in superoxide, we strained SMCs with Polyethylene Glycol Superoxide Dismutase (PEG-SOD) and this blunted the increased red fluorescence signal that was previously observed.

Hydrogen peroxide is an important byproduct of cellular metabolism, especially in the vasculature. When produced at high concentrations it is capable of causing DNA strand breaks, but at low concentrations it plays an important signaling role [94]. We wanted to study, whether cyclic strain also increases levels of the more stable hydrogen peroxide. The Amplex Red assay was used to measure levels of hydrogen peroxide after strain (Fig 3.9) and we observed that SMCs strained for 4 hours show a significant approximately 4-fold increase in  $H_2O_2$  levels ( $p < 0.05$ ) compared to non-strained cells. Note that this increase represents a snapshot of the  $H_2O_2$  levels after 4 hours of cyclic strain, and is not a cumulative measurement.

I



II

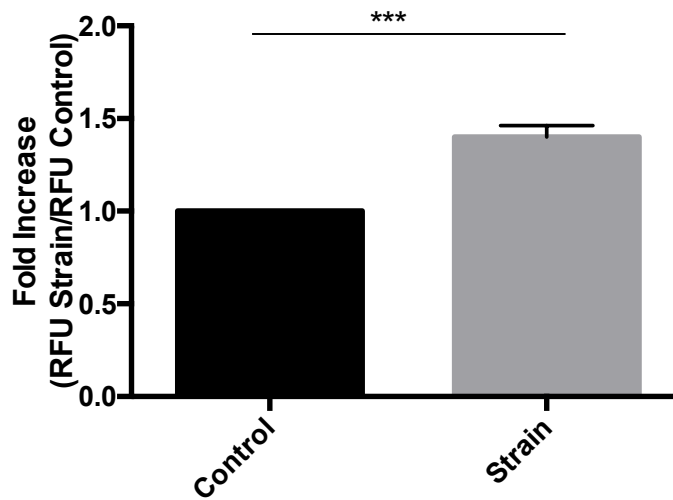


**Figure 3.8: Cyclic Strain for 4 hours Increases Superoxide ( $O_2^{\bullet-}$ )** (I) Superoxide levels were measured using the hydrocyanine-3 fluorescent dye. RASMs were strained for 4 hours prior to the addition of hydrocyanine-3 dye. Fluorescence images were then taken at 10X magnification for N=3. Representative images are shown. (I and II) An increase in superoxide levels was observed in the cells strained for 4 hours (panel b) compared to the unstrained control (panel a). Quantification in II. \*\*\*p<0.001, N=3

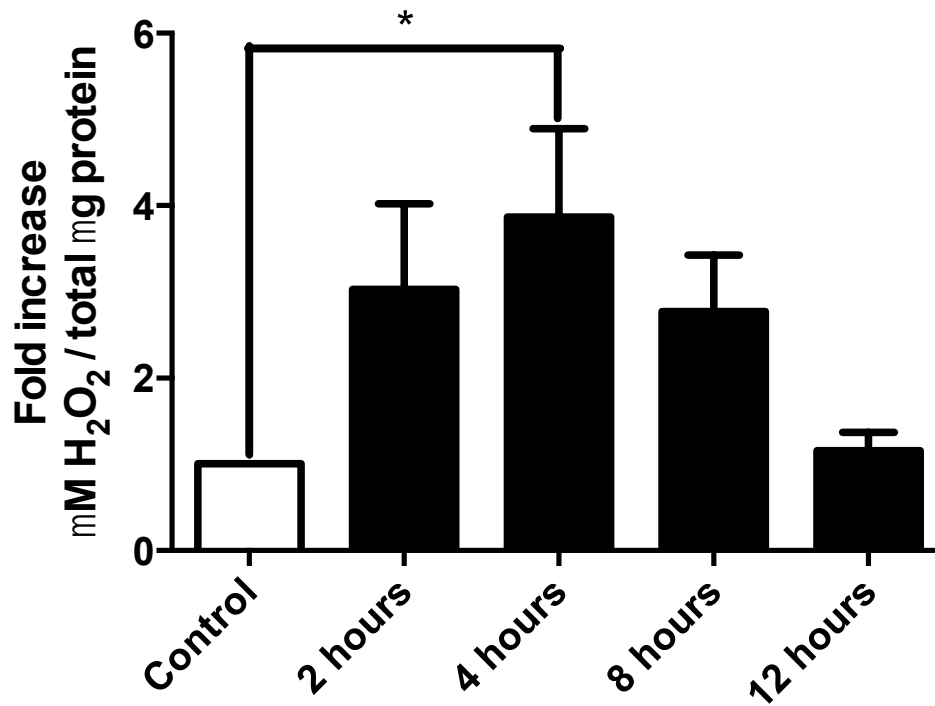


**Figure 3.9: Cyclic Strain Significantly Increases H<sub>2</sub>O<sub>2</sub>** Amplex Red Assay was used to measure levels of hydrogen peroxide. Total concentration of H<sub>2</sub>O<sub>2</sub> was normalized to total protein and the fold increase plotted against control at each time point. Control sample represents RASMs exposed to no strain for 12 hours. All other samples were obtained by straining RASMs for 2, 4, 8, and 12 hours at 10% strain. \*p<0.05 for N=4

## **NADPH oxidases play an Important Role in Mediating Cyclic Strain-induced Increase in OPN Expression in Culture**

NADPH oxidases are an important enzymatic source of ROS in SMCs, and we wanted to determine if they were upstream of cyclic strain-induced ROS and OPN expression. In this set of experiments, we used two inhibitors of NADPH oxidases – diphenyliodonium (DPI) and apocynin – while cyclically straining vascular smooth muscle cells.

DPI is used as a non-competitive inhibitor of flavoenzymes – and NADPH oxidases belong to this family of enzymes [120]. It was originally discovered to be a hypoglycemic agent that could block respiration and gluconeogenesis [120], but was later discovered to block the activity of flavoenzymes such as NADPH oxidases, nitric oxide synthases, and xanthine oxidase [120]. DPI is thought to abstract an electron from the FAD subunit which results in a radical. This then binds irreversibly to the FAD subunit of NADPH oxidases, irreversibly and rapidly blocking their activity [75, 121].

Apocynin is another non-specific NADPH oxidase inhibitor used in these studies that is believed to inhibit the assembly of the NADPH oxidase subunits. Apocynin is also known to have ROS scavenging activity [122, 123].

SMCs strained for 24 hours in the presence of DPI demonstrated a significant decrease in OPN protein expression compared to untreated, strained RASMS (Fig 3.10). Similar decreases in OPN expression were measured in the SMCs strained in the presence of apocynin (Fig 3.11). These data suggest that NADPH oxidases potentially play a role in mediating mechanical strain dependent increases in ROS and OPN. Although further studies will have to be conducted to identify which specific NADPH oxidase mediates these strain-induced increases in OPN.

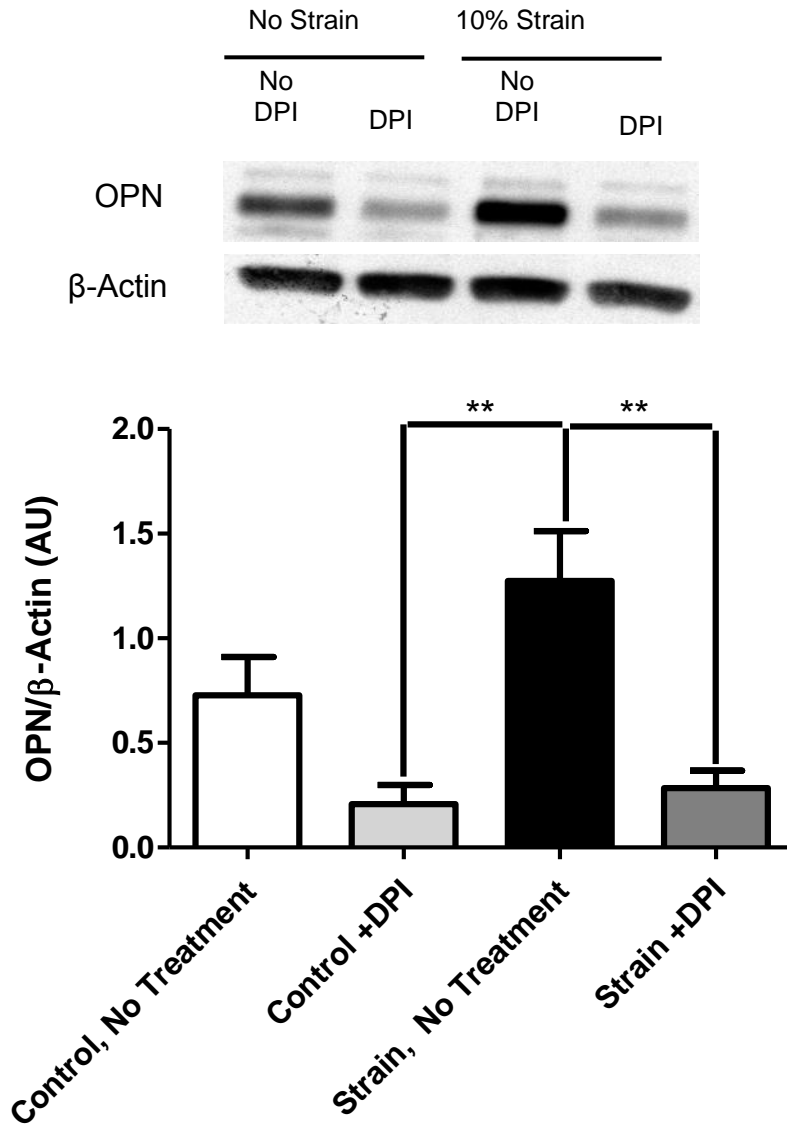


**Figure 3.10: Strain-Induced Increase in OPN Expression was Blunted in the Presence of DPI**

OPN protein levels were measured using Western Blot analysis and normalized to  $\beta$ -Actin expression. The 1<sup>st</sup> lane is the control sample obtained from RASMs not exposed to strain and DPI, 2<sup>nd</sup> lane is the sample obtained from non-strained RASMs with DPI, 3<sup>rd</sup> lane is the sample from RASMs strained for 24hrs without any DPI, and the 4<sup>th</sup> lane is sample obtained from RASMs strained for 24h in the presence of DPI. \*\* $p < 0.01$ , N = 3. We observed that strain-dependent increase in OPN was blunted in the presence of DPI.

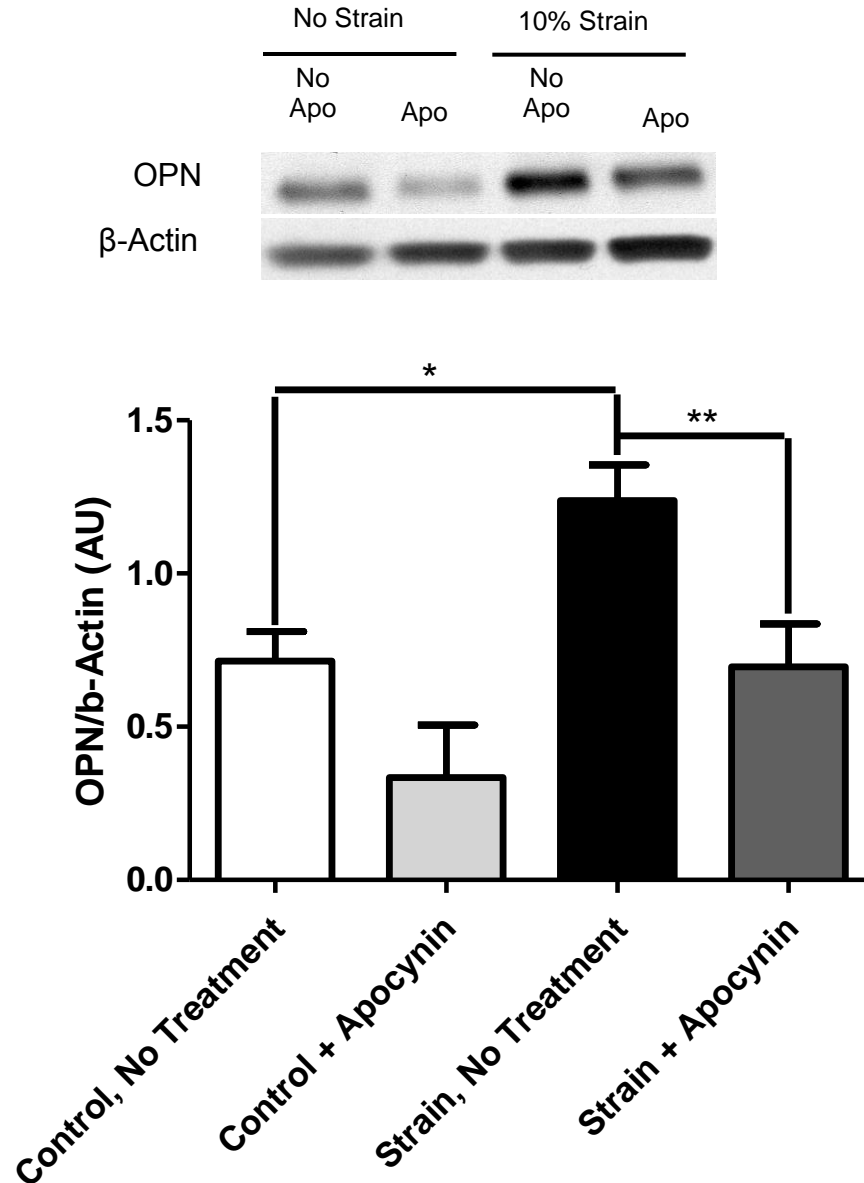


**Figure 3.11: Strain-Induced Increase in OPN Expression was Blunted in the Presence of Apocynin** OPN protein levels were measured using Western Blot analysis and normalized to  $\beta$ -Actin expression. The 1<sup>st</sup> lane is the control sample obtained from RASMs that were not exposed to cyclic strain or apocynin, 2<sup>nd</sup> lane is the sample obtained from non-strained RASMs, but exposed to apocynin only, 3<sup>rd</sup> lane is the sample from RASMs cyclically strained for 24hrs without any apocynin, and the 4<sup>th</sup> lane is the sample from RASMs cyclically strained for 24h and also exposed to apocynin. \* $p < 0.05$ , \*\* $p < 0.01$ , N = 3

## Discussion

Early *in-vitro* studies using aortic smooth muscle, in the late 1970s, by Leung et al. focused on the effect of cyclic strain on the synthesis of extra-cellular matrix proteins. It was discovered that there was a significant increase in the rate of synthesis of collagen, hyaluronate, and chondroitin 6-sulfate [124]. It was further noted in this study that the increase in ECM protein synthesis was not dependent on an increase in cell number or DNA synthesis rates [124]. Another early study looked at the effect of pulsatile stretching on the orientation of smooth muscle cells, and it was observed that more than 75% of the cells reoriented themselves within 45 degrees of a line at a right angle in the direction of stretch [125]. Finally, Lundberg et al highlighted that mechanical strain impacts cell proliferation and that this was dependent on the ECM composition and origin of the SMC [126]. These early studies highlight the physical behavior of smooth muscle cells and their impact on ECM in response to stretch. However, the specific contribution of elevated cyclic strain in accelerating the process of arterial inflammation has not been adequately explored, and the basic underlying molecular mechanisms leading to hypertension associated vascular complications still remain largely unknown.

Therefore, the primary objective of this aim was to use an *in-vitro* system to study the impact of cyclic mechanical strain on the expression of the potent pro-inflammatory protein, osteopontin (OPN), and its regulation in aortic smooth muscle cells. Our hypothesis was that cyclic strain would elevate OPN expression and that this would occur via a redox sensitive pathway. To our knowledge, the results of these studies provide first evidence that

- 1) OPN is upregulated with cyclic mechanical strain in cultured vascular smooth muscle cells as we observed significant increases in OPN mRNA, cellular protein, and secreted protein (Fig 3.4-3.6).

- 2) this upregulation of OPN protein was maximal at 10% Strain (Fig 3.7), and that,
- 3) cyclic strain-induced OPN is potentially mediated by NADPH oxidases – the primary enzymatic source of ROS in the vasculature (Fig 3.10-3.11). However, the specific NADPH oxidase regulating this process, still remains to be determined.

Indeed, many of our results are corroborated by other studies from our group and other researchers who focus on the strain-dependent regulation of proteins involved in vascular remodeling and inflammation in arteries. For example, in one study by Grote et al., cyclic strain was shown to impact proteins involved in vascular remodeling such as matrix metalloproteinases (MMPs), that are responsible for the breakdown of the vascular ECM scaffold [79]. This study also went onto prove that cyclic strain of SMCs increased release of the proenzyme and mRNA expression of MMP-2, and that this was mediated by NADPH oxidase-derived ROS [79]. Our results implicate a role for NADPH oxidases in mediating increases in cyclic strain-induced OPN.

Our results from aim 1 also validate previous findings that highlight that the cyclic nature of the mechanical stimulus is critical in observing these changes. Studies from our groups and others have shown previously that a significant increase in hydrogen peroxide is observed only in the setting where cyclic strain (1Hz, 20% strain) was applied to aortic endothelial cells [4, 127]. In cells that were exposed to a static strain (only 20% strain) no increase in hydrogen peroxide was observed [4]. These observations, therefore, prompted us to conduct our experiments in aim 1 using cyclic and not static strain.

We also observe increased levels of both superoxide and hydrogen peroxide with cyclic strain (Fig 3.8 and 3.9) and these are supported by several studies in literature. Some *in-vitro* and *ex-vivo* studies have shown that a cyclic strain of 10% and 20% stimulate an increase in superoxide [127-129], however, strain magnitudes of 5% and 6% fail to do so [127-129]. These results suggest

that a minimum threshold strain magnitude *maybe* necessary for the active production of ROS in these cells. Our experiments were conducted at a strain magnitude of 10%, and we do see significant increases in ROS as early as 4 hours, and hence these findings are in line with previous studies as described in literature. Our results from the strain dependent experiments also show that there is a maximal increase of OPN at 10% strain, but a lower increase at the higher strain magnitudes (15% and 20%). We speculate that this lower OPN expression at higher strain magnitudes, may imply a maladaptive response of aortic SMCs as they experience higher strain magnitudes.

With regard to the regulation of OPN, studies by Lyle et al. have demonstrated that OPN mRNA and OPN protein (both cellular and secreted) expression are increased in the presence of hydrogen peroxide in cultured SMCs [7]. We observe in this aim that ROS (such as hydrogen peroxide and superoxide) are increased with cyclic strain. We further note that inhibiting NADPH oxidases, a major source of these ROS, reduces OPN expression. These results together, therefore, strongly suggest that cyclic strain-dependent increase in OPN is redox-sensitive, and further validate the observations made by Lyle et al [7].

As for the time course of the increase in OPN in our studies, it was interesting to note that both OPN mRNA and protein expression were upregulated only at the 24-hour time point (Fig 3.5). On the other hand, ROS levels (both superoxide and hydrogen peroxide) were increased at the earlier 4-hour time point (Fig 3.8 and 3.9). This suggests that there may be a delay in OPN transcription, in response to cyclic strain. Studies on the direct effects of hydrogen peroxide on OPN expression, have in fact shown that there are late (18h) transcriptional increases in OPN protein expression, regulated by the binding of the redox sensitive transcription factors AP-1 and NF- $\kappa$ B, to the OPN promoter region, in response to hydrogen peroxide treatment [7]. These results

validate our observations, and provide a possible explanation for the delayed increase of OPN protein expression in response to cyclic strain, despite the early increase in hydrogen peroxide.

Finally, it has been documented that AngII, a critical mediator of vasoconstriction and blood pressure, upregulates OPN expression in SMCs [130]. AngII is well documented to increase levels of NADPH oxidase-derived ROS [45], and therefore, these ROS maybe the potential mediators by which AngII-dependent increase in OPN occurs as well, which further supports the findings of this study.

As for some of the limitations and assumptions made in this study, a major assumption made for the purpose of this study, was that the applied mechanical strain is equal to the actual mechanical strain experienced by the cells. This assumption, however, is not entirely true as noted by the results of a finite element analysis (FEA) of the strain profiles of these flexible membranes [131]. The FEA simulations suggest that the regions of the membrane located off the loading post experience large radial strains and small circumferential strains, while the regions located directly above the loading post experience equal, but large radial and circumferential strains (see Fig 3.2). This potential inconsistency in the biaxial strain experienced by all cells within the Flexercell device, may explain why we fail to see a strain dose-dependent change in OPN expression as observed in Figure 3.7. In future experiments, separating cells from the regions located off the post from those located directly above the post, may give us clearer answers on the effect of cyclic strain on OPN expression.

Overall the results of this aim support the following conclusions:

- 1) that OPN is indeed a mechanosensitive protein whose expression is upregulated with cyclic strain in vascular smooth muscle cells, independent of strain magnitude, and that

- 2) the strain-dependent increase in OPN is mediated by NADPH-oxidases and potentially by ROS, although future studies are needed to further clarify the specific NADPH oxidase(s) and specific ROS that mediate this increase.

Our *in-vitro* results provide a novel mechanism for the strain-dependent regulation of OPN and a potential target to consider while designing therapeutics to address the severe cardiovascular disease pathologies that arise as a result of hypertension, where cyclic mechanical forces are chronically dysregulated.

**CHAPTER 4:**  
**HYPERTENSION UPREGULATES OSTEOPONTIN VIA A H<sub>2</sub>O<sub>2</sub> DEPENDENT  
MECHANISM**

*SPECIFIC AIM 2:*

*To determine if osteopontin expression is increased in a murine model of hypertension and if this increase is H<sub>2</sub>O<sub>2</sub>-dependent*

**Introduction**

Hypertension has been recognized as a major risk factor for several inflammatory diseases of the cardiovascular system such as atherosclerosis, myocardial infarctions (MI), and strokes [2, 24, 25]. Uncontrolled hypertension leads to alterations in the aorta including oxidative stress, significant increases in inflammatory chemokines [132] infiltrating leukocytes and macrophages, and changes in extra-cellular matrix (ECM) components such as elastin and collagen [133], all leading up to hypertrophy and aortic adaptive or maladaptive remodeling.

Oxidative stress has been inextricably linked to inflammation of the aorta. ROS have been shown to have pathological effects on a wide range of biomolecules, as well as modulate transcription factors and redox-sensitive signal transduction pathways [134]. AngII and mechanical stress are stimuli known to rapidly increase ROS levels by promoting the assembly of NADPH oxidase enzymes [88]. Hypertension induces long term exposure of the vasculature to these stimuli, which then results in the upregulation and increased activation of NADPH oxidase (NOX), and ultimately sustained increases in ROS levels [88]. These in turn activate signaling pathways that include c-Jun N-terminal kinase (JNK), mitogen-activated protein kinase (MAPK), and redox-sensitive transcription factors such as AP-1 and NF- $\kappa$ b [135-137]. NF- $\kappa$ b is known to serve as a transcription factor for several cytokines and adhesion molecules such as VCAM-1,

ICAM-1, and E-selectin [7, 138, 139]. These events lead to the activation and infiltration of inflammatory cells including leukocytes, macrophages, and monocytes. These cells in turn produce more ROS which leads to a self-perpetuating cycle of oxidative stress and inflammation which in turn results in the remodeling of the arterial wall and its potential degeneration.

Osteopontin (OPN) has recently emerged as a key factor in the progression of atherosclerosis and vascular wall remodeling [115]. Studies have shown that OPN promotes adhesion and migration of macrophages [140] and SMC proliferation [141]. Elevated OPN mRNA has been identified in human atherosclerotic lesions within the carotid, coronary, and aorta [5, 115, 142, 143]. Finally, mice overexpressing OPN show an increase in medial thickness and neointimal formation after arterial balloon injury [110].

In addition to these studies and our results from Aim 1 that show an increase in osteopontin (OPN) with cyclic strain *in-vitro*, we were strongly motivated to investigate whether OPN was increased in the aorta with the onset of hypertension. We wanted to further identify if this increase in OPN was mechanistically linked to the more stable ROS, hydrogen-peroxide. We used two well established models of murine hypertension that involved continuous infusion of the vasoactive factors –AngII and NE. We further utilized a genetic murine model that overexpresses catalase specifically in vascular smooth muscle cells (SMCs) in order to test the role of hydrogen peroxide in regulating OPN expression. This SMC-specific catalase overexpression mouse model was developed and well characterized by our laboratory previously [81].

## Methods

### Animals

Eight to ten week old male C57BL/6 mice were purchased from Jackson Laboratories (Bar Harbor, ME). Transgenic mice with smooth muscle cell (SMC)-specific catalase overexpression ( $Tg^{SMC-Cat}$ ) were bred in-house in the Department of Animal Resources at Emory University.  $Tg^{SMC-Cat}$  mice have elevated expression of human catalase through the SMC-specific smooth muscle myosin heavy chain promoter and were characterized previously [144]. For all experiments, eight to ten week old  $Tg^{SMC-Cat}$  were compared with WT littermates. It is important to note that these  $Tg^{SMC-Cat}$  mice are on a C57BL/6 background. The animals were housed and cared for according to the guidelines approved by the Emory University Institutional Animal Care and Use Committee (IACUC).

### Osmotic Minipump Implantation

Mice were anesthetized using 1% isoflurane (oxygen delivered at 0.5L/min with 2% isoflurane for induction and 1% isoflurane for maintenance). Ang-II (Sigma Aldrich, A6402) at a dose of 0.75mg/kg/day or NE (Sigma Aldrich, A9512) at 5.6mg/kg/day were infused via a primed mini-osmotic pump (Alzet mini-osmotic pump, Model 2004). The pumps were inserted subcutaneously, on the back. Following surgery, mice were administered buprenorphine (1mg/kg, SC), once on the day of surgery, and then as needed.

## **Measurement of Systolic Blood Pressure**

Mice were first acclimatized to the tail-cuff plethysmograph (Visitech© Corporation) for at least three consecutive days. Systolic blood pressure was then measured prior to and after infusion of AngII or NE.

## **Immunohistochemistry**

Mice were euthanized by slow CO<sub>2</sub> inhalation and tissues were perfused with saline and fixed with 10% buffered formalin. Whole aortas were excised, paraffin embedded, and cut into 5 µm sections. Enzyme treatment was performed for antigen retrieval using protease K 10ug/ml for 30 minutes, before incubation with OPN antibody (1:100 in 5% BSA, R&D), followed by incubation with anti-goat secondary antibody (1:400 in 5% BSA; Vector Labs) and incubation with streptavidin QDot 655 (1:200 in 5% BSA; Invitrogen). Images were acquired from a Zeiss Axioskope microscope equipped with an AxioCam camera.

## **Protein Analysis**

Mice were euthanized by slow CO<sub>2</sub> inhalation. Aortas were rapidly cleared of excessive perivascular fat and snap frozen in liquid nitrogen and stored at minus 80°C until further processing. Aortas were homogenized on ice using 500-1000uL of Hunter's Buffer. The homogenized samples were then centrifuged at 4°C and the resulting supernatant used. Total protein quantification was first performed via the Bradford assay using a BSA Standard Curve. The protein supernatant was then boiled after the addition of a 1X Laemmli's buffer and β-mercaptoethanol. 10-20 µg of total protein from each sample was then loaded onto a precast 10%

polyacrylamide gel and allowed to run in an electrophoresis chamber at 200V for approximately an hour. The separated proteins were transferred onto a nitrocellulose membrane at 100V for 2 hours at 4°C. The nitrocellulose membrane was blocked for 1 hour at room temperature in 5% milk (Biorad) prepared with a solution of 1% TBS/0.1% Tween (TBST). The membrane was then incubated with OPN primary antibody used at a dilution of 1:500 (R&D systems). Secondary antibody (donkey anti-goat, Biorad) was used at a dilution of 1:2000. Both primary and secondary antibodies were diluted in 5% milk (Biorad) prepared with a solution TBST. The membranes were washed 3 times for 10 minutes between primary and secondary incubations using TBST and finally incubated with chemiluminescent detection reagent (Amersham ECL). Kodak Scientific Imaging Film was then exposed to the processed membrane for around 30 seconds to 2 minutes in a dark room. The developed film was scanned and analyzed by densitometry analysis for OPN protein expression and normalized to the housekeeping protein  $\beta$ -Actin. The primary  $\beta$ -Actin antibody for normalizing the OPN protein data was used at a dilution of 1:2000 and was obtained from Cell Signaling. The secondary antibody used was anti-Rabbit at a 1:2000 dilution as well, and obtained from Biorad.

### **RNA Isolation and Quantitative Real-time Polymerase Chain Reaction**

RNA was extracted from aortas that were snap frozen using the RNEasy kit from Qiagen, Valencia, CA, and according to protocol. RNA levels from each sample was quantified using absorbance values at 260nm obtained using a benchtop spectrophotometer. cDNA was first prepared from the obtained aortic mRNA using Superscript III reverse transcriptase following a well-established protocol. cDNA was purified using Qiagen PCR purification minispin columns. OPN mRNA levels were measured by amplification of cDNA using an Applied Biosystems

thermocycler with primers specific for mouse OPN (QuantiTect Primers, Qiagen, and SYBR green dye. Copy numbers were calculated by the instrument software from standard curves of genuine templates. Standards were previously made by amplifying murine aortic OPN PCR products and calculating the copy number based on the concentration and amplicon length of the OPN gene. OPN copy numbers were normalized per million copies of the housekeeping gene 18s.

### **Statistics**

All results are presented as mean  $\pm$  SEM and analyzed using ANOVA or t-test using GraphPad <sup>TM</sup> Prism Software (GraphPad Prism), followed by Bonferroni or Tukey multiple comparisons test. A p-value  $< 0.05$  was considered significant.

## Results

### **Angiotensin-II (AngII) and Norepinephrine (NE) Increase Systolic Blood Pressure**

We used two distinct vasoactive agents to induce hypertension in C57BL/6 mice – AngII and NE. We used mini-osmotic pumps to continuously infuse AngII (0.75mg/kg/day) or NE (5.6mg/kg/day) for seven days. This time point was used as it captures the earliest stages of aortic inflammation and remodeling with hypertension [81, 133].

We measured systolic blood pressure (SBP) in these mice using tail-cuff plethysmography prior to and after infusion of AngII or NE and this is shown in Figure 4.1. We observed a significant increase in SBP in mice treated with either AngII or NE. AngII treated mice had a mean SBP of  $169 \pm 4$  mmHg, with a 51% increase over untreated wild-type controls (WT) controls. Similarly, NE treated mice had a mean SBP of  $149 \pm 4$  mmHg, and a 32% increase in SBP compared to WT mice. Interestingly, we noticed a much more significant increase in systolic blood pressure with AngII infusion compared with NE infusion.

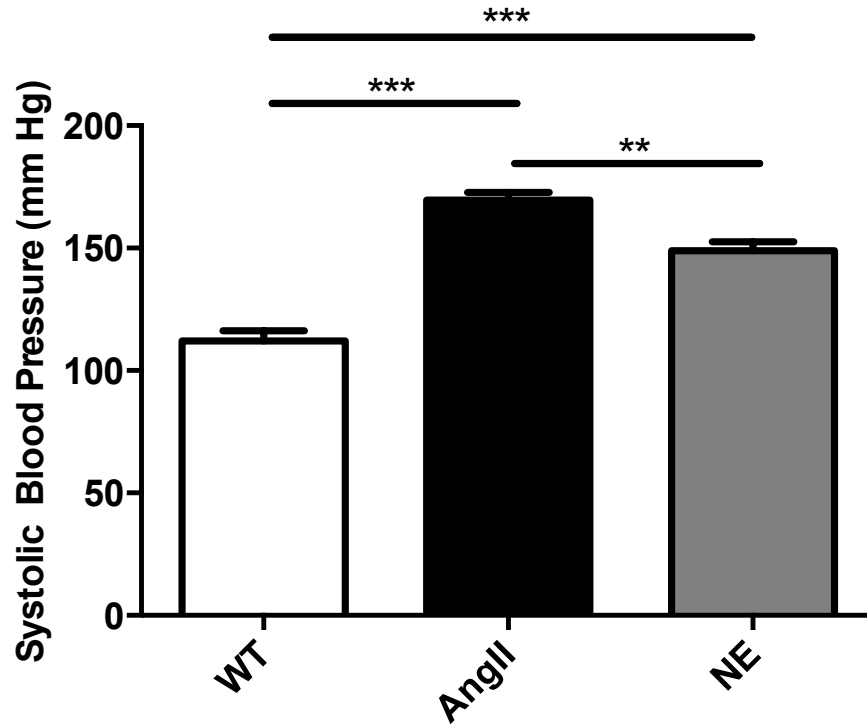


**Figure 4.1: Continuous Infusion of AngII or NE for 7 days Significantly Increase Systolic Blood Pressure** There was approximately a 51% and 32% increase in systolic blood pressure with Angiotensin-II (AngII) and Norepinephrine (NE) infusion respectively. \*\* $p < 0.01$ , \*\*\* $p < 0.001$ ,  $N = 6$ .

## **Angiotensin-II (AngII) and Norepinephrine (NE) Increase Osteopontin (OPN) mRNA and Protein Expression in Whole Aortas**

Following 7 days of treatment with AngII or NE and measurement of systolic blood pressure, whole aortas (including both thoracic and abdominal regions) were excised and cleared of excessive perivascular adipose tissue. We first measured OPN mRNA levels in these aortas using quantitative real-time polymerase chain reaction (qRT-PCR). We observed a significant increase in OPN mRNA levels in aortas from animals treated with AngII (approximately 8-fold increase) and a trending increase with NE treatment (around 1.6-fold increase) compared to their WT controls as seen in Figure 4.2. Furthermore, AngII treated aortas expressed almost a 2.2-fold higher level of OPN mRNA expression compared with NE treated mice, suggesting that AngII may play an even more potent role in eliciting an inflammatory response within the vasculature as compared with NE. Interestingly, this increase in OPN mRNA expression with AngII treatment follows the same trend as observed with the increase in SBP in AngII treated mice (see Fig 4.1), further suggesting a possible synergy between elevated mechanical wall strain due to hypertension and AngII alone, although this remains to be further explored.

Analysis of OPN protein in aortic tissues was analyzed via Western blotting and results are shown in Figures 4.3 and 4.4. It was revealed that OPN protein expression was significantly increased in the AngII treated mice and NE treated mice.

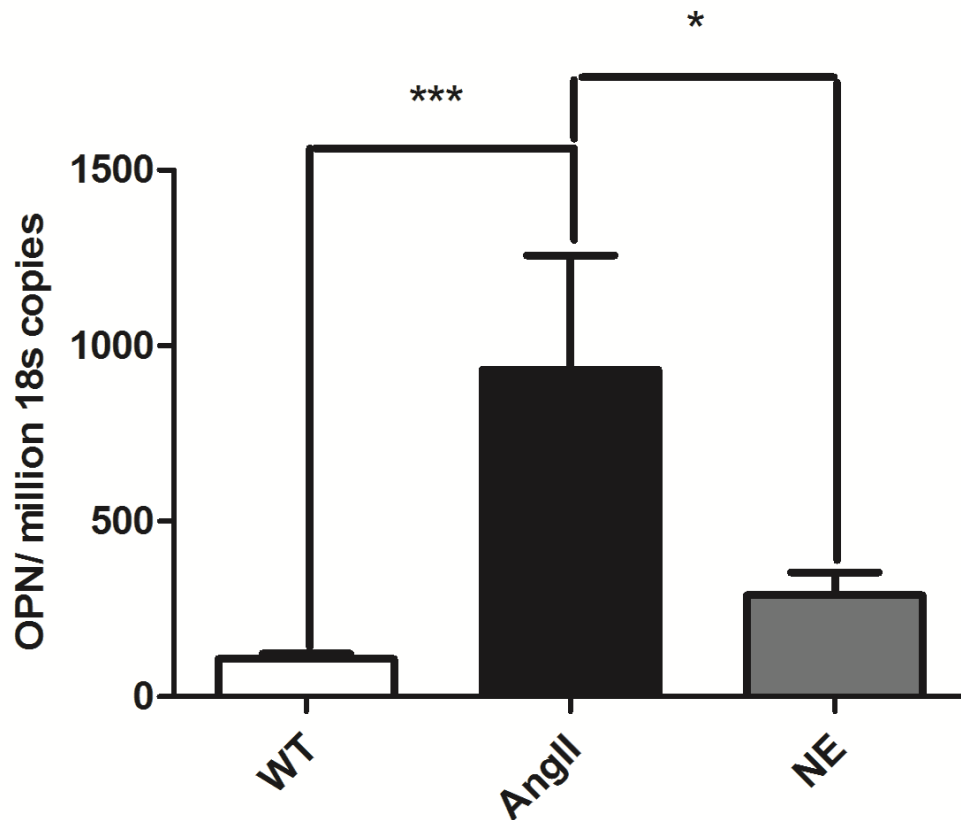


**Figure 4.2: OPN mRNA expression is upregulated in aortas of mice treated with AngII for 7 days** Real time PCR quantification of OPN mRNA, followed by normalization with a million copies of the 18s housekeeping gene was performed on samples from aortas obtained from mice infused for 7 days with AngII and NE. OPN expression is upregulated from baseline in both AngII and NE treated groups, but there is statistically significant differences only in the AngII treated group. AngII treated aortas have significantly higher OPN mRNA compared with NE treated aortas too. \*\*\* $p < 0.001$ , \* $p < 0.05$ , WT=25, AngII=12, NE=11.

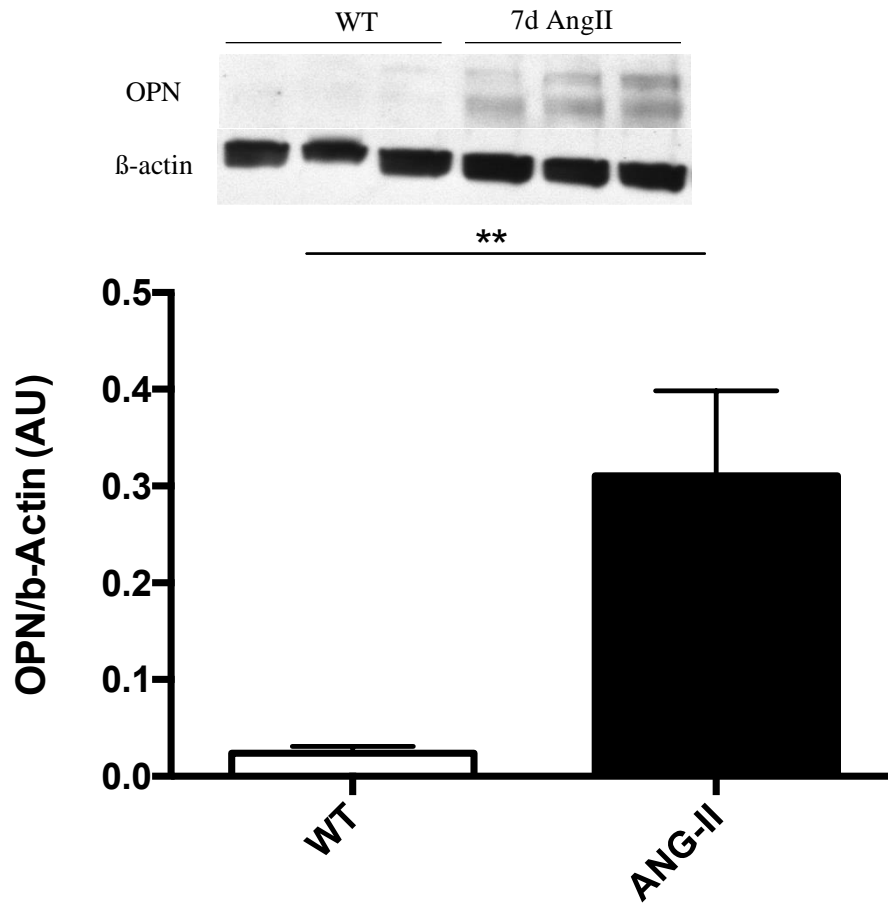


**Figure 4.3: 7 day AngII Infusion Increases OPN Protein Expression in the Aorta** OPN protein expression in the aorta of mice was measured following 7 days of both AngII infusion using Western Blot Analysis. A significant increase in OPN protein expression was observed in AngII treated mice compared with the non-treated control, WT mice. \*\*p<0.01, N=3.

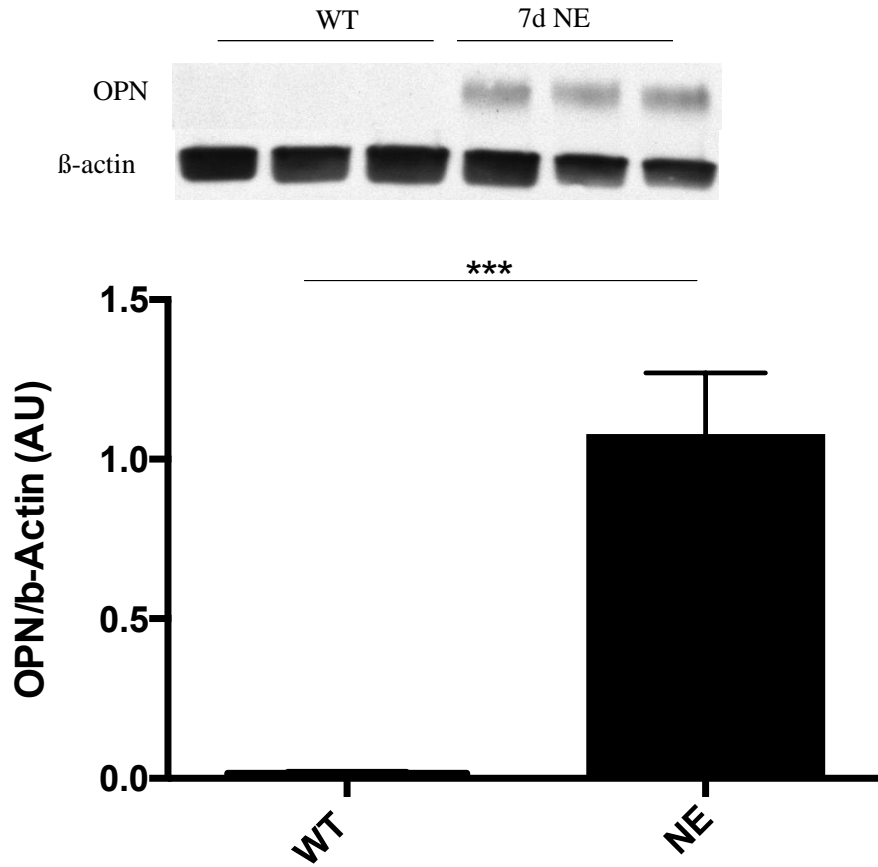


**Figure 4.4: 7 day NE Infusion Increases OPN Protein Expression in the Aorta** OPN protein expression in the aorta of mice was measured following 7 days of both NE infusion using Western Blot Analysis. A significant increase in OPN protein expression was observed in NE treated mice compared with the non-treated control, WT mice. \*\*\*p<0.001, N=3.

## **Osteopontin (OPN) Protein Expression is Primarily localized to the Medial Layer with Hypertension**

Motivated by the differences observed in both OPN mRNA using RT-PCR (Fig 4.2) and protein observed using Western Blot analysis (Figs 4.3-4.4), we used immunohistochemistry, to identify differences in the expression pattern and localization of OPN with both AngII and NE treatment. First, it was observed that OPN expression is almost entirely absent in WT, healthy baseline aortas, as very little to almost no red fluorescence intensity (specific to OPN protein) was observed (Fig 4.5, panel a). Secondly, we observe that both AngII and NE treatment induce a dramatic increase in OPN expression (Fig 4.5, panels b and c). Third, we observe that medial thickness is increased and OPN expression appears to be much higher in the AngII treated aortas (Fig 4.5, panel b) compared with NE treated aortas (Fig 4.5, panel c), once again suggesting the more potent role that AngII plays in mediating both the SBP and inflammatory responses of the aortic wall. Finally, we observe that OPN expression is primarily localized to the medial layer of the aorta – suggesting that the primary site of expression of OPN was from the smooth muscle cells of the media (Fig 4.5). The medial layer of the aorta is primarily responsible for withstanding and responding to the cyclic mechanical strain associated with blood flow due to systole and diastole, and hence it is not surprising to observe that with elevated blood pressure, the SMCs of the medial layer respond by upregulating the expression of OPN protein, which could ultimately lead to the adaptive or maladaptive remodeling of the vessel wall. Differences in medial thickness with AngII treated are further evaluated and quantified in Aim 3.

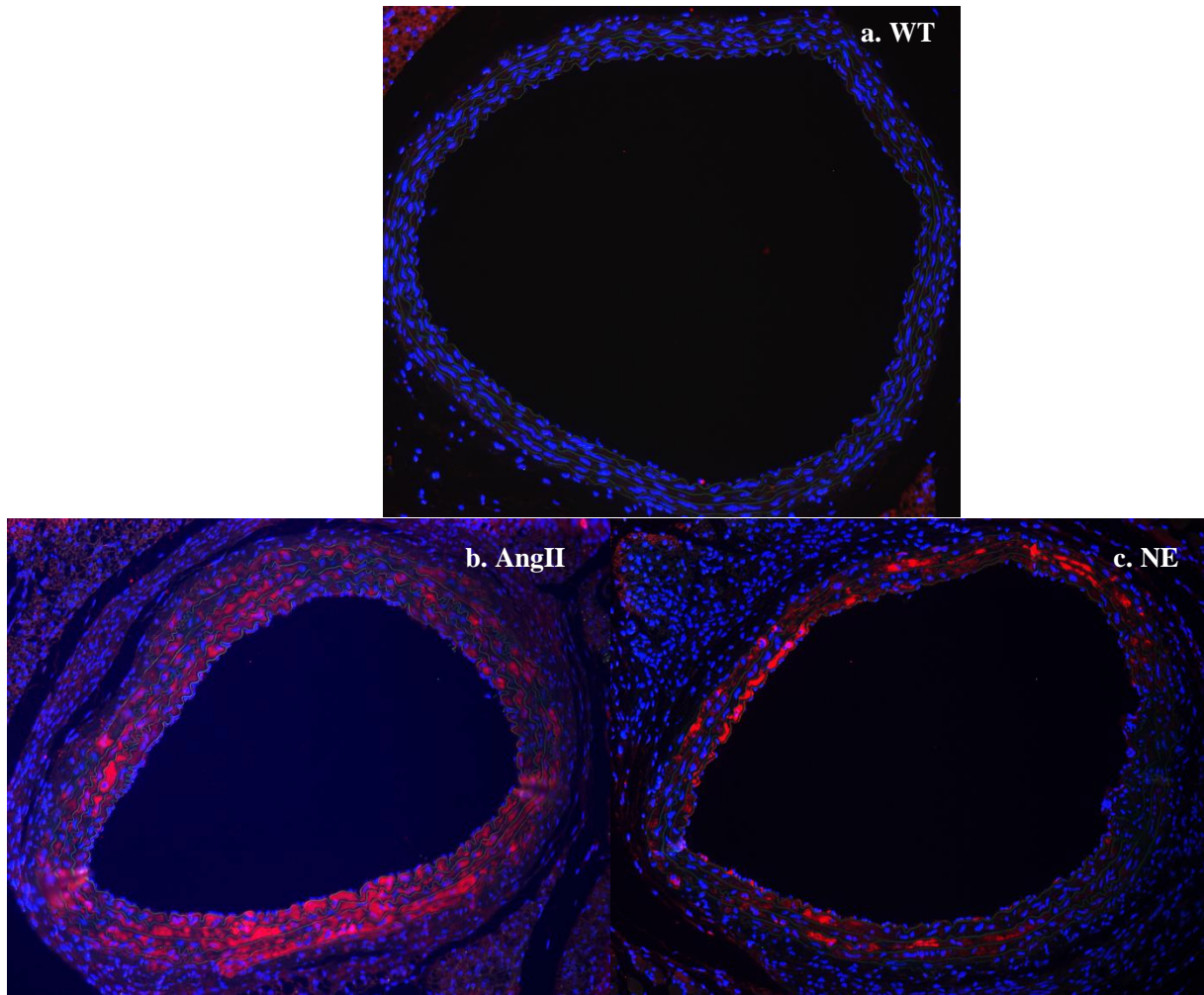


**Figure 4.5: OPN expression was Increased with Hypertension and Localized Primarily to the Media** OPN expression in SMCs of the aorta in mice after 7-day AngII and NE infusion compared to WT control as measured by immunohistochemistry. **RED=OPN**, **BLUE=DAPI**. Representative images are shown and were taken at 10X for an N=4

## **Hydrogen Peroxide Scavenging Mediated by Catalase Blunts Increased OPN expression with Hypertension in Murine Aortas**

So far we have investigated the differences in OPN expression in wild-type (WT) baseline and hypertensive aortas. We next wanted to determine if catalase-mediated scavenging of H<sub>2</sub>O<sub>2</sub> produced specifically in vascular smooth muscle cells protects the aorta against this hypertension related increase in pro-inflammatory OPN expression. Hence, we treated transgenic mice with smooth muscle cell (SMC)-specific catalase overexpressing (Tg<sup>SMC-Cat</sup>) and WT animals with AngII or NE for 7 days. We observed a significant increase in blood pressure in both strains of mice with both treatments (Fig 4.6). This result indicated that blood pressure was not affected at baseline with overexpression of catalase, but with hypertensive stimuli such as AngII and NE, blood pressure was increased similarly in these Tg<sup>SMC-Cat</sup>, just as is observed in WT mice.

Finally, we measured OPN protein levels using Western Blot analysis in these aortas at 7 days post infusion with AngII or NE. We observed that there was a significant increase in OPN expression in the WT mice with either AngII or NE expression (Fig 4.7) as was already previously seen (Figs 4.3-4.5), but there was a dramatic blunting of OPN expression in the aortas of the catalase overexpressing (Tg<sup>SMC-Cat</sup>) mice (Fig 4.7). Our results show that reducing H<sub>2</sub>O<sub>2</sub> production in the medial layer of the aorta imparts a protective environment against the inflammatory increase in OPN expression. This result is further supported by other studies from our group that have shown protection of the aorta against the inflammatory effects of hypertension. For example, transgenic catalase overexpressing mice have been shown to be protected against vascular hypertrophy with hypertension induced by 14 days of AngII infusion [81]. Furthermore, it has been shown that both pharmacologic infusion and genetic overexpression of catalase protected aortas against aneurysmal formation [145].

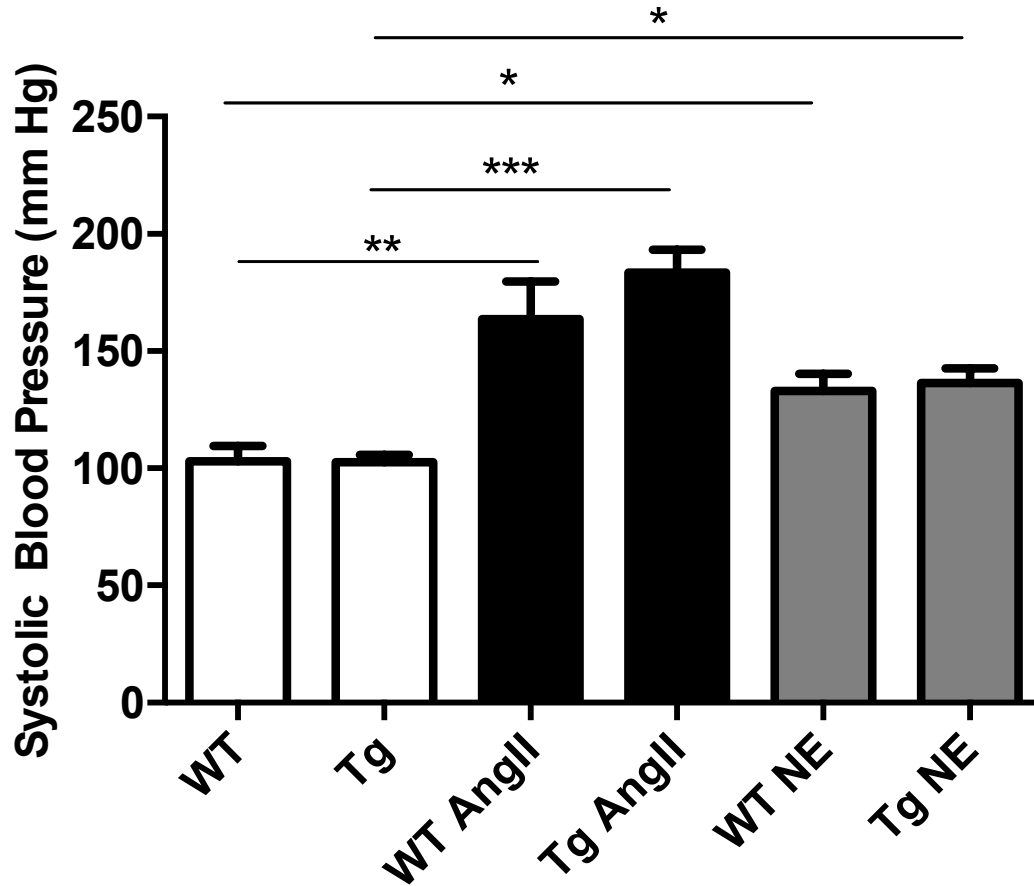


**Figure 4.6: Systolic Blood Pressure is Increased in both WT and Transgenic Catalase Overexpressing Mice in both models of hypertension** Systolic blood pressure was measured in catalase overexpressing and wild type (WT) mice at baseline and following 7 days of AngII or NE infusion using tail-cuff plethysmography N=3-4, \*p<0.05, \*\*p<0.01, and \*\*\*p<0.001.

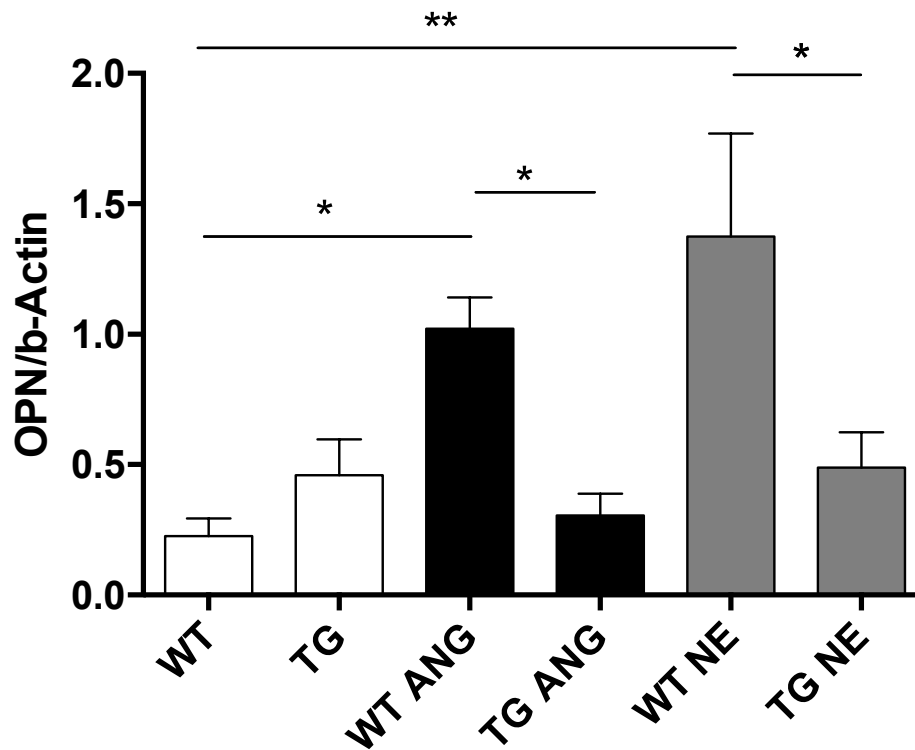
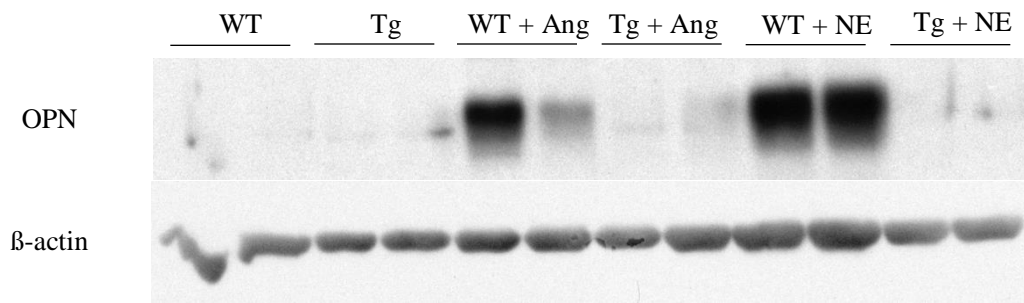


**Figure 4.7: Hypertensive Smooth Muscle Cell Catalase overexpressing mice ( $Tg^{SMC-Cat}$ ) showed attenuated OPN levels** OPN protein was measured using Western Blot analysis in aortas from WT and  $Tg^{SMC-Cat}$  mice made hypertensive using 7-day AngII and NE infusion for N=6-8. Representative blot shown. \*p<0.05, \*\*p<0.01.

## Discussion

For this aim, we used two murine models of hypertension and an existing strain of mice that overexpress catalase specifically within vascular smooth muscle cells. We hypothesized that increased oxidative stress, specifically related to increased hydrogen peroxide, led to aortic inflammation by upregulation of the pro-inflammatory protein, osteopontin (OPN). We tested this hypothesis by analyzing levels of OPN mRNA and protein at baseline and with hypertension. We also histologically analyzed expression of OPN within the aorta after inducing hypertension. Finally, we measured OPN protein expression with hypertension utilizing the transgenic catalase overexpressing mice (Tg<sup>SMC-Cat</sup>). Overall the results of this aim demonstrate that H<sub>2</sub>O<sub>2</sub> indeed alters inflammation of the aorta by regulating the expression of OPN in the setting of hypertension. Specifically, we have shown that:

- a) hypertension-related stimuli (whether humoral or mechanical) can lead to a direct increase in pro-inflammatory protein expression
- b) the medial layer of arteries plays an important role in sensing and responding to changes in the mechanical milieu, especially in relation to hypertension
- c) catalase which is an antioxidant against H<sub>2</sub>O<sub>2</sub>, plays a pivotal role in protecting arteries against pro-inflammatory stimuli in response to hypertension

It has been shown that OPN levels are increased in blood plasma of hypertensive human subjects [146]. Early studies exploring the role of OPN in the vasculature have shown that it plays an important role in accelerating AngII-dependent atherosclerosis and aneurysm formation [146]. OPN was further proven to play an important role in mediating the recruitment of macrophages to the arterial wall in the setting of AngII-mediated inflammation in the aorta [146]. Isoda et al have also shown that overexpression of OPN in the vasculature is related to a significant increase in

medial thickening with aging and neointimal formation with arterial injury [110]. However, the mechanism by which hypertension is related to OPN is still unknown.

Our results from Chapter 3 suggest that mechanical strain indeed leads to an increase in OPN expression *in-vitro*. We also show in this aim that OPN is upregulated in the aorta through the use of two independent humoral factors (namely AngII and NE) and that both cause an increase in blood pressure (Fig 4.2-4.5). This suggests that elevated vascular wall strain due to hypertension *may* in fact be the common stimulus responsible for increased OPN and ultimately the progression of inflammation in the aorta. However, delineating the independent effects of humoral versus mechanical factors on inflammation in the aorta with hypertension are impossible to clarify using an animal model alone, and call for further *in-vitro* and *in-vivo* studies, or a combination thereof.

Some of the other models of hypertension that maybe utilized in future studies to further clarify the role of humoral and mechanical factors in regulating OPN expression. The aortic coarctation model used by Ollerenshaw et al involved the creation of an aortic stenosis of constant diameter by the tying of a silk ligature between the origins of the two renal arteries [57]. This coarctation induced a region of high blood pressure above the coarctation and normal blood pressure, below [57]. Some of the results of this study have already shown that there was a significant increase in the medial thickness of the aorta above the coarctation at 9 and 20 days post procedure [57]. Analysis of OPN expression above and below the coarctation would provide a better understanding on the specific role of elevated mechanical strain on OPN expression.

The two-kidney, one-clip model of hypertension developed by Goldblatt et al. is another model that maybe used to study the effects of a gradual and chronic increase in blood pressure on the aorta. However, the increase in blood pressure induced by this model maybe influenced by changes to components of the RAAS system (such as renin and angiotensin), and therefore

delineating the effects of humoral versus mechanical signals maybe more challenging, if utilizing this model.

Furthermore, continuous infusion of both AngII and NE for 7 days does increase blood pressure, although AngII alone seems to increase blood pressure significantly more compared with NE (Fig 4.1). This observation is supported by a previous study that showed that mean arterial pressure was higher in carotid arteries of animals treated with AngII as compared with NE [147].

In addition to having a more potent effect on blood pressure, we also know that AngII can have an independent effect on OPN expression in SMCs [130]. The studies performed by Remus et al have shown that OPN mRNA and protein expression are significantly increased in SMCs with 24 hours of treatment with 100nM of AngII [130]. However, the effect of NE alone on OPN expression in SMCs is yet to be identified. Finally, it is important to note that both humoral and mechanical factors are most likely working synergistically towards causing inflammation of the aorta, and therefore, the combined effects of these factors ought to be critically analyzed in future studies.

AngII is known to increase blood pressure via several actions – namely vasoconstriction, sympathetic nervous stimulation, and increased aldosterone production [148]. AngII acts mostly via G-protein coupled receptors – namely - AT<sub>1</sub> or AT<sub>2</sub> receptors [149] The AT<sub>1</sub> receptor (AT<sub>1</sub>R) is known to primarily mediate all the classically known physiological actions of AngII. These receptors are expressed by numerous cell types and organs ranging from kidney, vascular and immune system, adrenal, heart, and both peripheral and central nervous system [149]. In the kidney, activation of AT<sub>1</sub>R by AngII leads to increased sodium reabsorption and renal vasoconstriction [144, 149]. In the vasculature, AT<sub>1</sub>R is known to increase peripheral resistance and induce vasoconstriction [144].

AngII binding to AT<sub>1</sub> receptors on the membrane of cells is known to cause the dissociation of G-coupled protein receptors (GPCRs) [150]. This dissociation is typically related to the intracellular loops of the receptor, activation of the phospholipase C (PLC), cleavage of phosphoinositides to form inositol triphosphate (IP<sub>3</sub>) and diacylglycerol (DAG) [150]. IP<sub>3</sub> then causes the release of calcium ions from intracellular Ca stores, while activated AT<sub>1</sub> receptors also cause calcium channels to open within the cell membrane [150].

Norepinephrine (NE) is released by the sympathetic nervous system and adrenal medulla. Typically, NE released by the sympathetic nervous system is taken up by the nerves [151]. However, at times of high sympathetic nerve activation, there is a dramatic increase in the concentration of NE in the bloodstream as well. NE causes a significant transient increase in heart rate and contractility via  $\beta_1$  adrenoceptors [151]. It also causes significant vasoconstriction in arteries via  $\alpha_1$  and  $\alpha_2$  adrenoceptors [151]. The overall response to NE in the cardiovascular system is an increase in blood pressure, via increases in cardiac output and systemic vascular resistance [151].

The three  $\alpha_1$  receptors are coupled to the G<sub>q</sub> $\alpha$  pathway, that stimulates phospholipase C (PC) and generates the second messengers inositol (1, 4, 5,) – triphosphate (IP<sub>3</sub>) and diacylglycerol (DAG), which mobilizes intracellular calcium ions, activates protein kinase C (PKC), and in some tissues activates sodium-hydrogen, sodium-calcium exchangers, or potassium channels [150]. The three  $\alpha_2$  adrenergic receptors couple to the G<sub>i</sub> receptor, which inhibits cyclic adenosine 3', 5'-monophosphate (cAMP)-dependent protein kinase A (PKA) [150]. Finally, the  $\beta$ -AR subtypes are also G-coupled receptors which activate the adenylyl cyclase cAMP-PKA signaling pathway [150].

Studies in the 1990s showed that OPN was synthesized by smooth muscle, endothelial cells, and macrophages in human primary and restenotic coronary atherosclerotic plaques [152]. Work by O'Brien et al have shown that OPN mRNA and protein were abundant in human primary and restenotic coronary artery lesions, but almost undetectable within the intima or media of non-diseased coronary arteries [152]. We observe similar patterns from the histological results of this aim. We see that OPN expression is almost undetectable in the media or intima of the aortic cross-sections of healthy, WT mice (Fig 4.5, panel a). However, there is a dramatic increase in OPN expression, primarily localized within the medial layers of the aorta with AngII and NE treatment. It is interesting to note that the pattern of increase in OPN expression within the aortic cross sections (Fig 4.5) is similar to the pattern of increase in systolic blood pressure with AngII or NE treatment (Fig 4.1). These observations lead us to speculate that the medial layer is sensitive to and responds to changes in vascular wall strains as a result of varying blood pressure.

Literature suggests that the healthy aorta experiences a circumferential strain of about 10-15% [153, 154]. In this aim, we observed that the healthy aorta *in-vivo* had very little to almost no OPN expression at baseline (Fig 4.5), but our results from Aim 1 show that SMC's exposed to 10% strain in the stretch device, get a very robust upregulation of OPN expression (Fig 3.4-3.7). These results at first appear to be in contradiction to each other, however, a closer look reveals that these differences maybe attributed to the known differences in properties of SMCs within the aorta *in-vivo*, and those grown in culture. It is known that SMCs often exist on a spectrum of intermediate morphologies, in which contractile and synthetic SMCs, represent the two ends [155]. Contractile SMCs often have a spindle-shaped and elongated morphology, whereas synthetic SMCs have a cobblestone morphology [155]. Synthetic SMCs contain a large number of organelles involved in protein synthesis, and exhibit faster growth and migratory rates [155]. In

the healthy aorta, SMCs tend to have more of a contractile phenotype, however, when cultured the levels of contractile protein makers are known to gradually decrease [156]. In our studies, SMCs grown in culture tend to have features similar to that of synthetic SMCs, which is why they are quiesced under serum free conditions prior to experiments, in order to better assess the response and behavior of SMCs to various stimuli.

Physical factors are also known to have a significant impact on the phenotypic modulation of SMCs. It is known that mechanical forces such as circumferential strain increase the expression of ECM and contractile phenotype in SMCs of blood vessels [155], and this constant exposure to mechanical strain maybe a reason why OPN expression was present at low concentrations in the healthy aorta. Quiesced, non-strained, SMCs grown in culture had a similar phenotype and expressed low levels of OPN as well. However, upon exposure of these quiesced, SMCs to mechanical strain increased OPN expression, suggesting that a change to the mechanical strain environment experienced by these SMCs in-fact induces the expression of pro-inflammatory proteins including OPN.

ROS-mediated inflammation of arteries has been well established in literature, in the setting of a plethora of cardiovascular disease pathologies. Several studies have delved into elucidating the specific role of H<sub>2</sub>O<sub>2</sub> in mediating inflammatory processes. Of specific interest to this project, we note that several studies demonstrate that H<sub>2</sub>O<sub>2</sub> mediates abdominal aortic aneurysm (AAA) formation through the use of the Tg<sup>SMC-Cat</sup> mouse model [133, 145]. A remarkable decrease in aortic dilatation, MMP activity, and SMC apoptosis was observed in Tg<sup>SMC-Cat</sup> aortas compared with WT mice following treatment with CaCl (used in order to induce AAA) [145]. Another study demonstrated that Tg<sup>SMC-Cat</sup> following AngII treatment had better protected mechanical properties and altered matrix protein expression leading to a complete

absence of AAA incidence [133]. These studies highlight the vital role of H<sub>2</sub>O<sub>2</sub> in mediating inflammation within the vasculature.

Another relevant observation from a previous study has shown that both WT and Tg<sup>SMC-Cat</sup> treated with AngII for 14 days exhibit a significant increase in systolic blood pressure and vascular hypertrophy [81]. We observe similar results in both murine groups with 7 days of AngII and NE treatment suggesting that 1) blood pressure goes up as early as 7 days, and that 2) Tg<sup>SMC-Cat</sup> mice are sensitive to both AngII and NE treatment by responding with elevated systolic blood pressure. Finally, it is known that aortic segments from Tg<sup>SMC-Cat</sup> mice have a significant attenuation in H<sub>2</sub>O<sub>2</sub> levels with AngII treatment compared with WT aortic segments [81]. This attenuation in H<sub>2</sub>O<sub>2</sub> with hypertension in the aorta may be the primary reason for the blunted increase in OPN expression we observed in both the AngII and NE treated Tg<sup>SMC-Cat</sup> mice as seen in Fig 4.7. These data reveal a definite mechanistic link between H<sub>2</sub>O<sub>2</sub> and OPN. This observation is further corroborated by published work of Lyle et al. Some of the *in-vitro* data show that OPN is upregulated over a time course of 24 hours and with varying doses of H<sub>2</sub>O<sub>2</sub> treatment [7]. This work suggests that increases in OPN expression in response to H<sub>2</sub>O<sub>2</sub> occur at early time points via translational modifications, and at later time points via transcriptional changes. It was also shown that OPN expression was decreased in the setting of hind-limb ischemia in Tg<sup>SMC-Cat</sup> mice as compared with WT mice [114].

Taking all our results from Aim 2, we have shown in summary that:

- 1) AngII and NE-dependent hypertension upregulates OPN mRNA and protein expression in the aorta
- 2) Hypertension-dependent increase in OPN is mostly localized to the medial layer of the aorta, and

- 3) Overexpression of catalase, which is an antioxidant against  $H_2O_2$ , protects the aorta against the pro-inflammatory increase in OPN.

These data provide evidence that  $H_2O_2$  plays a pivotal role in mediating hypertension-related inflammation within the vasculature, and this link might be critical in developing effective preventative and therapeutic strategies in the treatment and management of hypertension related vascular complications.

**CHAPTER 5:**  
**EXPLORING THE ROLE OF OSTEOPONTIN IN AORTIC BIOMECHANICS WITH  
HYPERTENSION**

*SPECIFIC AIM 3:*

*To determine the contribution of osteopontin to the mechanical properties of the aorta at baseline and in the setting of hypertension*

**Introduction**

The aorta plays an important role in the transportation and collection of blood from various organs and tissues of the body. The material components that provide primary structure to the aorta include endothelial and smooth muscle cells, elastin, and collagen [157, 158]. The mechanical behavior of the aorta is clearly linked to its material composition. There is significant alteration to the material environment of the aorta in the setting of hypertension. These changes are mediated by the cellular components of the aorta that sense changes in mechanical strain and stress. These responses to hypertension, within the aorta, lead to its growth and remodeling, which ultimately translates to altered physiologic or pathophysiologic mechanical behavior.

When the healthy aorta is isolated, it typically undergoes a reduction in its diameter by 20% and length by around 40%, indicating that the cellular and protein components of the aorta are typically under tension [14]. Blood pressure within the aorta induces further strain of about 10-20% [15]. These pre-stresses and strains indicate that under physiological conditions, the aorta operates in the high strain region of its stress-strain curve [13, 15].

In the setting of hypertension, changes in material or structure in response to the altered stresses and strains begin at the cellular level [41, 159]. The existing body of literature suggests that with hypertension, smooth muscle cells first hypertrophy, proliferate, and produce excess

ECM proteins, which ultimately leads to a thickened and stiffer vessel wall that allows intramural stresses to return toward normal values [160-163]. Some of the geometric and mechanical parameters that highlight the mechanical behavior of the aorta and that are explored in this chapter include thickness of the vessel wall, aortic diameter under varied intramural pressures, and local compliance. Compliance measurements reflect upon the ability of the aortic wall to expand with varying levels of intraluminal pressure and are closely linked to and controlled by the vessel geometry and composition. We further explored the microstructure and material composition of the aorta by histological analysis of proteins such as collagen and elastin.

A key player and mediator of vascular pathophysiology that has recently emerged in literature, is the matricellular protein, osteopontin (OPN). It is known that OPN mediates AngII-induced vascular hypertrophy, and is a potent chemoattractant for macrophages and leukocytes, that could bring in extra-cellular matrix degrading enzymes, such as matrix metalloproteinases (MMPs). It's role in mediating hypertrophy and inflammation within the aorta, led us to hypothesize that the lack of OPN in mice may alter the biomechanics of the aorta, with hypertension. We also observed in Chapter 4 that OPN is significantly upregulated in the setting of disease hypertension within the aorta, however, it is unknown whether OPN alters the mechanical properties of the hypertensive aortic wall. In this chapter, therefore, we utilize OPN knockout (KO) mice and explore changes in the material, geometric, and mechanical parameters under baseline and angiotensin-II-induced hypertensive conditions. We only used the AngII model of hypertension for this aim, however, future studies should consider other models of hypertension as well, including NE infusion, for a thorough analysis of the effects of the lack of OPN on hypertension-dependent changes of the biomechanics of the aorta.

## **Methods**

### **Animals**

Eight to twelve week old male C57BL/6 (WT) mice or OPN Knockout (KO) mice were purchased from Jackson Laboratories (Bar Harbor, ME). The animals were housed and cared for according to the guidelines approved by the Emory University Institutional Animal Care and Use Committee (IACUC).

### **Osmotic Minipump Implantation**

Mice were anesthetized using 1% isoflurane (oxygen delivered at 0.5L/min with 2% isoflurane for induction and 1% isoflurane for maintenance). AngII (Sigma Aldrich, A6402) at a dose of 0.75mg/kg/day was infused via a primed mini-osmotic pump (Alzet mini-osmotic pump, Model 2004). The pumps were inserted subcutaneously, on the back. Following surgery, mice were administered buprenex (1mg/kg, SC), once prior to surgery, and then as needed.

### **Measurement of Systolic Blood Pressure**

Mice were first acclimatized to the tail-cuff plethysmograph (Visitech© Corporation) for at least three consecutive days. Systolic blood pressure was then measured prior to and after infusion of AngII.

### **Measurement of Aortic *In-Vivo* Length, Aorta Isolation, and Preparation**

Mice were first euthanized via CO<sub>2</sub> asphyxiation. The thoracic cavity was opened and the aorta cleared of excessive connective tissue. Prior to excision, a small ruler was placed beside, and at the same focal plane as that of the aorta. An image of the intact aorta and ruler was taken using

a dissection microscope camera. This image was then opened in Image J, and a conversion factor (for pixels-to-mm) generated, based on the distance between two tick marks (1mm) on the ruler. A straight line was drawn from the start of the descending aorta until the end of the thoracic aorta (near the celiac trunk). The distance of this line was then calculated by Image J, based on the previously generated pixel-to-mm conversion factor, and is approximately the *in-vivo* length of the aorta.

After excision, the fatty tissue surrounding the aorta was carefully removed. Care was taken to make sure that the intercostals, celiac trunk, mesenteric and renal arteries were left still attached to the aorta. Following the removal of fat, the intercostals and remaining branches were tied off with silk suture filaments, each fastened away from the surface of the aorta to prevent the knots from interfering with the expansion of the aorta under pressurization. During cleaning and the course of the experiments, the aorta was maintained in sterile 1X PBS with a pH of 7.4. The region of the aorta being tested was the thoracic region.

The aorta was then cannulated onto a 200 $\mu$ m diameter glass cannula in a multiaxial computer-controlled vessel isolation device similar to one that has been previously described [164]. The aorta and cannula were suspended into a bath containing 1X PBS and 10 $\mu$ M sodium nitroprusside (SNP) to ensure that the aorta was fully dilated during the testing process. The aorta was perfused through the two glass cannula which allows for the precise control of the luminal pressure. These cannulae are attached to two computer controlled linear motion actuators that can allow for the careful control of the vessel length during the mechanical test. The device was placed above an inverted microscope and real time images of the aorta acquired at a magnification of 2.5x in a temperature controlled incubator. The device allows for the precise maintenance of

intraluminal pressure and axial length of the aorta, while simultaneously recording the outer diameter of the vessel.

### **Mechanical Testing of Aortas**

Following cannulation, the unloaded length of the aorta was first measured and the vessel was then preconditioned. Fixed length pressure-diameter tests were then performed at varying axial stretches ( $\lambda$ ) ranging from  $\lambda=1.3, 1.4, 1.5, 1.6, 1.7, 1.8,$  and  $1.9$ . Here axial stretch,  $\lambda$ , is defined as the ratio of the loaded vessel length to the unloaded vessel length. During the pressure-diameter tests, the aorta was inflated from 10mm to 200mm Hg at the axial stretches previously listed and the outer diameter of the aorta continuously recorded, with two loading and unloading cycles for each axial stretch.

### **Pressure-Diameter (P-D) Curves and Compliance Analysis**

Following mechanical testing, pressure-diameter (P-D) curves were generated from the raw data obtained from the device. The P-D curves for all aortas followed a biphasic trend that include regions of low deformation under low pressures, a linear increasing region under mid-range pressures, and finally a flat deformation plateau at peak pressures.

Local compliance of the aortas was calculated at 20mmHg increments to generate pressure-dependent compliance versus pressure curves. A linear trend line was applied to the pressure-diameter curves 10mm Hg above and below an indicated pressure in order to obtain local compliance values.

## **Histological Analysis**

Following mechanical testing, aortas were fixed with 10% buffered formalin. Aortas were then paraffin embedded and cut into 5  $\mu\text{m}$  increment sections. Sections were then stained with hemotoxylin and eosin (H&E) for analysis of gross aortic morphology, Verhoff's van Geison Elastic Stain for elastic laminae, and Masson's Trichrome Stain for collagen. Medial thickness, elastin interlamellar gap, and length of the aorta were calculated using Image J Software.

## **Statistics**

All results are presented as mean  $\pm$  SEM and analyzed using ANOVA or t-test using GraphPad <sup>TM</sup> Prism Software (GraphPad Prism), followed by Bonferroni multiple comparisons test. A p-value  $< 0.05$  was considered significant.

## Results

### **Systolic Blood Pressure is Increased in Both WT and OPN KO Mice with Angiotensin-II**

#### **Treatment**

We used mini-osmotic pumps to continuously infuse AngII (0.75mg/kg/day) in both wild type (WT) and OPN KO mice. We measured systolic blood pressures (SBPs) in WT mice at baseline and WT mice that were infused with AngII for three, seven, and fourteen days. We also measured SBPs in OPN KO mice at baseline and in those infused with AngII for seven days.

We observed a significant increase in SBP in WT mice treated with AngII at all three time points – three, seven, and fourteen days compared to the baseline WT controls (Fig 5.1). Three day AngII treated mice had a mean SBP of  $152 \pm 7$  mm Hg, with a 41% increase over baseline WT, while seven and fourteen day AngII infused mice had a mean SBP of  $161 \pm 4$  mmHg and  $171 \pm 3$  mmHg, with a 49% and 59% increase over baseline WT controls, respectively. These increases were statistically significant.

OPN KO mice had a baseline SBP of  $114 \pm 2$  mmHg, and when treated with AngII for seven days increased by 42% to  $162 \pm 6$  mmHg.

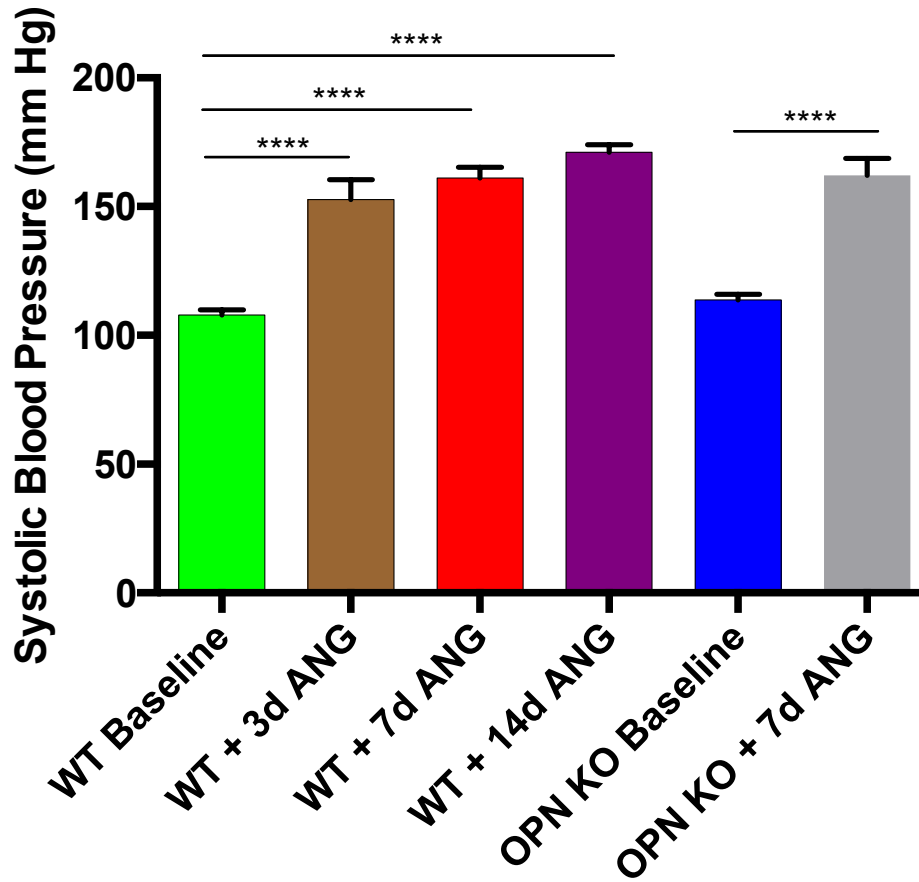


**Figure 5.1: Systolic Blood Pressure is Significantly Increased in both WT and OPN KO mice with AngII infusion** Baseline SBPs were similar in both WT and OPN KO mice. There was a significant increase in SBP in WT treated with AngII for 3, 7 and 14 days, and also in the OPN KO mice treated with AngII for 7 days compared with their corresponding baseline controls. \*\*\*\*p<0.0001, N=4-6

## **In-Vivo Aortic Length Is Not Altered with Angiotensin-II Treatment in WT or in OPN null mice**

To determine whether there was any difference in the axial environment of the aorta *in-vivo*, we measured the length of the aorta while still intact and inside the animal. We observed no significant differences in the *in-vivo* length of the aorta among all treatment groups, reflecting that there are no alterations to the axial environment or tension of the vessel. The *in-vivo* length of the aorta was measured via Image J analysis as previously mention and the average length of the aorta (thoracic and suprarenal region) was  $19.5 \pm 0.5\text{mm}$  among all treatment groups (Fig 5.2). We further determined the *in-vivo* stretch needed for mechanical testing based on the ratio between this calculated in-vivo length and the unloaded ex-vivo length of the excised aorta. The in-vivo axial stretch was determined to be  $\lambda=1.7$  (in most cases).

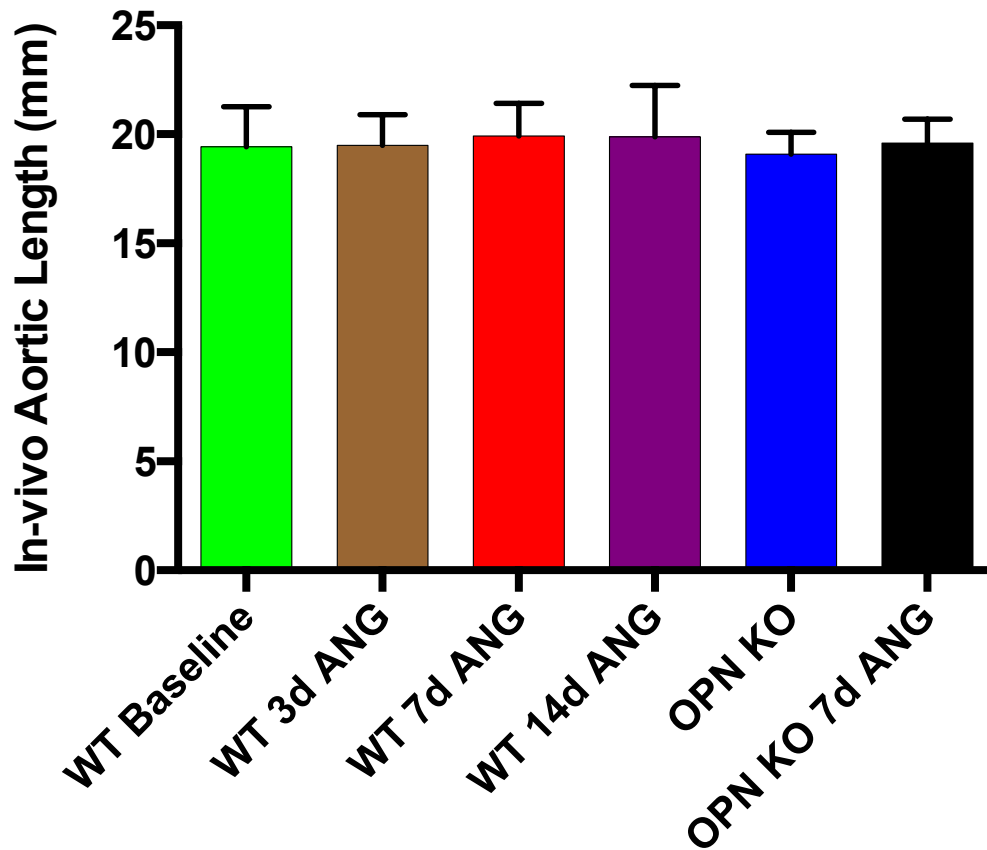


**Figure 5.2: In-Vivo Length of WT and OPN KO Aortas is not Altered with AngII Treatment**

The in-vivo length of the aorta was determined at baseline and with 3, 7, or 14 days of AngII treatment in WT mice, and at baseline and with 7 days of AngII treatment in OPN KO mice. No significant differences were observed. N=6-11

### **Angiotensin-II Infusion Increases Aortic Diameter, but does not alter Aortic Compliance**

We wanted to first determine how AngII-induced hypertension would affect aortic mechanics over the time course of 3, 7, or 14 days. The P-D curves (Fig 5.3) demonstrated a biphasic behavior which reflects reduced vessel expansion at lower pressures and stiffening at higher pressures. We observe a significant increase in diameter with AngII treatment at low and mid-range pressures of 20, 40, and 60 mm Hg. Statistical analysis revealed that there was no significant change in aortic diameter with three days of AngII treatment at all pressures compared with the baseline WT diameters, although there appears to be a trending increase. Seven days of AngII infusion, however, induced a significant increase in diameter at 20 and 40 mmHg, while fourteen days of AngII infusion induced a significant increase at 20, 40, and 60 mm Hg. This increase in aortic diameter suggests that AngII-induced hypertension causes the vessel to remodel in order to compensate for the elevated blood pressure as early as potentially three days, and definitively by seven and fourteen days.

Analysis of the local pressure-dependent compliance (Fig 5.4) obtained by calculating the slope of P-D data revealed a bell-shaped curve with minimum compliance observed at low (20mm Hg) and high pressures (100mm Hg and higher) and maximal compliance at mid-range pressures (40-80mm Hg). However, there was no statistical difference in the compliance properties of these aortas with AngII treatment, suggesting that these murine aortas are able to adaptively remodel in a robust and rapid manner at time points as early three days lasting up to fourteen days. Further histological analysis revealed the microstructural changes that occur in these aortas at these time points.

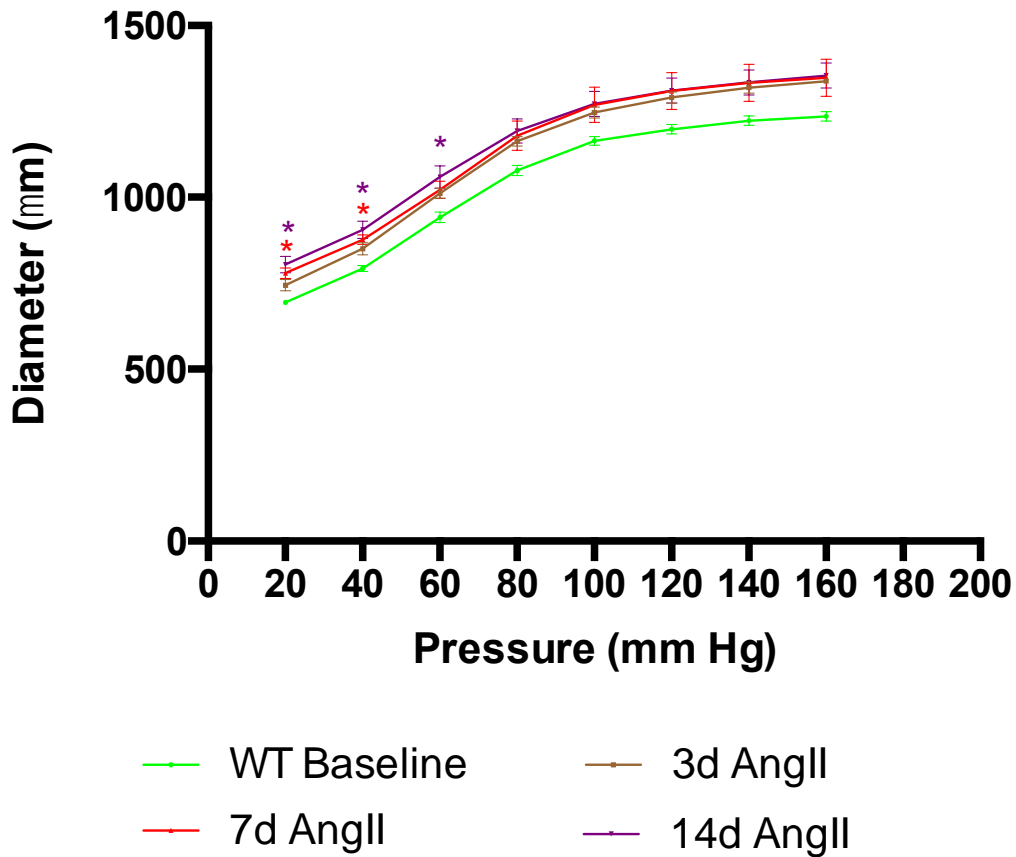


**Figure 5.3: AngII-induced Hypertension Increases Aortic Diameter** Mechanical testing of WT aortas treated with AngII for 3, 7, and 14 days revealed a significant increase in vessel diameter at the early and mid-range pressures of 20-60mm Hg. Seven day AngII treatment caused an increase in diameter at 20 and 40mm Hg (\*  $p < 0.05$  7d AngII vs WT Baseline), while fourteen day AngII treatment increased diameters at 20, 40, and 60mm Hg (\*  $p < 0.05$  7d AngII vs WT Baseline). N=6 for WT Baseline, N=4 for 3d AngII, N=5 for 7d AngII, and N=4 for 14d AngII treated mice.

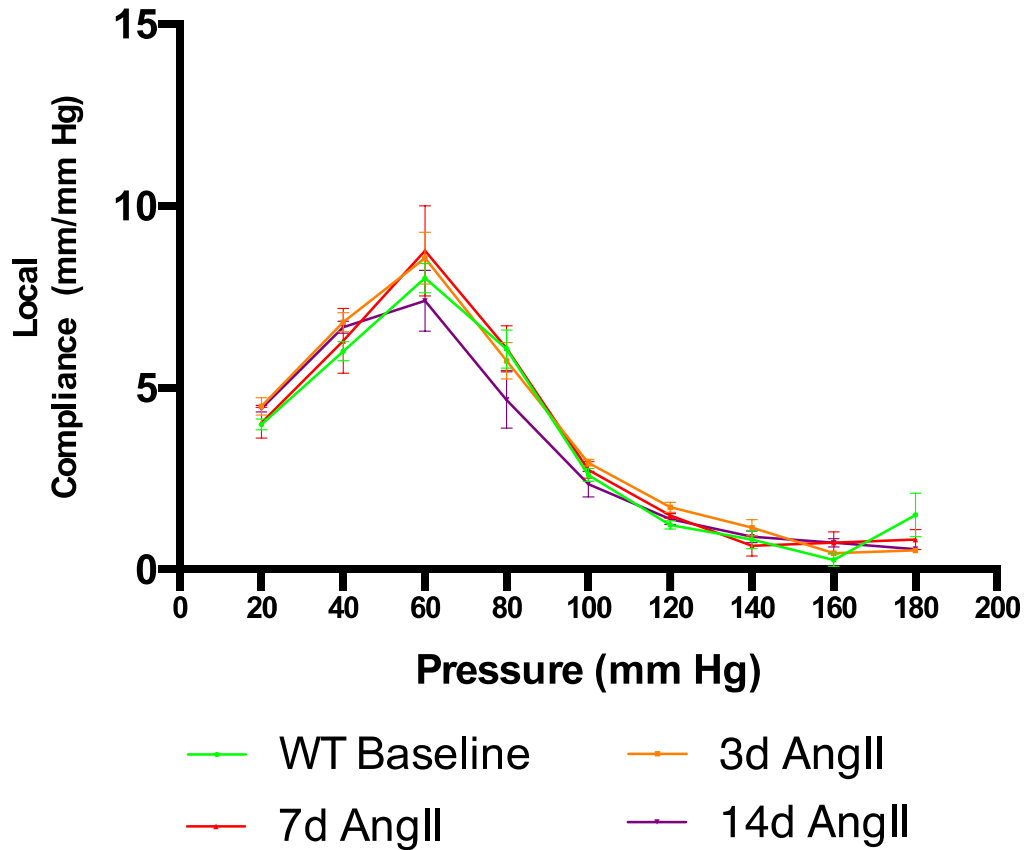


**Figure 5.4: Pressure-Dependent Local Compliance is not Altered in murine WT aortas with AngII Treatment at 3, 7 or 14 days** Analysis of local compliance obtained by calculating the slope of P-D curves of WT aortas treated with AngII for 3, 7, and 14 days revealed no changes in aortic compliance. N=6 for WT Baseline, N=4 for 3d AngII, N=5 for 7d AngII, and N=4 for 14d AngII treated mice.

## **Angiotensin-II Infusion Increases Medial Thickness of the Aorta**

Representative images of aortic cross sections of aortas obtained from baseline WT mice and WT mice treated for three, seven, and fourteen days with AngII are shown in Figure 5.5. The images reveal that the baseline WT aortic wall (Fig 5.5, top left panel) comprises of 4-5 concentric elastic lamellae as shown by H&E Stain. The medial thickness of the aorta is significantly increased with AngII treatment for three, seven, or fourteen days as compared to the baseline WT mice aortic cross sections (quantified in Fig 5.6). Another notable difference is the presence of a thicker adventitial layer that reveals infiltration of inflammatory cells and abundance in collagen in the seven and fourteen day AngII treated samples (Fig 5.5, bottom left and right panels) as compared to the baseline WT or three day treated samples.

Finally, the medial layer of the aortic wall appears to have uniformly thickened with AngII treatment, suggesting that these aortas have all adaptively remodeled. Furthermore, we do *not* observe any elastin breaks or separation in the layers of the aortic wall, and the aortic wall appears to be relatively intact in all treatment groups. These observations provide evidence in support of our previous observation that shows no change in the compliance properties of aortas treated with AngII for three, seven, or fourteen days, suggesting that they have all successfully adaptively remodeled (Fig 5.4).

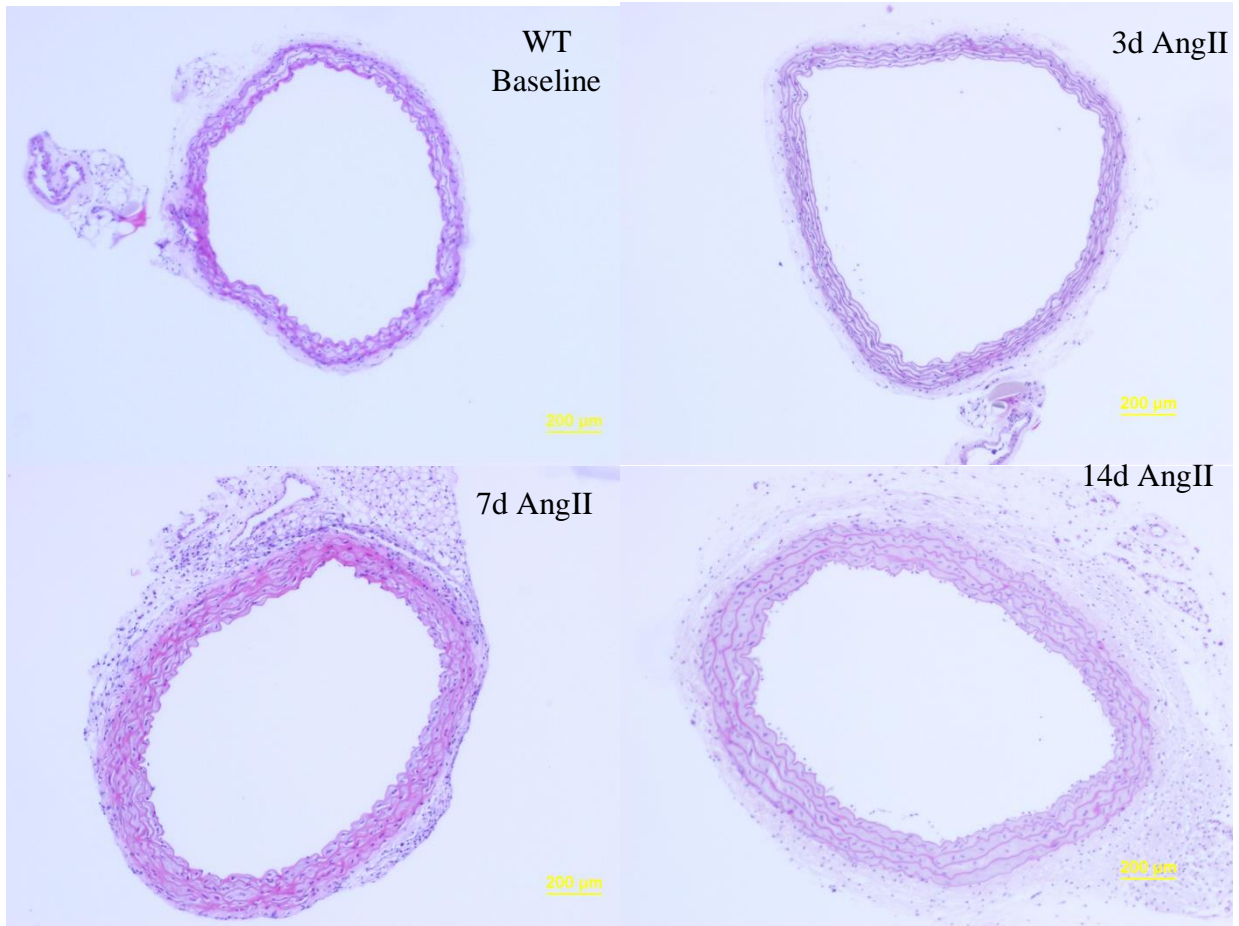


**Figure 5.5: Medial Thickness is Increased with 3, 7, or 14 day AngII infusion** Representative images reveal aortic microstructures of samples obtained from WT mice at baseline or treated with AngII for 3, 7, or 14 days and stained with hemotoxylin and eosin (H&E). We observe a uniform increase in medial thickness of these aortas at all three time points. N=6 for all groups.

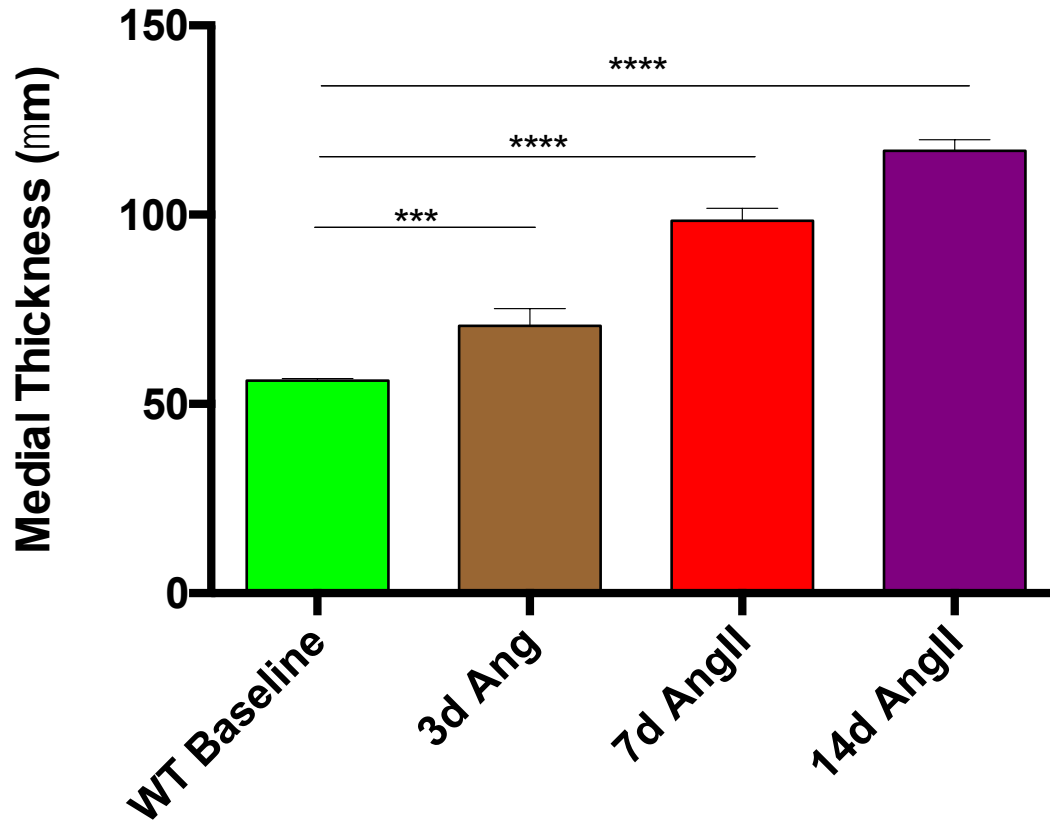


**Figure 5.6: Medial Thickness of Aorta Increases with AngII Treatment** We observe a significant and stepwise incremental increase in medial thickness of the aorta with treatment with AngII for three, seven, and fourteen days. \*\*\* $p < 0.001$  and \*\*\*\* $p < 0.0001$  for  $N=6$  for all groups.

## **Aortic Diameter and Compliance is Altered in OPN null mice**

Osteopontin (OPN) is an important mediator of arterial inflammation and remodeling in response to ischemia and injury [113, 114, 140]. However, it is unknown if OPN mediates arterial remodeling in response to hypertension. In order to determine its potential role, we used OPN null mice and treated them with AngII for 7 days, which is the earliest time point we observe changes in the mechanical behavior of the aorta (Fig 5.3).

The P-D curves obtained from OPN KO mice (Fig 5.7) revealed a biphasic behavior similar to the WT mice which reflects reduced vessel distension at lower pressures and stiffening at higher pressures. However, the most surprising observation was that OPN KO mice have significantly higher aortic diameters at all pressures (low, mid-range, and high) at *both* baseline conditions and when treated with AngII. Seven days of AngII infusion increases outer aortic diameter at 20 and 40 mmHg as was already previously noted (Fig 5.3).

We analyzed local pressure-dependent compliance curves of OPN KO mice (Fig 5.8) obtained by calculating the slope of P-D data and it also revealed a similar bell-shaped curve with minimum compliance observed at low (20mm Hg) and high pressures (100mm Hg and higher) and maximal compliance at mid-range pressures (40-80mm Hg). We observed that OPN KO aortas at baseline had a statistically higher compliance at the mid-range pressure of 60mm Hg compared with baseline WT aortas ( $10.3 \pm 0.4$  versus  $8.02 \pm 0.39$  mm/mm Hg, respectively). OPN KO aortas treated with AngII had significantly lower compliance at 60mm Hg compared with OPN KO baseline aortas ( $8.70 \pm 0.53$  versus  $10.3 \pm 0.4$  mm/mm Hg, respectively). Therefore, the results of these mechanical tests reflect that OPN does indeed have an impact on the mechanical properties of the aorta. Evaluation of the microstructure through histological analysis provide further interpretation of these data.

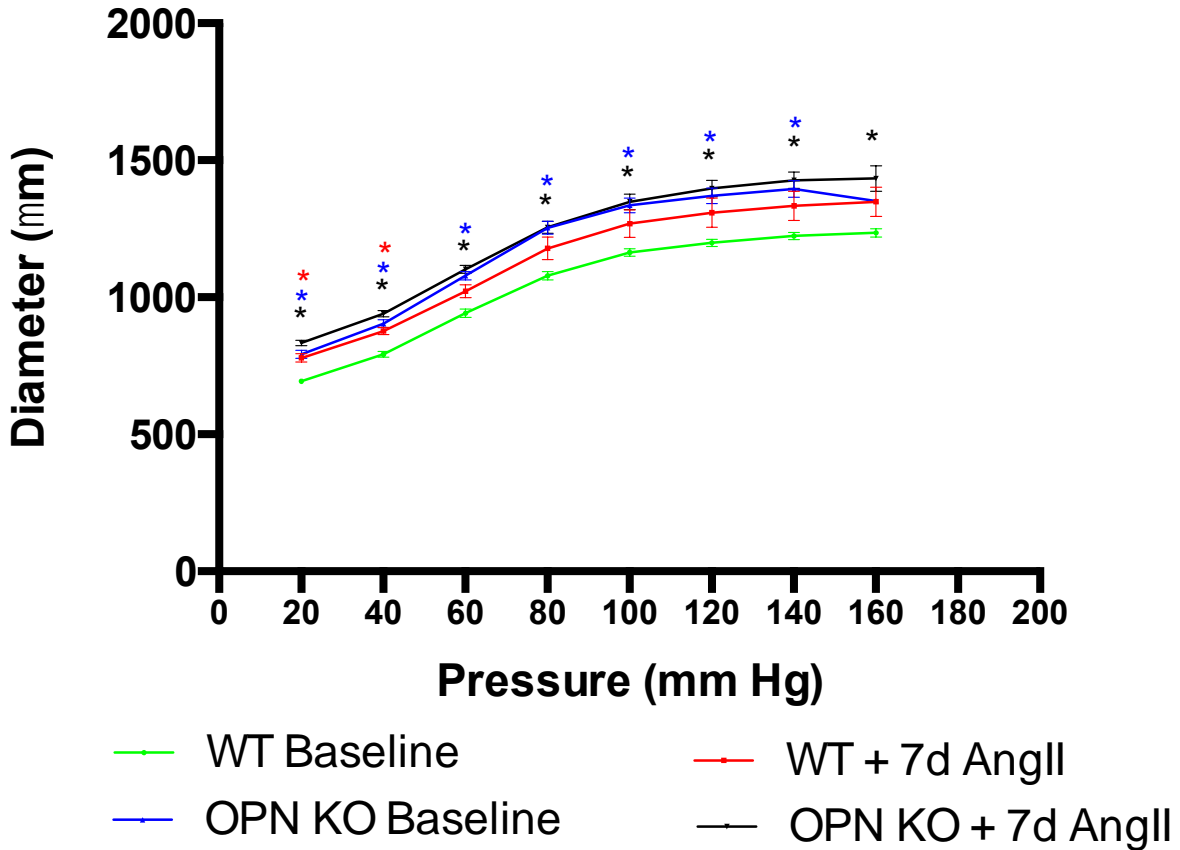


**Figure 5.7: OPN KO Aortas Have Dramatically Higher Aortic Diameter with and without AngII treatment** Mechanical testing of OPN KO and WT aortas at baseline conditions and treated with AngII for seven days revealed significantly higher vessel diameters at all pressures. OPN KO aortas at baseline had significantly higher diameters at all pressures except 160mm Hg (Blue \*  $p < 0.05$  OPN KO Baseline vs WT Baseline). Seven day AngII treated OPN KO mice had elevated diameters at all pressures (Black \*  $p < 0.05$  OPN KO Baseline vs WT Baseline). Finally, seven day AngII treated WT aortas have increased diameters at 20mm Hg and 40mm Hg (Red\*  $p < 0.05$  7d AngII vs WT Baseline). N=6 for WT Baseline, N=5 for WT + 7d AngII treated mice, N=5 for OPN KO Baseline, and N=6 for OPN KO + 7d AngII treated mice.

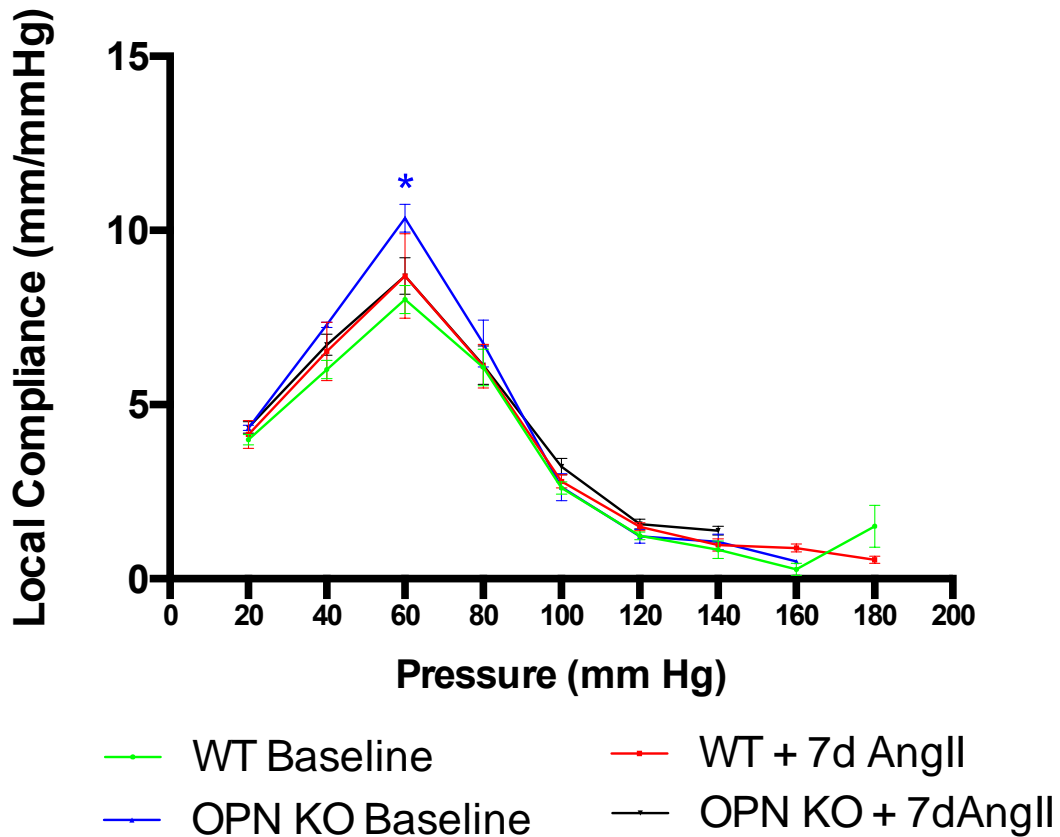


**Figure 5.8: OPN KO aortas have Higher Maximal Compliance than WT aortas** Mechanical testing of OPN KO and WT aortas at baseline conditions and treated with AngII for 7 days revealed a significant increase in compliance in OPN KO aortas. OPN KO aortas at baseline had greater local compliance at 60mm Hg compared with both WT baseline and OPN KO aortas treated with AngII (Blue \*  $p < 0.05$  OPN KO Baseline vs. WT Baseline). N=6 for WT Baseline, N=5 for 7d AngII treated WT mice, N=5 for OPN KO Baseline, and N=4 for OPN KO + 7d AngII treated mice.

## **Osteopontin KO Aortas Have Altered Microstructural Features and are Protected against Inflammatory Infiltration with Hypertension**

Representative images of aortic cross sections from WT and OPN KO mice treated with seven days of AngII are shown in Figure 5.9. We observe differences between WT and OPN KO aortas even under baseline conditions. These OPN KO aortas appear to have a moderate increase in medial thickness as compared to WT aortas (Fig 5.9 top left and bottom left panels). However, this difference may be attributed to the difference in elastin fiber structure and organization in the OPN KO. We observe that baseline OPN KO aortas appear to have elastin fibers that are straighter and more widely spaced (Fig 5.11, top left and bottom left panels). On the other hand, baseline WT aortas have elastin lamellae that are wavier, more undulated, and tightly spaced (Fig 5.11, top left and bottom left panels). This inter-lamellar elastin gap is quantified in Figure 5.12.

As was previously noted in Figure 5.5 and 5.6, medial thickness is significantly increased in WT mice treated with AngII for seven days (Fig 5.9-5.10). These hypertensive WT mice also have a thickened adventitia abundant in collagen and inflammatory cells (Fig 5.9-11, top right). Interestingly, we observe an increase in medial thickness in AngII-treated OPN KO mice, but these aortas *do not* have a thick adventitial layer, abundant in collagen, suggesting that these mice are protected against inflammatory cell infiltration (Fig 5.9-11, bottom right).

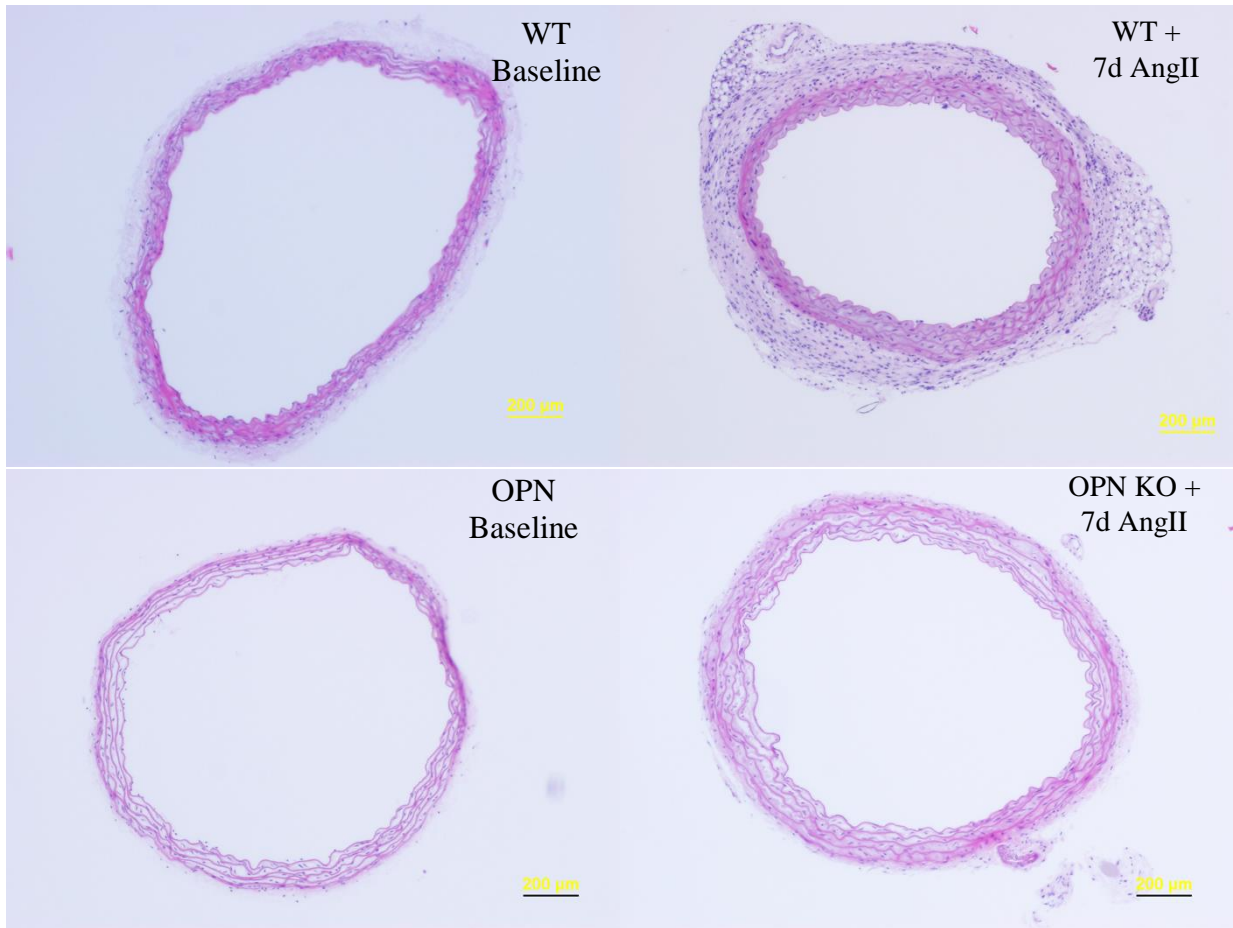


**Figure 5.9: Hypertensive OPN KO mice are Protected against Adventitial Inflammation**

Representative images reveal aortic microstructures of samples obtained from WT mice and OPN KO mice at baseline or treated with AngII for seven days stained with H&E. OPN KO aortas appear to have a slightly increased medial thickness due to widely spaced elastin fibers, that also appear to be more unfolded as compared to the elastin in WT aortas. There is also significantly greater thickening of the adventitia in the WT mice treated with AngII compared with the OPN KO mice treated with AngII. N=6 for all groups.

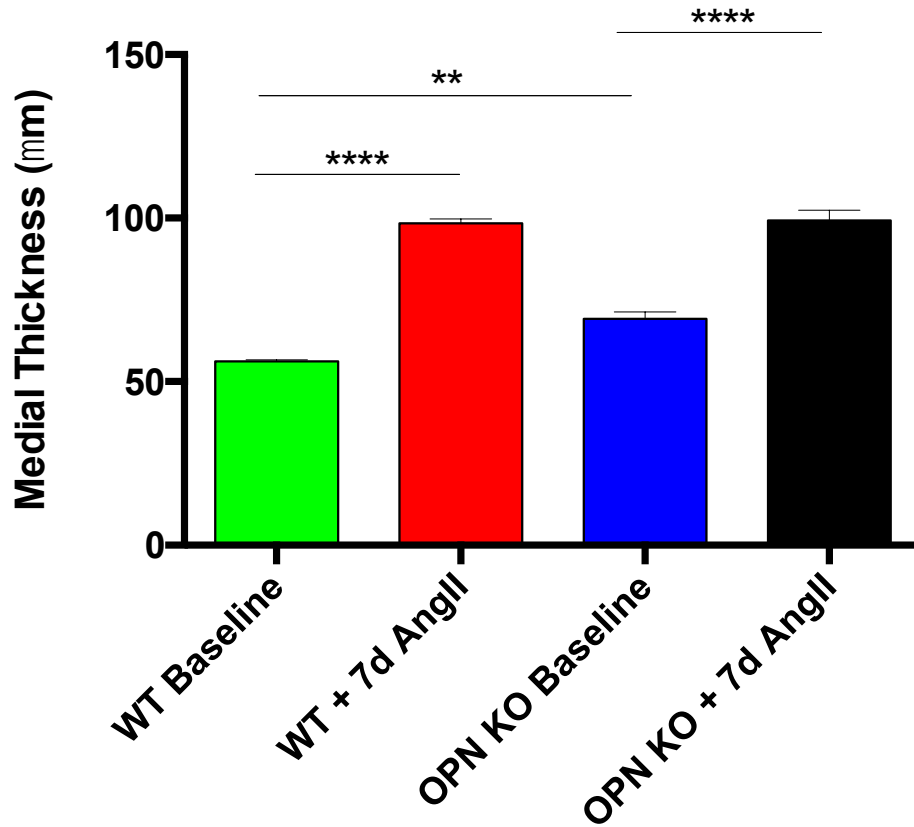


**Figure 5.10: AngII Infusion Induces Medial Thickening in Both WT and OPN KO aortas**  
 Treatment with 7 days of AngII significantly increased medial thickness in both WT and OPN KO aortas. There also appears to be an increase in medial thickness of baseline OPN KO aortas.  
 \*\*p<0.01 and \*\*\*\*p<0.0001. N=6 for all groups.

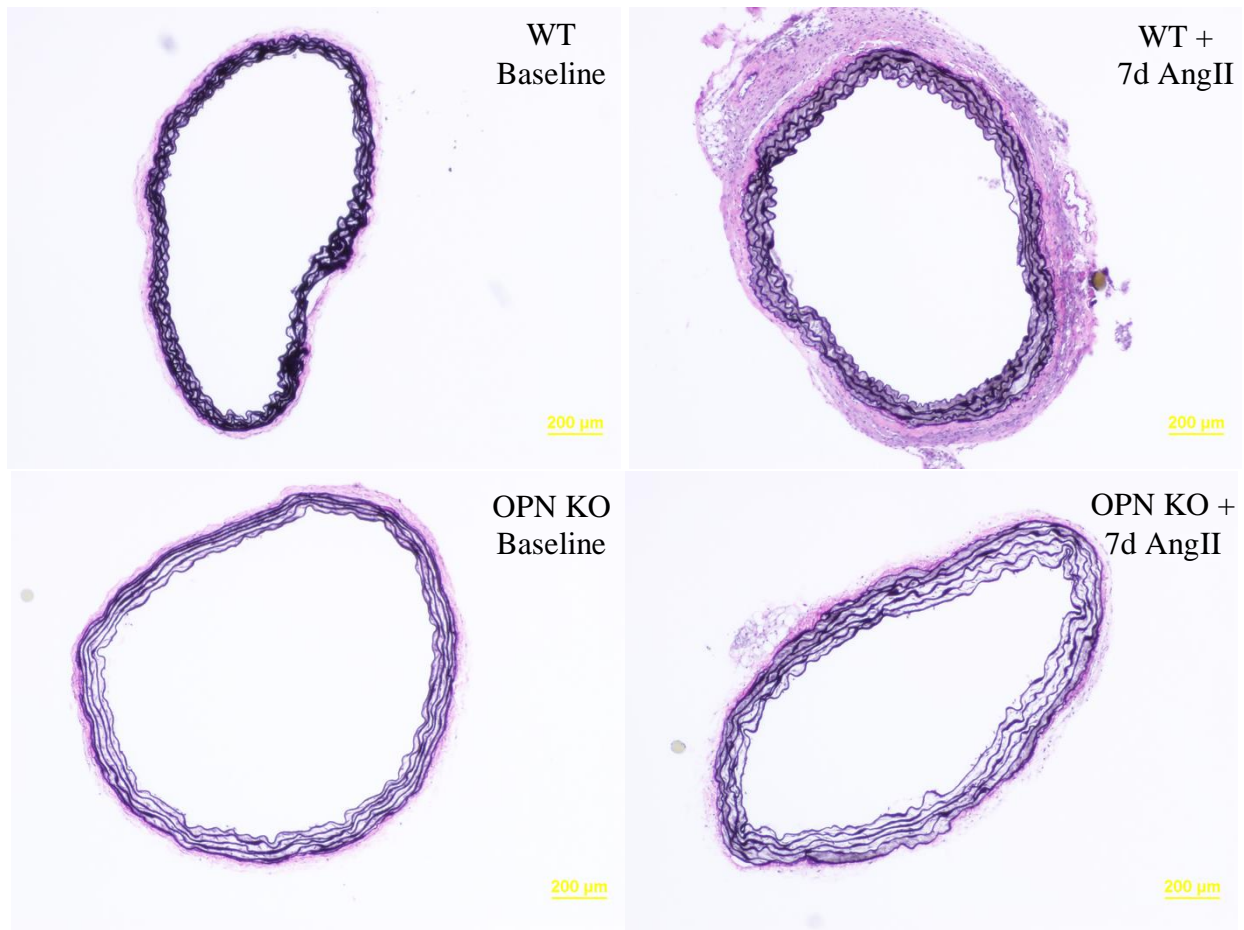


**Figure 5.11: OPN KO Aortas Have Altered Elastin Organization** WT and OPN KO aortas were stained with Verhoff's van Geisson to identify differences in elastin organization. We observe that the elastin lamellae in baseline WT aortas (top left) appear more undulated, wavy, and closely spaced, while those in the baseline OPN KO aortas (bottom left) appear to have straighter fibers and more widely spaced organization. 7-day AngII treatment of both WT and OPN KO aortas appears to increase the gap between the elastin lamellae (top right and bottom right). N=3 for WT baseline, N=6 for all other groups.

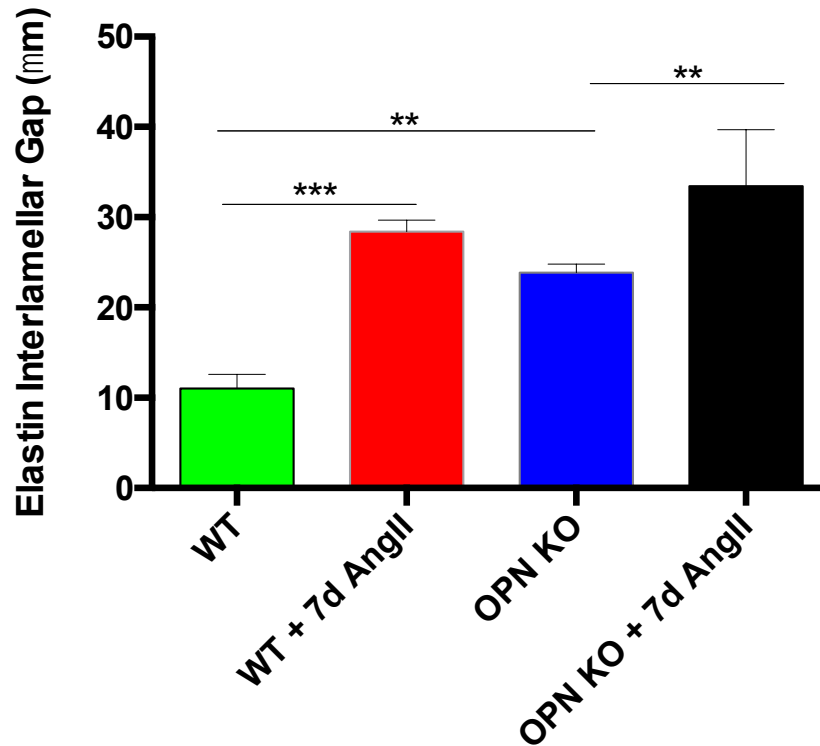


**Figure 5.12: OPN KO Aortas Have Increased Elastin Interlamellar Gaps** The shortest distance between the elastin lamellae at multiple points on the aorta were measured using ImageJ software and quantified for the various treatment groups shown in the previous figure. Baseline OPN KO and AngII treated WT and OPN KO aortas have greater elastin interlamellar gaps compared with baseline WT aortas. \*\* $p < 0.01$ , \*\*\* $p < 0.001$ . N=3 for WT Baseline, N=6 for all other groups.

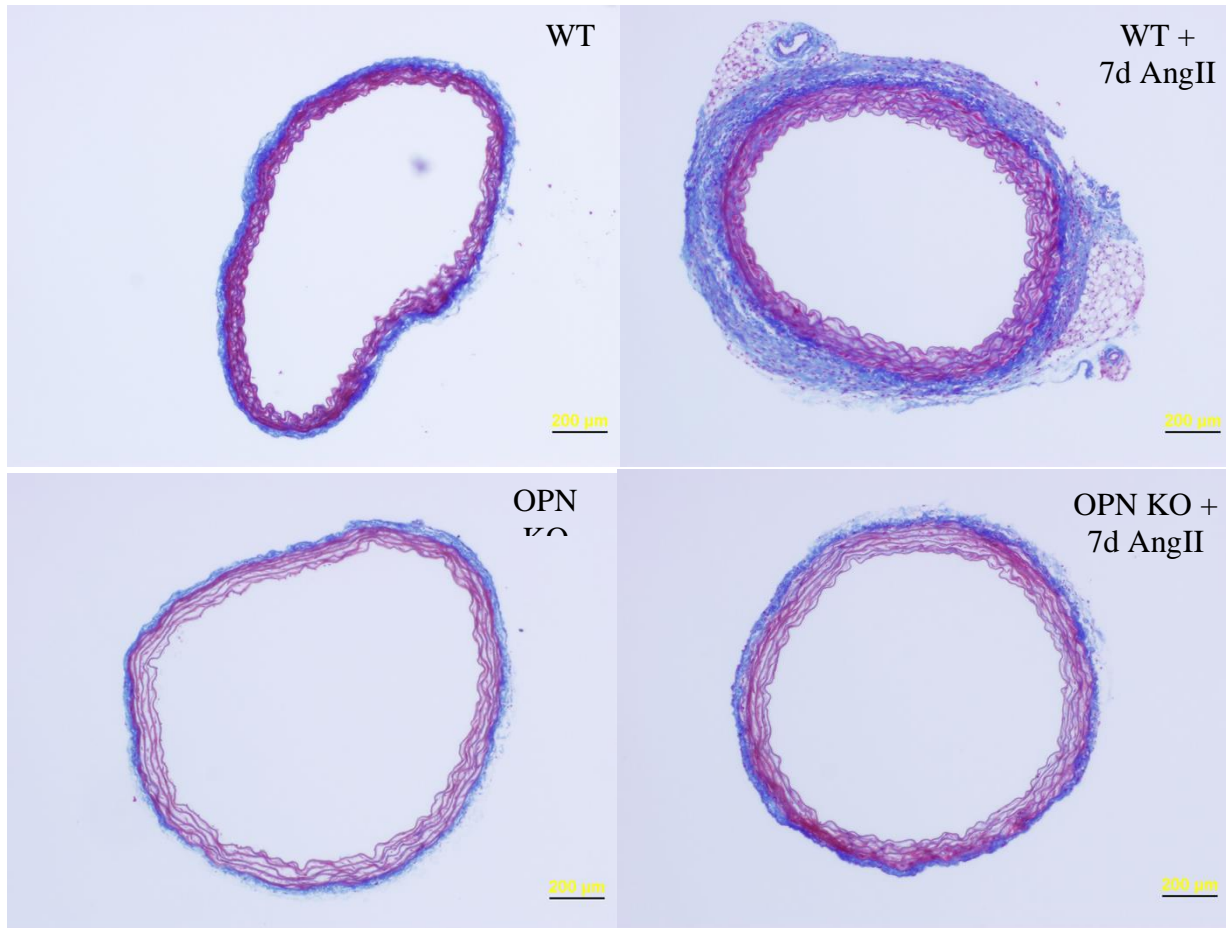


**Figure 5.13: Hypertensive OPN KO have Reduced Adventitial Collagen, Adventitial Thickening, and Inflammation** Aortic cross-sections were stained with Masson's Trichrome in order identify differences in collagen (stained blue). WT mice treated with AngII for seven days (top right) appear to have a striking increase in collagen in the adventitial layer of the aorta as compared with baseline WT levels (top left). Interestingly, aortas from OPN KO mice treated with AngII for seven days appear to have significantly lower levels of collagen in the adventitia, suggesting that it plays a role in mediating adventitial inflammation with hypertension (bottom right). N=3 for WT Baseline, N=6 for all other groups.

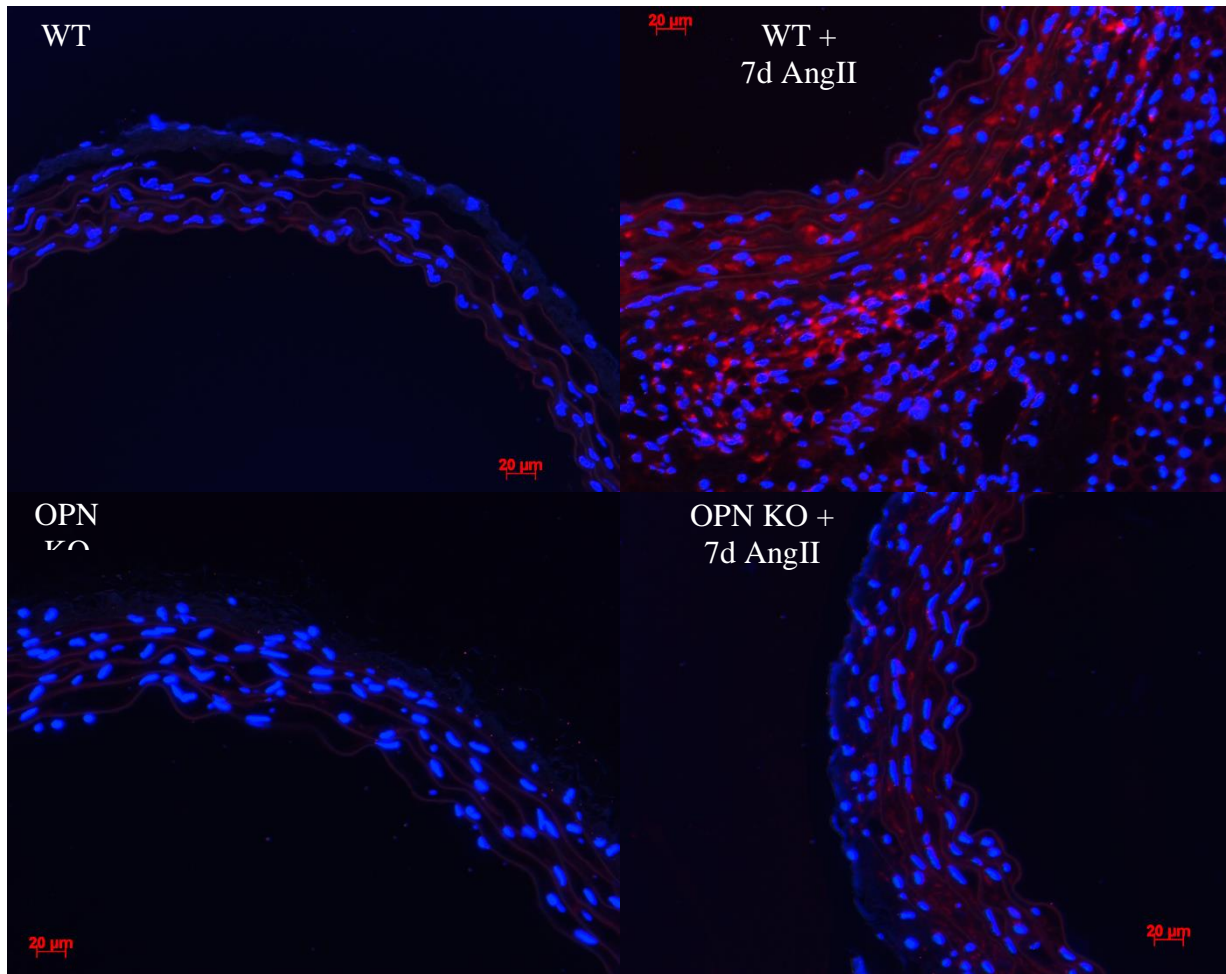


**Figure 5.14: Hypertensive OPN KO have Significantly Reduced Inflammation** Aortic cross-sections were stained to for CD107b (also known as Mac3) in order identify invasion of macrophages within the aorta. WT mice treated with AngII for seven days (top right) appear to have a striking increase in Mac-3 expression within the aorta as compared with baseline WT levels (top left). Interestingly, aortas from OPN KO mice treated with AngII for seven days appear to have significantly lower level to almost no expression of Mac-3, suggesting that OPN KO mice are protected against AngII-induced inflammation (bottom right). N=3 for WT Baseline, OPN KO Baseline, and OPN KO with 7d AngII, and N=4 for WT with 7d AngII.

## Discussion

Osteopontin (OPN) has been shown to play an important role in vascular physiology and pathophysiology. While several studies have highlighted its role as a mediator of inflammation [95, 165], angiogenesis [7], tumor growth [166], and tissue remodeling, its unique role in mediating vascular biomechanics in the setting of hypertension is still unclear. Our initial working hypothesis for this aim was that the lack of OPN would contribute to changes in the mechanical properties of the aorta only in the setting of hypertension and not under basal conditions. Our rationale for this hypothesis was that OPN is almost absent in WT aortas under baseline conditions, and therefore, we expected to not observe any mechanical differences in OPN KO aortas under baseline conditions as well. Moreover, results from several clinical studies and our findings from aims 1 and 2, show that OPN expression is significantly increased only in the presence of a vascular insult or elevated mechanical stress.

To test our hypothesis, we measured pressure versus diameter (PD) and compliance behavior of OPN KO and WT aortas under healthy and AngII-induced hypertensive conditions. We further characterized the morphology of these aortas via a thorough histological analysis. Overall, the results of these studies demonstrate that OPN does indeed significantly change the biomechanical properties of the aorta, however, to our surprise this was true under *both* healthy and diseased settings.

Prior to commencing our studies with OPN KO aortas, we wanted to determine the earliest time point at which biomechanical differences in WT aortas are most pronounced with AngII treatment. Most studies that have explored hypertension related arterial compliance changes, have done so only in human subjects, and have not carefully explored the time scales over which these changes occur [167-170].

We therefore performed a time course study, and analyzed PD and local compliance curves obtained from aortas of WT mice treated with AngII for three, seven, or fourteen days. We hypothesized that AngII-induced hypertension in WT mice would cause stiffening of aortas, which would be evident via a decrease in compliance of these aortas. Our time course studies revealed that there is a significant increase in diameter and medial thickness of aortas at all three time points, however, there was no change in the compliance properties of these aortas. This suggests that murine aortas are capable of rapid and adaptive remodeling to compensate for the increased vascular strain due to elevated blood pressure. Our results showing increased pressure dependent diameters in AngII treated mice are in agreement with previous findings that also show that aortas undergo hypertrophy with AngII-induced hypertension [32, 42, 45]. We subsequently chose to perform our OPN KO studies at the seven-day time point because this was the earliest time point at which we observed pressure-dependent diameter changes.

The next objective of this aim was to explore how the absence of OPN in aortas would affect aortic biomechanics. Our results show that pressure-diameter (PD) curves of OPN KO aortas are significantly displaced upward at baseline compared with baseline WT aortas. OPN KO aortas also exhibit higher compliance at mid-range pressures compared with baseline WT aortas. This suggests that OPN might play an important role in mediating vascular mechanics even under baseline conditions. These results are similar to those found in an early study that explored the role of OPN in vascular physiology under basal conditions. This study demonstrated that carotid arteries obtained from OPN KO mice exhibit greater diameters than WT mice at physiological pressures [171]. The study also showed that OPN KO carotids have greater elasticity at higher physiological pressures such as 125mm Hg and 175mm Hg [171]. We observe, however, that baseline OPN KO aortas demonstrate greater compliance only at mid-range, sub-physiologic

pressures, with the most significant difference observed at 60mm Hg. This difference in compliance maybe attributed to the fact that the aorta is a much larger vessel capable of reaching peak compliance at earlier pressures compared with the smaller carotid arteries. Aortas also have a very different ultrastructure as compared with carotid arteries.

Our histological analysis reveals that OPN KO aortas have increased medial thickness at baseline, but this increase may be attributed to the straighter and more widely spaced elastic lamellae. In an intact, unloaded artery, elastin fibers typically appear undulated and wavy like those seen in the WT aorta (shown in the top left panel of Fig 5.11) [172]. However, as the transmural pressure increases, these elastin fibers straighten out as they begin to bear load, and continue to remain straight at physiologic pressure [172]. The arteries that were histologically analyzed in this study were all in the unloaded state when fixed, but it is interesting to note that the morphology of the elastin fibers of the baseline OPN KO aortas resemble that of a pressurized artery. This unique “loaded” morphology of elastin, even in the unloaded state, might suggest why OPN KO aortas at baseline distend significantly greater than WT aortas when pressurized. A more thorough evaluation of the regulation, organization, and function of other associated structural ECM proteins (such as collagen), and cell types such as smooth muscle cells (SMCs), needs to be performed for a better interpretation of these data.

For the final objective of this aim, we tested OPN KO aortas with AngII for 7 days and discovered that these aortas also have significantly higher PD curves when compared with P-D curves of WT AngII-treated aortas. This result suggests that OPN may also be responsible for the mechanical distension of the aorta in the setting of hypertension. Finally, it is important to observe from our histological analysis that AngII treated OPN KO aortas are dramatically protected against adventitial thickening and inflammation which is predominant in the AngII treated WT aortas (Figs

5.9, 5.11, and 5.13). A similar finding, but in the setting of neointimal formation was observed by Myers et al. In this study, OPN KO ligated carotid arteries showed significantly lesser neointimal formation than the ligated carotid arteries obtained from WT mice [171]. This study also showed an absence of leukocyte infiltration in histologic sections obtained from ligated carotid sections of OPN KO mice [171].

While this study provides us with interesting insights on the role of OPN in mediating the biomechanics of the aorta, there are several limitations that need to be considered while interpreting these results and considered while designing future experiments. A limitation of this study was the lack of characterization of the axial mechanics, residual stresses and strains, and ECM organization of these OPN KO aortas. Conducting fixed length axial force-pressure tests, opening angle measurements, and a more careful analysis of ECM organization via confocal would shed more light on these properties of the aorta. Confocal imaging of the aorta while being pressurized would allow us to observe differences in the structure and organization of the ECM. One can take z-stack images and images of the structure of elastin and collagen, harnessing the auto-fluorescence properties of these proteins.

Another limitation of this study was our inability to capture the stress-strain properties of the aorta of the different treatment groups. While local compliance data provides us with some insight into the mechanical differences between the treatment groups, stress-strain properties provide a better reflection of the true mechanical properties of biologic tissues [173]. Circumferential vessel stress and strain are defined as follows:

$$\text{Circumferential Stress } (\sigma_{\theta}) = \frac{P_i d_i}{h} \text{ -----[173, 174]}$$

where,  $P_i$  = Aortic Pressure,  $d_i$  = inner diameter of aorta,  $h$  = vessel wall thickness (calculated by subtracting inner diameter from outer diameter of the aorta)

$$\text{Circumferential Strain } (\varepsilon_{\theta}) = \frac{d_{\text{mean}} - D_{\text{mean}}}{D_{\text{mean}}} \text{ -----[173, 174]}$$

where,  $d_{\text{mean}} = (d_o + d_i)/2$  is the mean diameter, and  $D_{\text{mean}}$  is the in-vivo reference configuration

As the formulae above reflect, calculation of stress-strain properties requires measurement of both vessel outer-diameter and inner-diameter values, however, our device setup was only able to capture outer diameter and aortic pressure values. Hence, we were unable to analyze the real stress-strain properties of the aorta, given the lack of inner diameter data. Histological analysis reveals the inner diameter and medial thickness values at the unloaded configuration, therefore, we *may* use these values to approximate circumferential stress and strain values, but it is important to note that as transmural aortic pressure increases, the inner diameter ( $d_i$ ) and outer diameter ( $d_o$ ) increase, while the vessel wall thickness ( $h$ ) decreases and this would alter the estimated circumferential stress values. This reduced vessel wall thickness and increased inner diameter would translate to overall increases in circumferential stress and strain values.

In summary, we have shown that OPN does in fact have a significant impact on altering the biomechanical properties and morphology of the aorta. This was demonstrated by use of a transgenic OPN knockout (KO) mouse model that allowed us to delineate the specific role of OPN in the aorta. The combination of biomechanical data demonstrating differences in pressure-dependent diameter and compliance parameters, and histological evidence showing differences in medial and adventitial thickening, and elastin organization, strongly suggest that OPN plays an important role in regulating the mechanical properties of the vasculature in the absence or presence of disease.

**CHAPTER 6:**  
**SUMMARY, LIMITATIONS, FUTURE DIRECTIONS**

**Summary**

The primary objective of this thesis was to determine the role and regulation of osteopontin (OPN) in the aorta in the setting of hypertension. This was accomplished 1) through the use of an *in-vitro* model where mechanical strain was applied to aortic smooth muscle cells, 2) the use of two *in-vivo* models of murine hypertension, and 3) finally, the *ex-vivo* mechanical testing of OPN knockout (KO) aortas.

The effects of elevated blood pressure on the cells of the aorta such as the smooth muscle cells are myriad and complex. Several clinical and animal studies have supported the hypothesis that both increased mechanical strain and humoral factors play a role in mediating inflammation of the aorta. However, there is still a need to isolate the potential effects of each factor in a controlled manner; thus in aims 1 and 2 of this project we used an *in-vitro* system of mechanical strain and two distinct *in-vivo* models of hypertension in order to identify how each of these factors independently contributed to the expression of the pro-inflammatory OPN in the aorta. In aim 2, we further tested whether OPN was regulated by hydrogen peroxide (H<sub>2</sub>O<sub>2</sub>) through the use of a transgenic mouse model that overexpresses human catalase (an enzyme that scavenges H<sub>2</sub>O<sub>2</sub>) specifically in smooth muscle cells. The results of our studies from aims 1 and 2 produced the following results:

- 1) Mechanical strain, in the setting of hypertension, has a significant effect on elevating expression of OPN in aortic smooth muscle cells, as determined by both the *in-vitro* and *in-vivo* experimental tests used.
- 2) The hypertension-dependent increase in OPN is regulated by hydrogen peroxide

Despite it being known that OPN plays an important role in mediating vascular growth and remodeling, especially under inflammatory conditions, there is a significant lack of data available on whether it directly modulates the mechanical properties of the diseased aorta. We therefore mechanically tested OPN knockout (KO) aortas under both healthy and hypertensive conditions in aim 3 of this project to clarify its potential role in the biomechanics of large arteries. The results of aim 3 show us that:

- 1) OPN regulates pressure-dependent diameter properties and the matrix environment of the aorta
- 2) OPN has a significant impact on the maximal compliance properties under healthy conditions.
- 3) AngII-treated OPN KO aortas are protected against AngII-induced medial hypertrophy and adventitial inflammation

Overall our results deepen our understanding of hypertension mediated vascular inflammation and highlight the role of OPN in altering aortic biomechanics. Taken together, these results have important implications in the design and development of preventative or therapeutic strategies aimed against the consequences of hypertension.

## **Limitations and Future Considerations**

*Aim 1: Establish if mechanical strain in-vitro increases osteopontin*

The first limitation of this aim was the assumption that smooth muscle cells (SMCs) from all regions of the flexible membrane culture wells experience equal biaxial strains (in both the radial and circumferential direction) upon cyclic strain in the Flexercell™ device. However, a study by Vande Geest et al in which a finite element analysis was conducted to identify the complete strain field for the membranes of the Flexercell™ device, highlighted that the strain profiles of the regions of the membrane located directly above the loading post are different from the regions located off the post [131]. Based on the results of the biaxial simulations that were performed in this study, the biaxial and tangential strains for a circular region directly above the loading post were shown to be approximately equal, validating a state of equibiaxial strain for this region of the membrane. However, the region of the membrane located off the loading post was shown to produce large radial strains and small circumferential strains (Fig 6.1). The inconsistencies in the strain profile across the surface of the flexible culture membranes maybe one of the reasons why we failed to see an increasing cyclic strain magnitude-dependent response in OPN expression (Fig 3.7). Therefore, in future mechanical strain experiments, separating cells located directly above the loading post from those growing off the loading post, prior to analysis, will allow us to better resolve the effects of a single magnitude of mechanical strain.

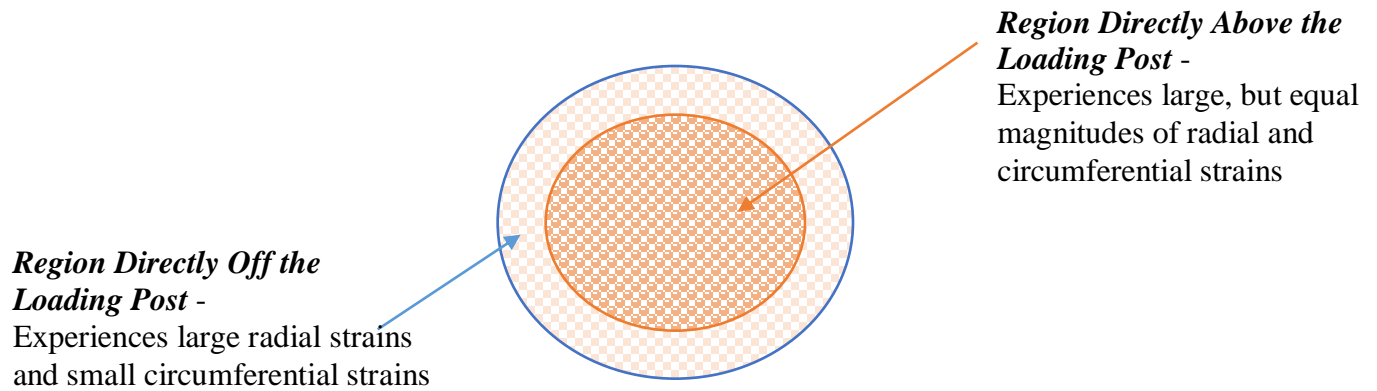


**Figure 6.1: Different regions of the flexible membrane well experience different strain profiles** A finite element analysis of the biaxial flexible membrane surface showed that the regions directly above the loading post experience large but equal magnitudes of radial and circumferential strains, however, the regions located off the loading post experience large radial strains and small circumferential strains. These results suggest that cells cultured on these plates experience a range of strains, that may contribute to the variability in results observed when conducting cyclic strain experiments.

The second limitation was the assumption that smooth muscle cells (SMCs) of the aorta experience an average cyclic strain of around 10%. There are several clinical and animal studies that have analyzed average aortic strains in both humans and animals, however, there is significant variability in the magnitudes of the aortic strain reported [119, 154, 175]. For example, a study by Bell et al reported that the circumferential strain experienced by the descending aorta averages around 12.2% (in men) to 13.7% (in women) [119]. Another study by Vogt et al showed that there is dramatic variability in the average circumferential strain measured across healthy aortas, from one subject to the next, with values ranging from as low as 6% to as high as 23% [153].

The ascending aorta experiences longitudinal strain (along the long axis of the aorta), as a result of the displacement of the sino-tubular junction, during systole [176]. This longitudinal displacement produces negative radial strain and circumferential strain, and maybe a biomarker of aortic stiffness [119]. However, there are very small longitudinal strains experienced by the descending aorta as reported in the literature [175, 177].

Based on these studies, we performed a strain-dependent study to see if OPN levels would vary with increasing strain magnitudes. We observed the most significant increase in OPN at 10%

strain. We, therefore, chose this strain magnitude for all our subsequent studies. In reality, however, SMCs likely experience a range of strains, depending on the region they are harvested from, the corresponding aortic geometry of the region, and the healthy or diseased state of the aorta. For future experiments, a careful *in-vivo* analysis of the range of strains experienced by the aorta, under varying conditions and at different locations of the aortic wall, prior to harvesting SMCs for *in-vitro* mechanical strain experiments, would allow us to more accurately recapitulate the mechanical environment sensed by these cells *in-vivo*.

Finally, another limitation of this aim is the lack of clarity on the role of hydrogen peroxide ( $H_2O_2$ ), in regulating the increase of OPN with mechanical strain. We conducted a study where we strained SMCs for 24 hours in the presence of PEG-Catalase. Media was harvested from these cells and an ELISA conducted to analyze secreted OPN levels, however, no significant effect of catalase on OPN levels was observed (Appendix, Fig A.1).

Given this result, we analyzed PEG-Catalase activity over the course of 24 hours in media. It was observed that PEG-Catalase incubated at  $37^\circ C$  for 24 hours drastically loses its activity within the first 6 hours of incubation (Appendix, Fig A.2). We, therefore, redesigned our experiment (Appendix, Fig A.3) such that SMCs would be exposed to a steady dose of active PEG-Catalase over the entire time course of the experiment. We did this, by adding PEG-Catalase at regular 6 hour intervals to the SMCs that were being strained, for a total of 24 hours. However, the results of this experiment also did not show any significant changes in the strain-induced increase in OPN expression with the addition of catalase (Appendix, Fig A.4). These results suggest that PEG-Catalase may not be an ideal candidate for scavenging  $H_2O_2$ , at least in the *in-vitro* setting. In future studies, a more stable method to reduce  $H_2O_2$  levels within cells, via culture of catalase overexpressing SMCs or transient overexpression of catalase, may provide more

conclusive evidence regarding the role of hydrogen peroxide in strain-induced OPN expression. However, caution must be taken while using SMCs from transgenic smooth muscle cell specific catalase overexpressing mice. SMCs from mice aortas were used at the onset of this project to analyze their behavior in response to cyclic strain. However, we observed that SMCs do not attach well onto the flexible membrane culture plates, and have inconsistent responses when cyclically strained. On the other hand, SMCs obtained from rat aortas attached more strongly to the surface of the flexible membrane plates, and had consistent behavior in response to cyclic strain. Therefore, the species from where SMCs are obtained ought to be carefully considered and experimental conditions optimized prior to testing.

*Aim 2: To determine if osteopontin expression is increased in a murine model of hypertension and if this increase is H<sub>2</sub>O<sub>2</sub>-dependent*

The results of aim 2 demonstrated that hypertension-induced OPN expression was mediated by H<sub>2</sub>O<sub>2</sub>. However, a limitation of this study is that it is unclear whether this event is mediated by the global decrease of H<sub>2</sub>O<sub>2</sub> within the entire aortic wall or the local decrease of H<sub>2</sub>O<sub>2</sub> specific to SMCs. There are studies from our lab (unpublished) that have suggested that AngII-treated mice that overexpress catalase specifically in macrophages are protected against inflammation and AAA formation. This finding implicates that the global decrease in H<sub>2</sub>O<sub>2</sub> within the aortic wall may be the underlying cause for the protection of the aorta against AngII-mediated increase in OPN. This hypothesis may be tested in the future by fluorescent staining of H<sub>2</sub>O<sub>2</sub> within segments of the aorta, which would clarify whether global or local decrease in H<sub>2</sub>O<sub>2</sub> is responsible for OPN reduction in the setting of AngII-induced hypertension. Co-staining aortic cross-sections

for OPN and H<sub>2</sub>O<sub>2</sub> may further elucidate the underlying mechanism responsible for regulating OPN expression.

A second limitation of this study was a lack of clarity on the role of superoxide in mediating hypertension-dependent increase of OPN. Our results from aim 1 suggest that superoxide is indeed upregulated in the setting of mechanical strain (Fig 3.8). It is also known from animal studies that hypertensive arterial tissues have higher levels of superoxide [178]. Therefore, in order to deepen our understanding of the range of ROS at work in the regulation of OPN, it is important in future studies to analyze the role of this molecule. This maybe done via pharmacologic intervention through the use of the superoxide scavenging enzyme, namely superoxide dismutase (SOD). As an alternate approach, transgenic SOD overexpressing mice or SOD KO 1 and 2 mice may also be used in order to explore the role of superoxide in regulating hypertension-induced OPN expression.

Another limitation of this study is the lack of validation of the finding that H<sub>2</sub>O<sub>2</sub> regulates hypertension-induced increases in OPN, using an alternative approach. While there are no reported changes in vascular physiology of the transgenic smooth muscle-specific overexpressing catalase strain of mice under baseline conditions (as characterized in [81]), it is unknown if there may be compensatory changes affecting other organ systems, as a result of this catalase overexpression. It is therefore important to validate these findings in the future using an alternative approach to decrease levels of H<sub>2</sub>O<sub>2</sub> within the aorta. One technique that may be considered for future experiments could involve pharmacologic intervention via the continuous infusion of PEG-catalase using a jugular catheter.

*Aim 3: To determine the contribution of osteopontin to the mechanical properties of the aorta at baseline and in the setting of hypertension.*

A limitation of our work in aim 3 is the lack of characterization of axial mechanics of the OPN KO aorta under healthy and hypertensive conditions. Even though our preliminary analysis suggested that there is no significant difference between the *in-vivo* length of the aortas of OPN KO and WT mice under baseline and hypertensive conditions, a more thorough analysis is necessary to clarify the role of OPN in mediating *both* circumferential and axial mechanics. This role may be clarified via axial force-length and axial force-pressure tests using the mechanical testing setup previously described by Gleason et al.

A second limitation of this aim was the lack of characterization of residual strains within the OPN KO and WT aortas under baseline and hypertensive conditions. Opening angles of blood vessels can be obtained by bisecting segments of the aorta cutting which results in the stress-free configuration of the vessel. Opening angles are a reflection of the residual circumferential strain within the inner and outer wall of a blood vessel, and also reflect differences in its material and mechanical properties. Given that we observed differences in medial hypertrophy, adventitial inflammation, elastin fiber organization and collagen expression in both the OPN KO and WT baseline and AngII-treated groups, characterization of the opening angles in the future could further validate these changes that we observed.

A third limitation of aim 3, is our interpretation or lack thereof, of the histology data showing altered elastin fiber organization of OPN KO aortas. Our data showed that OPN KO aortas at baseline have altered elastin fiber structure as compared to WT aortas. OPN KO aortas at baseline had elastin fibers that were straighter and exhibiting larger elastin interlamellar gaps (Fig

5.12-5.13), while WT aortas at baseline had elastin fibers that were wavy, undulating, and tightly spaced in concentric layers. It would be important in future studies to perform a more detailed analysis of the elastin and collagen organization of OPN KO and WT aortas. This may be done via confocal imaging of the aorta at different intraluminal pressures. A custom biomechanical device as developed by Gleason et al., that fits on an inverted confocal microscope maybe used to visualize the microstructure and ECM organization across the entire wall of unfixed, live OPN KO and WT aortas at different transmural pressures and axial stretches. Furthermore, the z-stack data obtained from this device would also allow for the precise calculation of the adventitial thickness (from collagen images) and medial thickness (from elastin images).

There is also a lack of data in aim 3 regarding the behavior of AngII treated OPN KO or WT aortas at later time points (21, 28 days or more). In this study, we look at early changes (3, 7, or 14 days of AngII treatment) in mechanical and morphological behavior of aortas. While we do in fact observe changes in the pressure-dependent diameter metrics of WT and OPN KO aortas at these early time points, we do not observe any changes in the compliance properties of these aortas. The lack of change in compliance properties in WT aortas at 3, 7, or 14 days of AngII treatment suggests that these aortas are able to perfectly remodel and adapt to increases in blood pressure. Therefore, based on our results from these early time point studies, we hypothesize that arterial stiffness in WT mice increases only under conditions of prolonged, untreated hypertension (21 days or longer) and that OPN KO mice are protected against this AngII-induced stiffening. Hence, future studies should evaluate the mechanical behavior of these OPN KO and WT aortas at later time points of AngII-induced hypertension. Finally, we only use a single model of hypertension to study the effects of OPN on the biomechanics of the aorta. In the future, it is important to utilize

multiple models of hypertension including norepinephrine (NE), which we have used in aim II to in order validate and expand our findings from this aim.

### **Implications**

Hypertension has a direct impact on vascular hypertrophy, and is a known risk factor for the development of atherosclerosis [81]. This atherogenic potential of hypertension has been proposed to exist, due to the pro-inflammatory state within the arterial wall, elicited by elevated blood pressure [2]. It is already well established in literature that one of the early changes in hypertension is the generation of reactive oxygen species (ROS) within the vessel wall [2, 39, 46, 77, 80, 90, 134]. These increased ROS levels, result in the upregulation of redox-sensitive gene products such as MCP-1 and VCAM-1, that lead to the infiltration of leukocytes and macrophages, ultimately resulting in either atherosclerosis or vascular hypertrophy [49, 89, 134, 179]. The results of this thesis provide a novel mechanism by which this pro-inflammatory state is developed in the aorta, via osteopontin (OPN). Our results have shown that OPN is significantly upregulated, in smooth muscle cells with the application of mechanical strain, and in the aorta with elevated blood pressure. We have further observed that this hypertension-induced increase in OPN is mediated by hydrogen peroxide. Overall these results provide a novel redox-sensitive mechanism by which hypertension, induces inflammation within the aorta.

This work has also provided unique insights on the role of OPN in regulating the mechanics of blood vessels. In OPN knockout (KO) aortas, it was interesting to note that the pressure-dependent diameter curves had an upward shift (or larger diameters), when compared to aortas expressing OPN (from WT mice), under both baseline and hypertensive conditions. Baseline OPN KO aortas also had a greater maximal compliance (at 60mm Hg) compared to WT aortas, suggesting that OPN may be playing a role in regulating mid-range pressure compliance properties

of blood vessels. Adventitial inflammation and vascular hypertrophy were significantly attenuated in hypertensive OPN KO mice compared to hypertensive WT mice. There was also a blunting in collagen expression in the hypertensive OPN KO aortas. Finally, our histological analysis revealed that OPN KO aortas had altered elastin fiber morphology compared to WT aortas at baseline conditions. In the future, a more detailed analysis on elastin fiber orientation and organization is necessary, to understand the role of OPN in the regulation of elastin morphology and function.

These novel insights into the redox-sensitive expression of OPN and its contribution to arterial biomechanics, together, provides us with a clearer understanding of the progression of atherosclerosis in the setting of hypertension. This knowledge should be carefully considered in the future design of therapies and strategies aimed against the consequences of hypertension, the most common being atherosclerosis.

Finally, these findings on the redox-sensitive regulation of OPN, imply that it may also be upregulated via a similar signaling pathway, in the setting of the formation of aortic abdominal aneurysms (AAAs). There are animal studies that have already established OPN's role in the formation of AAA [180]. There are studies that have also explored the association between OPN polymorphisms and AAA formations, however, no association was observed between the five single nucleotide polymorphisms or haplotypes of the OPN gene and AAA formation or aortic diameter [181]. However, it was shown that the serum concentration of OPN had an association with AAA formation. Taking these results and our studies one step further, we speculate that OPN may also serve as a useful biomarker not only for AAAs, but for other vascular inflammation-related complications as well, such as AAAs or atherosclerosis.

Previous work from our group and others, have also revealed parallel changes that occur in the early stages of AAA formation and hypertension-related atherosclerosis – such as significant

oxidative stress, increase in pro-inflammatory proteins, and infiltration of macrophages and leukocytes into the vessel wall. All these findings taken together reveal a critical role for osteopontin in mediating vascular inflammation and its consequences that range from atherosclerosis to AAAs.

### **Conclusion**

This work has provided evidence, for the first time, that osteopontin (OPN) is a mechanosensitive inflammatory product expressed by SMCs of the aorta. We have identified that OPN is upregulated with hypertension and have demonstrated a causal role of H<sub>2</sub>O<sub>2</sub> in mediating this increase. Finally, we have identified a novel role for OPN in mediating the structure and mechanics of the aorta under both a healthy and hypertensive context. As highlighted in this chapter, the findings of this work provide additional questions and render alternative directions to pursue, in the context of hypertension-induced vascular inflammation. These findings give us novel insights into the pathogenesis of inflammation and a deeper understanding of the relation between molecular and mechanical events within the aorta.

APPENDIX

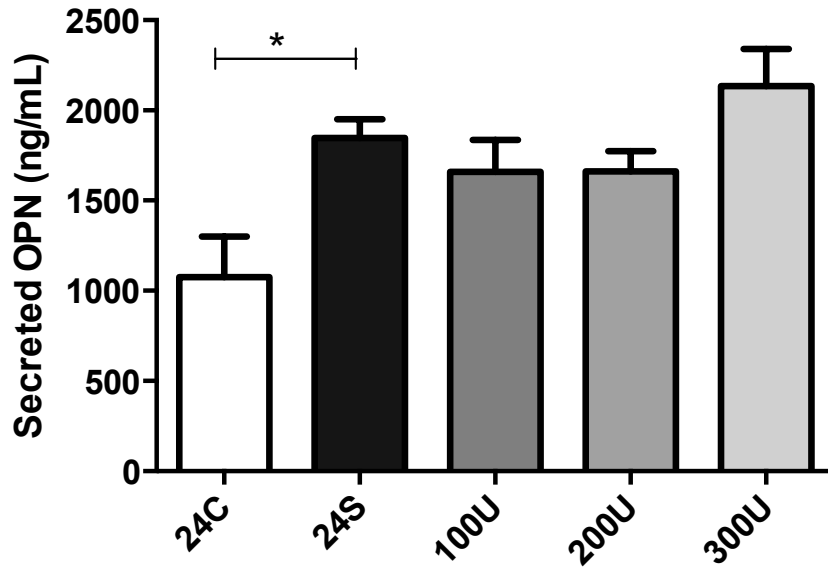


**Figure A.1: Cyclic Strain-induced Increase in OPN was not Affected with 24 hours PEG-Catalase Treatment** We measured secreted OPN expression in cells strained and treated with PEG-Catalase for 24 hours. We observed a significant increase in secreted OPN expression with 24 hours of strain (black bar) compared to the non-strained control (white bar). However, no difference in OPN expression was observed in strained cells treated with PEG-Catalase treatment (U/mL) (gray bars) for an N=6

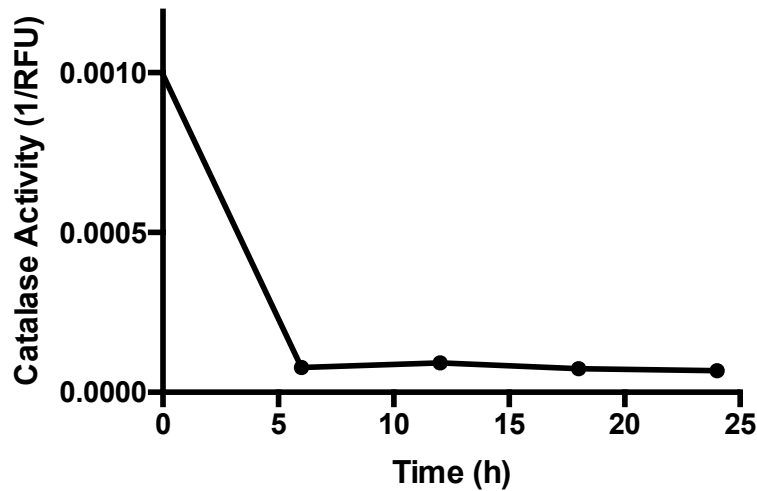


**Figure A.2: Catalase Activity in Cell Culture Medium Drops Within 6 hours** We observed that PEG-Catalase in Cell Culture Medium at 37°C drastically loses activity within the first 6 hours of incubation. We used 200U/mL of PEG-Catalase for this experiment.

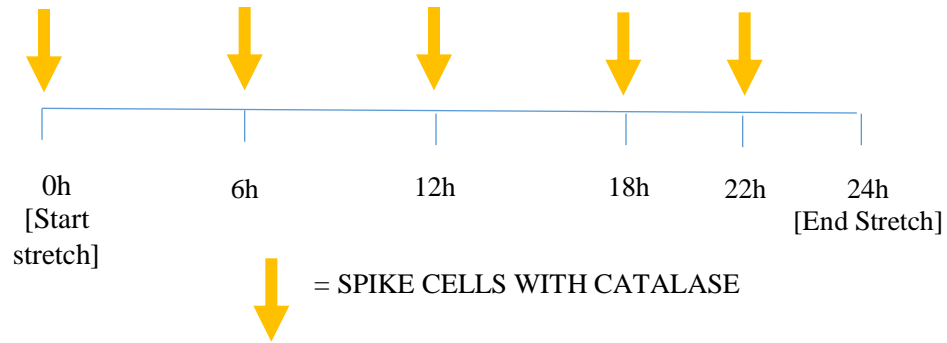


**Figure A.3: Updated Experimental Design to Account for Reduced Catalase Activity** In order to account for decreased PEG-Catalase activity within 6 hours of incubation, we updated the experimental design to include periodic spiking of strained SMCs every 6 hours (where PEG-Catalase would be added at the start 0h, 6h, 12h, 18h, and 22h of the test)

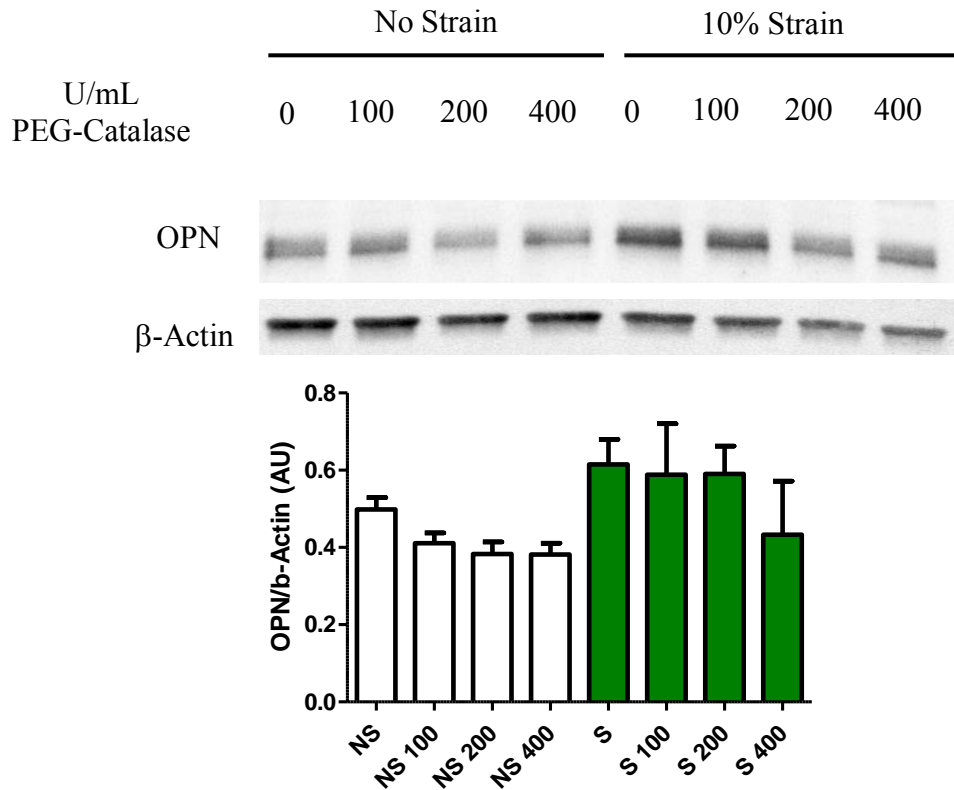


**Figure A.4: PEG-Catalase May Blunt Strained-induced cellular OPN at Higher Concentrations** OPN protein levels were measured using Western Blot analysis and normalized to β-Actin \* $p < 0.05$ , \*\* $p < 0.01$ ,  $N = 3$ . We observed a trending decrease in OPN expression with treatment of a higher concentration of PEG-Catalase at 400U/mL.

## REFERENCES

1. Victor, R.G., *Systemic Hypertension: Mechanisms and Diagnosis*, in *Braunwald's Heart Disease: Textbook of Cardiovascular Medicine*. p. 934-951.
2. Alexander, R.W., *Hypertension and the pathogenesis of atherosclerosis oxidative stress and the mediation of arterial inflammatory response: a new perspective*. *Hypertension*, 1995. **25**(2): p. 155-161.
3. Taylor, W.R., *Hypertensive vascular disease and inflammation: mechanical and humoral mechanisms*. *Current hypertension reports*, 1999. **1**(1): p. 96-101.
4. Taylor, W.R., *Mechanical deformation of the arterial wall in hypertension: a mechanism for vascular pathology*. *The American journal of the medical sciences*, 1998. **316**(3): p. 156-161.
5. Giachelli, C.M., et al., *Osteopontin is elevated during neointima formation in rat arteries and is a novel component of human atherosclerotic plaques*. *Journal of Clinical Investigation*, 1993. **92**(4): p. 1686.
6. Alameddine, F.M.F. and F.W.R. Taylor, *Role of Osteopontin in Hypertensive Vascular Hypertrophy*. 2002: p. 5-7.
7. Lyle, A.N., et al., *Hydrogen peroxide regulates osteopontin expression through activation of transcriptional and translational pathways*. *Journal of Biological Chemistry*, 2014.
8. *Know the Facts About High Blood Pressure*, in *Centers for Disease Control Website*, CDC, Editor 2015, CDC: Atlanta.
9. *High Blood Pressure Fact Sheet 2015*, in *Center For Disease Control Website*, CDC, Editor 2015: Atlanta.
10. Constanzo, L.S., *Cardiovascular Physiology*. *Physiology*, 2009(4): p. 113-184.
11. Augoustides, J.G., E.J. Pantn, and A.T. Cheung, *Thoracic Aorta*, in *Cardiac Anesthesiology*. p. 637-673.
12. Pappano, A.J. and W.G. Wier, *Hemodynamics*, in *Cardiovascular Physiology*. p. 119-134.
13. Silver, F.H., P.B. Snowhill, and D.J. Foran, *Mechanical Behavior of Vessel Wall: A Comparative Study of Aorta, Vena Cava, and Carotid Artery*. *Annals of Biomedical Engineering*, 2003. **31**(7): p. 793-803.

14. PATEL, D.J. and J.S. JANICKI, *Static elastic properties of the left coronary circumflex artery and the common carotid artery in dogs*. *Circulation Research*, 1970. **27**(2): p. 149-158.
15. Kalath, S., P. Tsipouras, and F.H. Silver, *Non Invasive Assessment of Aortic Mechanical Properties*. *Annals of Biomedical Engineering*, 1986. **14**: p. 513-524.
16. Papadaki, M. and S.G. Eskin, *Effects of Fluid Shear Stress on Gene Regulation of Vascular Cells*. *Biotechnol Prog*, 1997. **13**: p. 209-221.
17. Ueshima, H., *Epidemiology of Hypertension*, in *Cardiology*, Elsevier: Philadelphia. p. 523-534.
18. Goldstein, L.B., et al., *Guidelines for the primary prevention of stroke a guideline for healthcare professionals from the American Heart Association/American Stroke Association*. *Stroke*, 2011. **42**(2): p. 517-584.
19. Nwankwo, T., et al., *Hypertension Among Adults in the US - National Health and Nutrition Examination Survey, 2011-2012*, U.D.o.H.a.H. Services, Editor 2013, NCHS.
20. Pimenta, E., D.A. Calhoun, and S. Oparil, *Etiology and Pathogenesis of Systemic Hypertension*, in *Cardiology* 2009, Elsevier: Philadelphia. p. 511-522.
21. Savoia, C. and E.L. Schiffrin, *Inflammation in hypertension*. *Current opinion in nephrology and hypertension*, 2006. **15**(2): p. 152-158.
22. Vardulaki, K., et al., *Quantifying the risks of hypertension, age, sex and smoking in patients with abdominal aortic aneurysm*. *British journal of surgery*, 2000. **87**(2): p. 195-200.
23. Larson, E.W. and W.D. Edwards, *Risk factors for aortic dissection: a necropsy study of 161 cases*. *The American journal of cardiology*, 1984. **53**(6): p. 849-855.
24. Antikainen, R., P. Jousilahti, and J. Tuomilehto, *Systolic blood pressure, isolated systolic hypertension and risk of coronary heart disease, strokes, cardiovascular disease and all-cause mortality in the middle-aged population*. *Journal of hypertension*, 1998. **16**(5): p. 577-583.
25. Brunner, H.R., et al., *Essential hypertension: renin and aldosterone, heart attack and stroke*. *New England Journal of Medicine*, 1972. **286**(9): p. 441-449.
26. Chae, C.U., et al., *Blood pressure and inflammation in apparently healthy men*. *Hypertension*, 2001. **38**(3): p. 399-403.

27. Iwashima, Y., et al., *C-reactive protein, left ventricular mass index, and risk of cardiovascular disease in essential hypertension*. Hypertension Research, 2007. **30**(12): p. 1177.
28. Hwang, S.-J., et al., *Circulating adhesion molecules VCAM-1, ICAM-1, and E-selectin in carotid atherosclerosis and incident coronary heart disease cases the atherosclerosis risk in communities (ARIC) study*. Circulation, 1997. **96**(12): p. 4219-4225.
29. Zeisler, H., et al., *Serum levels of adhesion molecules in women with pregnancy-induced hypertension*. Wiener klinische Wochenschrift, 2001. **113**(15-16): p. 588-592.
30. Han, Y., M.S. Runge, and A.R. Brasier, *Angiotensin II induces interleukin-6 transcription in vascular smooth muscle cells through pleiotropic activation of nuclear factor- $\kappa$ B transcription factors*. Circulation Research, 1999. **84**(6): p. 695-703.
31. Fiebeler, A., et al., *Mineralocorticoid receptor affects AP-1 and nuclear factor- $\kappa$ B activation in angiotensin II-induced cardiac injury*. Hypertension, 2001. **37**(2): p. 787-793.
32. Owens, A.P., et al., *Angiotensin II Induces a Region-Specific Hyperplasia of the Ascending Aorta Through Regulation of Inhibitor of Differentiation 3*. Circulation Research, 2009. **106**(3): p. 611-619.
33. Owens, G.K., M.S. Kumar, and B.R. Wamhoff, *Molecular regulation of vascular smooth muscle cell differentiation in development and disease*. Physiological reviews, 2004. **84**(3): p. 767-801.
34. Thubrikar, M.J. and F. Robicsek, *Pressure-Induced Arterial Wall Stress and Atherosclerosis*. Annals of Thoracic Surgery, 1995. **59**: p. 1594-1603.
35. Weiss, D. and W.R. Taylor, *Deoxycorticosterone Acetate Salt Hypertension in Apolipoprotein E-/- Mice Results in Accelerated Atherosclerosis: The Role of Angiotensin II*. Hypertension, 2008. **51**(2): p. 218-224.
36. Dzau, V., *Circulating versus local renin-angiotensin system in cardiovascular homeostasis*. Circulation, 1988. **77**(6 Pt 2): p. I4-13.
37. Griendling, K.K., T. Murphy, and R.W. Alexander, *Molecular biology of the renin-angiotensin system*. Circulation, 1993. **87**(6): p. 1816-1828.
38. Lavoie, J.L. and C.D. Sigmund, *Minireview: overview of the renin-angiotensin system—an endocrine and paracrine system*. Endocrinology, 2003. **144**(6): p. 2179-2183.

39. Touyz, R.M., *Reactive Oxygen Species, Vascular Oxidative Stress, and Redox Signaling in Hypertension: What Is the Clinical Significance?* Hypertension, 2004. **44**(3): p. 248-252.
40. Kagami, S., et al., *Angiotensin II stimulates extracellular matrix protein synthesis through induction of transforming growth factor-beta expression in rat glomerular mesangial cells.* Journal of Clinical Investigation, 1994. **93**(6): p. 2431.
41. Gibbons, G.H., R. Pratt, and V.J. Dzau, *Vascular smooth muscle cell hypertrophy vs. hyperplasia. Autocrine transforming growth factor-beta 1 expression determines growth response to angiotensin II.* Journal of Clinical Investigation, 1992. **90**(2): p. 456.
42. Daemen, M., et al., *Angiotensin II induces smooth muscle cell proliferation in the normal and injured rat arterial wall.* Circulation Research, 1991. **68**(2): p. 450-456.
43. Vaughan, D.E., S.A. Lazos, and K. Tong, *Angiotensin II Promotes PAII in Cultured Endothelial Cells.* Journal of Clinical Investigation, 1995. **95**: p. 995-1001.
44. Galis, Z.S., et al., *Increased Expression of Matrix Metalloproteinases and Matrix Degrading Activity in Vulnerable Regions of Human Atherosclerotic Plaques.* Journal of Clinical Investigation, 1994. **94**: p. 2493-2503.
45. Griendling, K.K., et al., *Angiotensin II stimulates NADH and NADPH oxidase activity in cultured vascular smooth muscle cells.* Circulation Research, 1994. **74**(6): p. 1141-1148.
46. Griendling, K.K., *Oxidative Stress and Cardiovascular Injury: Part I: Basic Mechanisms and In Vivo Monitoring of ROS.* Circulation, 2003. **108**(16): p. 1912-1916.
47. Dikalova, A., *Nox1 Overexpression Potentiates Angiotensin II-Induced Hypertension and Vascular Smooth Muscle Hypertrophy in Transgenic Mice.* Circulation, 2005. **112**(17): p. 2668-2676.
48. Touyz, R.M., et al., *Expression of a functionally active gp91phox-containing neutrophil-type NAD (P) H oxidase in smooth muscle cells from human resistance arteries regulation by angiotensin II.* Circulation research, 2002. **90**(11): p. 1205-1213.
49. De Ciuceis, C., et al., *Reduced Vascular Remodeling, Endothelial Dysfunction, and Oxidative Stress in Resistance Arteries of Angiotensin II–Infused Macrophage Colony-Stimulating Factor–Deficient Mice Evidence for a Role in Inflammation in Angiotensin-Induced Vascular Injury.* Arteriosclerosis, thrombosis, and vascular biology, 2005. **25**(10): p. 2106-2113.

50. Giroud, C., J. Stachenko, and E.H. Venning, *Secretion of aldosterone by the zona glomerulosa of rat adrenal glands incubated in vitro*. Experimental Biology and Medicine, 1956. **92**(1): p. 154-158.
51. Chonko, A.M., et al., *The role of renin and aldosterone in the salt retention of edema*. The American journal of medicine, 1977. **63**(6): p. 881-889.
52. Brilla, C.G. and K.T. Weber, *Mineralocorticoid excess, dietary sodium, and myocardial fibrosis*. The Journal of laboratory and clinical medicine, 1992. **120**(6): p. 893-901.
53. Tank, A.W. and D. Lee Wong, *Peripheral and central effects of circulating catecholamines*. Compr Physiol, 2015. **5**(1): p. 1-15.
54. Blaes, N. and J.-P. Boissel, *Growth-Stimulating Effect of Catecholamines on Rat Aortic Smooth Muscle Cells in Culture*. Journal of Cellular Physiology, 1963. **116**: p. 167-172.
55. Armentano, R., et al., *Mechanical pressure versus intrinsic effects of hypertension on large arteries in humans*. Hypertension, 1991. **18**(5): p. 657-664.
56. Burton, A.C., *On the Physical Equilibrium of Small Blood Vessels*. American Journal of Physiology, 1951. **164**: p. 319-329.
57. Ollerenshaw, J.D., et al., *The effects of coarctation hypertension upon vascular inositol phospholipid hydrolysis in Wistar rats*. Journal of hypertension, 1988. **6**(9): p. 733-738.
58. Datla, S.R. and K.K. Griendling, *Reactive Oxygen Species, NADPH Oxidases, and Hypertension*. Hypertension, 2010. **56**(3): p. 325-330.
59. Knowles, R.G. and S. Moncada, *Nitric oxide synthases in mammals*. Biochemical Journal, 1994. **298**(Pt 2): p. 249.
60. Ignarro, L.J., et al., *Endothelium-derived relaxing factor produced and released from artery and vein is nitric oxide*. Proceedings of the National Academy of Sciences, 1987. **84**(24): p. 9265-9269.
61. Loscalzo, J., *Nitric oxide insufficiency, platelet activation, and arterial thrombosis*. Circulation research, 2001. **88**(8): p. 756-762.
62. Ignarro, L.J., *Endothelium-derived nitric oxide: actions and properties*. The FASEB Journal, 1989. **3**(1): p. 31-36.

63. Wu, M., et al., *Involvement of nitric oxide and nitrosothiols in relaxation of pulmonary arteries to peroxynitrite*. American Journal of Physiology-Heart and Circulatory Physiology, 1994. **266**(5): p. H2108-H2113.
64. Darley-usmar, V.M., et al., *The simultaneous generation of superoxide and nitric oxide can initiate lipid peroxidation in human low density lipoprotein*. Free Radical Research, 1992. **17**(1): p. 9-20.
65. White, C.R., et al., *Superoxide and peroxynitrite in atherosclerosis*. Proceedings of the National Academy of Sciences, 1994. **91**(3): p. 1044-1048.
66. Ushio-Fukai, M., et al., *P22phox is a critical component of the superoxide-generating NADH/NADPH oxidase system and regulates angiotensin ii-induced hypertrophy in vascular smooth muscle cells*. Journal of Biological Chemistry, 1996. **271**(38): p. 23317-23321.
67. Dikalov, S.I., et al., *Distinct roles of Nox1 and Nox4 in basal and angiotensin II-stimulated superoxide and hydrogen peroxide production*. Free Radic Biol Med, 2008. **45**(9): p. 1340-51.
68. Redon, J., et al., *Antioxidant activities and oxidative stress byproducts in human hypertension*. Hypertension, 2003. **41**(5): p. 1096-101.
69. Beckman, J.S. and W.H. Koppenol, *Nitric oxide, superoxide, and peroxynitrite: the good, the bad, and ugly*. American Journal of Physiology-Cell Physiology, 1996. **271**(5): p. C1424-C1437.
70. Thomas, S.R., P.K. Witting, and G.R. Drummond, *Redox control of endothelial function and dysfunction: molecular mechanisms and therapeutic opportunities*. Antioxidants & redox signaling, 2008. **10**(10): p. 1713-1766.
71. Chen, K., S.R. Thomas, and J.F. Keaney, *Beyond LDL oxidation: ROS in vascular signal transduction*. Free Radical Biology and Medicine, 2003. **35**(2): p. 117-132.
72. Griending, K.K. and G.A. FitzGerald, *Oxidative stress and cardiovascular injury part I: basic mechanisms and in vivo monitoring of ROS*. Circulation, 2003. **108**(16): p. 1912-1916.
73. Taniyama, Y. and K.K. Griending, *Reactive oxygen species in the vasculature molecular and cellular mechanisms*. Hypertension, 2003. **42**(6): p. 1075-1081.
74. Lassegue, B. and K.K. Griending, *NADPH Oxidases: Functions and Pathologies in the Vasculature*. Arteriosclerosis, Thrombosis, and Vascular Biology, 2009. **30**(4): p. 653-661.

75. Lambeth, J.D., *Nox enzymes, ROS, and chronic disease: an example of antagonistic pleiotropy*. *Free Radical Biology and Medicine*, 2007. **43**(3): p. 332-347.
76. Miller, F.J., et al., *Oxidative stress in human abdominal aortic aneurysms a potential mediator of aneurysmal remodeling*. *Arteriosclerosis, thrombosis, and vascular biology*, 2002. **22**(4): p. 560-565.
77. Griendling, K.K. and G.A. FitzGerald, *Oxidative stress and cardiovascular injury part II: animal and human studies*. *Circulation*, 2003. **108**(17): p. 2034-2040.
78. Rajagopalan, S., et al., *Reactive oxygen species produced by macrophage-derived foam cells regulate the activity of vascular matrix metalloproteinases in vitro. Implications for atherosclerotic plaque stability*. *Journal of Clinical Investigation*, 1996. **98**(11): p. 2572.
79. Grote, K., *Mechanical Stretch Enhances mRNA Expression and Proenzyme Release of Matrix Metalloproteinase-2 (MMP-2) via NAD(P)H Oxidase-Derived Reactive Oxygen Species*. *Circulation Research*, 2003. **92**(11): p. 80e-86.
80. Redon, J., *Antioxidant Activities and Oxidative Stress Byproducts in Human Hypertension*. *Hypertension*, 2003. **41**(5): p. 1096-1101.
81. Zhang, Y., et al., *Vascular hypertrophy in angiotensin II-induced hypertension is mediated by vascular smooth muscle cell-derived H<sub>2</sub>O<sub>2</sub>*. *Hypertension*, 2005. **46**(4): p. 732-7.
82. Banday, A.A., et al., *Mechanisms of oxidative stress-induced increase in salt sensitivity and development of hypertension in Sprague-Dawley rats*. *Hypertension*, 2007. **49**(3): p. 664-671.
83. Briones, A.M., et al., *Atorvastatin prevents angiotensin II-induced vascular remodeling and oxidative stress*. *Hypertension*, 2009. **54**(1): p. 142-149.
84. Gavrilu, D., et al., *Vitamin E inhibits abdominal aortic aneurysm formation in angiotensin II-infused apolipoprotein E-deficient mice*. *Arteriosclerosis, thrombosis, and vascular biology*, 2005. **25**(8): p. 1671-1677.
85. Lyle, A.N., *Modulation of Vascular Smooth Muscle Signaling by Reactive Oxygen Species*. *Physiology*, 2006. **21**(4): p. 269-280.
86. Hohler, B., B. Holzapfel, and W. Kummer, *NADPH Oxidase Subunits and Superoxide Production in Porcine Pulmonary Artery Endothelial Cells* *Histochem Cell Biology*, 2000. **114**: p. 29-37.

87. Sorescu, D., et al., *Superoxide production and expression of nox family proteins in human atherosclerosis*. *Circulation*, 2002. **105**(12): p. 1429-1435.
88. Lassegue, B. and R.E. Clempus, *Vascular NAD (P) H oxidases: specific features, expression, and regulation*. *American Journal of Physiology-Regulatory, Integrative and Comparative Physiology*, 2003. **285**(2): p. R277-R297.
89. Rodríguez-Iturbe, B., et al., *Oxidative stress, renal infiltration of immune cells, and salt-sensitive hypertension: all for one and one for all*. *American Journal of Physiology-Renal Physiology*, 2004. **286**(4): p. F606-F616.
90. Tanito, M., et al., *Enhanced Oxidative Stress and Impaired Thioredoxin Expression in Spontaneously Hypertensive Rats*. *Antioxidants and Redox Signaling*, 2004. **6**(1): p. 89-97.
91. Nishiyama, A., et al., *Possible contributions of reactive oxygen species and mitogen-activated protein kinase to renal injury in aldosterone/salt-induced hypertensive rats*. *Hypertension*, 2004. **43**(4): p. 841-848.
92. Moreno, M.a.U., et al., *Preliminary characterisation of the promoter of the human p22phox gene: identification of a new polymorphism associated with hypertension*. *FEBS Letters*, 2003. **542**(1-3): p. 27-31.
93. Li, J.-M. and A.M. Shah, *Endothelial cell superoxide generation: regulation and relevance for cardiovascular pathophysiology*. *American Journal of Physiology-Regulatory, Integrative and Comparative Physiology*, 2004. **287**(5): p. R1014-R1030.
94. Cai, H. and D.G. Harrison, *Endothelial dysfunction in cardiovascular diseases: the role of oxidant stress*. *Circulation research*, 2000. **87**(10): p. 840-844.
95. Denhardt, D.T., et al., *Osteopontin as a means to cope with environmental insults: regulation of inflammation, tissue remodeling, and cell survival*. *Journal of Clinical Investigation*, 2001. **107**(9): p. 1055.
96. Sodek, J., et al., *Novel Functions of the Matricellular Proteins Osteopontin and Osteonectin/SPARC*. *Connective Tissue Research*, 2002. **43**(2-3): p. 308-319.
97. Sodek, J., B. Ganss, and M.D. McKee, *Osteopontin*. *Critical Reviews in Oral Biology & Medicine*, 2000. **11**(3): p. 279-303.
98. Liaw, L., et al., *The adhesive and migratory effects of osteopontin are mediated via distinct cell surface integrins. Role of alpha v beta 3 in smooth muscle cell migration to osteopontin in vitro*. *Journal of Clinical Investigation*, 1995. **95**(2): p. 713.

99. Bayless, K.J., et al., *Osteopontin is a ligand for the alpha4beta1 integrin*. Journal of Cell Science, 1998. **111**(9): p. 1165-1174.
100. Barry, S.T., et al., *A regulated interaction between  $\alpha 5\beta 1$  integrin and osteopontin*. Biochemical and biophysical research communications, 2000. **267**(3): p. 764-769.
101. Denda, S., L.F. Reichardt, and U. Müller, *Identification of osteopontin as a novel ligand for the integrin  $\alpha 8\beta 1$  and potential roles for this integrin–ligand interaction in kidney morphogenesis*. Molecular biology of the cell, 1998. **9**(6): p. 1425-1435.
102. Smith, L.L., et al., *Osteopontin N-terminal domain contains a cryptic adhesive sequence recognized by  $\alpha 9\beta 1$  integrin*. Journal of Biological Chemistry, 1996. **271**(45): p. 28485-28491.
103. Senger, D.R., et al., *Adhesive properties of osteopontin: regulation by a naturally occurring thrombin-cleavage in close proximity to the GRGDS cell-binding domain*. Molecular biology of the cell, 1994. **5**(5): p. 565-574.
104. Lin, Y.-H. and H.-F. Yang-Yen, *The osteopontin-CD44 survival signal involves activation of the phosphatidylinositol 3-kinase/Akt signaling pathway*. Journal of Biological Chemistry, 2001. **276**(49): p. 46024-46030.
105. Weber, G.F., et al., *Receptor-ligand interaction between CD44 and osteopontin (Eta-1)*. Science, 1996. **271**(5248): p. 509-512.
106. O'Regan, A. and J.S. Berman, *Osteopontin: a key cytokine in cell-mediated and granulomatous inflammation*. International journal of experimental pathology, 2000. **81**(6): p. 373-390.
107. Patarca, R., R.A. Saavedra, and H. Cantor, *Molecular and cellular basis of genetic resistance to bacterial infection: the role of the early T-lymphocyte activation-1/osteopontin gene*. Critical reviews in immunology, 1992. **13**(3-4): p. 225-246.
108. Liaw, L., et al., *Altered wound healing in mice lacking a functional osteopontin gene (spp1)*. Journal of Clinical Investigation, 1998. **101**(7): p. 1468.
109. Rittling, S. and A. Chambers, *Role of osteopontin in tumour progression*. British journal of cancer, 2004. **90**(10): p. 1877-1881.
110. Isoda, K., *Osteopontin Plays an Important Role in the Development of Medial Thickening and Neointimal Formation*. Circulation Research, 2002. **91**(1): p. 77-82.

111. Speer, M., et al., *Smooth muscle cells deficient in osteopontin have enhanced susceptibility to calcification in vitro*. Cardiovascular Research, 2005. **66**(2): p. 324-333.
112. Wada, T., et al., *Calcification of vascular smooth muscle cell cultures inhibition by osteopontin*. Circulation Research, 1999. **84**(2): p. 166-178.
113. Duvall, C.L., et al., *The Role of Osteopontin in Recovery from Hind Limb Ischemia*. Arteriosclerosis, Thrombosis, and Vascular Biology, 2007. **28**(2): p. 290-295.
114. Lyle, A.N., et al., *Reactive oxygen species regulate osteopontin expression in a murine model of postischemic neovascularization*. Arteriosclerosis, thrombosis, and vascular biology, 2012. **32**(6): p. 1383-1391.
115. Okura, T., et al., *Osteopontin and carotid atherosclerosis in patients with essential hypertension*. Clinical Science, 2006. **111**(5): p. 319.
116. Okamoto, H., *Osteopontin and cardiovascular system*. Molecular and cellular biochemistry, 2007. **300**(1-2): p. 1-7.
117. Griendling, K., et al., *Characterization of phosphatidylinositol-specific phospholipase C from cultured vascular smooth muscle cells*. Journal of Biological Chemistry, 1991. **266**(23): p. 15498-15504.
118. Lyle, A.N., et al., *Poldip2, a Novel Regulator of Nox4 and Cytoskeletal Integrity in Vascular Smooth Muscle Cells*. Circulation Research, 2009. **105**(3): p. 249-259.
119. Bell, V., et al., *Longitudinal and circumferential strain of the proximal aorta*. Journal of the American Heart Association, 2014. **3**(6): p. e001536.
120. Riganti, C., et al., *Diphenyleneiodonium inhibits the cell redox metabolism and induces oxidative stress*. Journal of Biological Chemistry, 2004. **279**(46): p. 47726-47731.
121. Jaquet, V., et al., *Small-molecule NOX inhibitors: ROS-generating NADPH oxidases as therapeutic targets*. Antioxidants & redox signaling, 2009. **11**(10): p. 2535-2552.
122. Heumüller, S., et al., *Apocynin is not an inhibitor of vascular NADPH oxidases but an antioxidant*. Hypertension, 2008. **51**(2): p. 211-217.
123. Touyz, R.M., *Apocynin, NADPH Oxidase, and Vascular Cells A Complex Matter*. Hypertension, 2008. **51**(2): p. 172-174.
124. Leung, D., S. Glagov, and M.B. Mathews, *Cyclic stretching stimulates synthesis of matrix components by arterial smooth muscle cells in vitro*. Science, 1976. **191**(4226): p. 475-477.

125. Buck, R.C., *Behaviour of vascular smooth muscle cells during repeated stretching of the substratum in vitro*. *Atherosclerosis*, 1983. **46**(2): p. 217-223.
126. Lundberg, M.S., et al., *Actin isoform and  $\alpha 1B$ -adrenoceptor gene expression in aortic and coronary smooth muscle is influenced by cyclical stretch*. *In Vitro Cellular & Developmental Biology-Animal*, 1995. **31**(8): p. 595-600.
127. Hishikawa, K. and T.F. Luscher, *Pulsatile Stretch Stimulates Superoxide Production in Human Aortic Endothelial Cells*. *Circulation*, 1997. **96**(10): p. 3610-3616.
128. Hishikawa, K., et al., *Pulsatile stretch stimulates superoxide production and activates nuclear factor- $\kappa B$  in human coronary smooth muscle*. *Circulation Research*, 1997. **81**(5): p. 797-803.
129. Lehoux, S., et al., *Pulsatile Stretch–Induced Extracellular Signal–Regulated Kinase 1/2 Activation in Organ Culture of Rabbit Aorta Involves Reactive Oxygen Species*. *Arteriosclerosis, thrombosis, and vascular biology*, 2000. **20**(11): p. 2366-2372.
130. Remus, E.W., et al., *miR181a protects against angiotensin II-induced osteopontin expression in vascular smooth muscle cells*. *Atherosclerosis*, 2013. **228**(1): p. 168-174.
131. Geest, J.P.V., E.S. Di Martino, and D.A. Vorp, *An analysis of the complete strain field within Flexercell TM membranes*. *Journal of biomechanics*, 2004. **37**(12): p. 1923-1928.
132. Willett, N.J., et al., *An in vivo murine model of low-magnitude oscillatory wall shear stress to address the molecular mechanisms of mechanotransduction—Brief report*. *Arteriosclerosis, thrombosis, and vascular biology*, 2010. **30**(11): p. 2099-2102.
133. Maiellaro-Rafferty, K., et al., *Catalase overexpression in aortic smooth muscle prevents pathological mechanical changes underlying abdominal aortic aneurysm formation*. *American Journal of Physiology-Heart and Circulatory Physiology*, 2011. **301**(2): p. H355-H362.
134. Vaziri, N.D. and B. Rodríguez-Iturbe, *Mechanisms of Disease: oxidative stress and inflammation in the pathogenesis of hypertension*. *Nature Clinical Practice Nephrology*, 2006. **2**(10): p. 582-593.
135. Sen, C.K., *Antioxidant and redox regulation of cellular signaling: introduction*. *Medicine and Science in Sports and Exercise*, 2001. **33**(3): p. 368-370.
136. Hehner, S.P., et al., *Enhancement of T cell receptor signaling by a mild oxidative shift in the intracellular thiol pool*. *The Journal of Immunology*, 2000. **165**(8): p. 4319-4328.

137. Los, M., et al., *Hydrogen peroxide as a potent activator of T lymphocyte functions*. European journal of immunology, 1995. **25**(1): p. 159-165.
138. Kol, A., et al., *Chlamydial and human heat shock protein 60s activate human vascular endothelium, smooth muscle cells, and macrophages*. Journal of Clinical Investigation, 1999. **103**(4): p. 571.
139. Polla, B.S., et al., *Stress Proteins in Inflammation*. Annals of the New York Academy of Sciences, 1998. **851**(1): p. 75-85.
140. Giachelli, C.M., et al., *Evidence for a role of osteopontin in macrophage infiltration in response to pathological stimuli in vivo*. The American journal of pathology, 1998. **152**(2): p. 353.
141. Liaw, L., et al., *Osteopontin promotes vascular cell adhesion and spreading and is chemotactic for smooth muscle cells in vitro*. Circulation Research, 1994. **74**(2): p. 214-224.
142. Jonasson, L., et al., *Expression of class II transplantation antigen on vascular smooth muscle cells in human atherosclerosis*. Journal of Clinical Investigation, 1985. **76**(1): p. 125.
143. Majesky, M.W., et al., *Rat carotid neointimal smooth muscle cells reexpress a developmentally regulated mRNA phenotype during repair of arterial injury*. Circulation Research, 1992. **71**(4): p. 759-768.
144. Henriques, T., et al., *Androgen Increases AT1a Receptor Expression in Abdominal Aortas to Promote Angiotensin II-Induced AAAs in Apolipoprotein E-Deficient Mice*. Arteriosclerosis, Thrombosis, and Vascular Biology, 2008. **28**(7): p. 1251-1256.
145. Parastatidis, I., et al., *Overexpression of catalase in vascular smooth muscle cells prevents the formation of abdominal aortic aneurysms*. Arteriosclerosis, thrombosis, and vascular biology, 2013. **33**(10): p. 2389-2396.
146. Collins, A.R., et al., *Osteopontin modulates angiotensin II- induced fibrosis in the intact murine heart*. Journal of the American College of Cardiology, 2004. **43**(9): p. 1698-1705.
147. Wilson, S.K., *The effects of angiotensin II and norepinephrine on afferent arterioles in the rat*. Kidney Int, 1986. **30**(6): p. 895-905.
148. Fyhrquist, F., K. Metsärinne, and I. Tikkanen, *Role of angiotensin II in blood pressure regulation and in the pathophysiology of cardiovascular disorders*. Journal of human hypertension, 1995. **9**: p. S19-24.

149. Chen, D., et al., *AT1 Angiotensin Receptors in Principal Cells of the Collecting Duct Have Minimal Impact on Blood Pressure and the Development of Hypertension*. *Hypertension*, 2012. **60**(3\_MeetingAbstracts): p. A42.
150. Izzo, J.L., D.A. Sica, and H.R. Black, *Hypertension primer*. 2008: Lippincott Williams & Wilkins.
151. Klabunde, R., *Cardiovascular physiology concepts*. 2011: Lippincott Williams & Wilkins.
152. O'Brien, E.R., et al., *Osteopontin is synthesized by macrophage, smooth muscle, and endothelial cells in primary and restenotic human coronary atherosclerotic plaques*. *Arteriosclerosis, Thrombosis, and Vascular Biology*, 1994. **14**(10): p. 1648-1656.
153. Wittek, A., et al., *In vivo determination of elastic properties of the human aorta based on 4D ultrasound data*. *Journal of the mechanical behavior of biomedical materials*, 2013. **27**: p. 167-183.
154. Goergen, C.J., et al., *Influences of aortic motion and curvature on vessel expansion in murine experimental aneurysms*. *Arteriosclerosis, thrombosis, and vascular biology*, 2011. **31**(2): p. 270-279.
155. Rensen, S., P. Doevendans, and G. Van Eys, *Regulation and characteristics of vascular smooth muscle cell phenotypic diversity*. *Netherlands Heart Journal*, 2007. **15**(3): p. 100-108.
156. Christen, T., et al., *Mechanisms of neointima formation and remodeling in the porcine coronary artery*. *Circulation*, 2001. **103**(6): p. 882-888.
157. Canfield, T.R. and P.B. Dobrin, *Mechanics of blood vessels*. *Biomedical Engineering Handbook*, 1995. **1**: p. 19-1.
158. Dobrin, P.B., *Elastin, collagen, and the pathophysiology of arterial aneurysms*. *Development of aneurysms*. Georgetown, Texas.: Landis Bioscience, 2000: p. 42-73.
159. Humphrey, J.D., *Mechanisms of Arterial Remodeling in Hypertension: Coupled Roles of Wall Shear and Intramural Stress*. *Hypertension*, 2008. **52**(2): p. 195-200.
160. Coogan, J.S., J.D. Humphrey, and C.A. Figueroa, *Computational simulations of hemodynamic changes within thoracic, coronary, and cerebral arteries following early wall remodeling in response to distal aortic coarctation*. *Biomechanics and modeling in mechanobiology*, 2013: p. 1-15.

161. Wolinsky, H., *Comparison of medial growth of human thoracic and abdominal aortas*. Circulation research, 1970. **27**(4): p. 531-538.
162. Matsumoto, T. and K. Hayashi, *Mechanical and dimensional adaptation of rat aorta to hypertension*. Journal of biomechanical engineering, 1994. **116**(3): p. 278-283.
163. Pirard, L., et al., *In situ aortic allograft insertion to repair a primary aorto-esophageal fistula due to thoracic aortic aneurysm*. Journal of vascular surgery, 2005. **42**(6): p. 1213-1217.
164. Gleason, R., et al., *A multi-axial computer-controlled organ culture and biomechanical device for mouse carotid arteries*. Journal of biomechanical engineering, 2004. **126**(6): p. 787-795.
165. Ashkar, S., et al., *Eta-1 (osteopontin): an early component of type-1 (cell-mediated) immunity*. Science, 2000. **287**(5454): p. 860-864.
166. Crawford, H.C., L.M. Matrisian, and L. Liaw, *Distinct roles of osteopontin in host defense activity and tumor survival during squamous cell carcinoma progression in vivo*. Cancer Research, 1998. **58**(22): p. 5206-5215.
167. Glasser, S.P., et al., *Vascular compliance and cardiovascular disease: a risk factor or a marker?* American Journal of Hypertension, 1997. **10**(10): p. 1175-1189.
168. McVeigh, G.E., et al., *Age-related abnormalities in arterial compliance identified by pressure pulse contour analysis aging and arterial compliance*. Hypertension, 1999. **33**(6): p. 1392-1398.
169. Finkelstein, S.M. and J.N. Cohn, *First- and third-order models for determining arterial compliance*. Journal of Hypertension, 1992. **10**: p. S11-S14.
170. Ventura, H., et al., *Impaired systemic arterial compliance in borderline hypertension*. American heart journal, 1984. **108**(1): p. 132-136.
171. Myers, D.L., *Alterations of Arterial Physiology in Osteopontin-Null Mice*. Arteriosclerosis, Thrombosis, and Vascular Biology, 2003. **23**(6): p. 1021-1028.
172. Wagenseil, J.E. and R.P. Mecham, *Elastin in large artery stiffness and hypertension*. Journal of cardiovascular translational research, 2012. **5**(3): p. 264-273.
173. Fung, Y.-C., *Biomechanics: mechanical properties of living tissues*. 2013: Springer Science & Business Media.

174. Danpinid, A., et al., *In vivo characterization of the aortic wall stress–strain relationship*. Ultrasonics, 2010. **50**(7): p. 654-665.
175. Morrison, T.M., et al., *Circumferential and longitudinal cyclic strain of the human thoracic aorta: age-related changes*. Journal of vascular surgery, 2009. **49**(4): p. 1029-1036.
176. Kaess, B.M., et al., *Aortic stiffness, blood pressure progression, and incident hypertension*. Jama, 2012. **308**(9): p. 875-881.
177. Weber, T.F., et al., *Heartbeat-related displacement of the thoracic aorta in patients with chronic aortic dissection type B: quantification by dynamic CTA*. European journal of radiology, 2009. **72**(3): p. 483-488.
178. Somers, M.J., et al., *Vascular Superoxide Production and Vasomotor Function in Hypertension Induced by Deoxycorticosterone Acetate-Salt*. Circulation, 2000. **101**(14): p. 1722-1728.
179. Wind, S., et al., *Oxidative stress and endothelial dysfunction in aortas of aged spontaneously hypertensive rats by NOX1/2 is reversed by NADPH oxidase inhibition*. Hypertension, 2010. **56**(3): p. 490-497.
180. Bruemmer, D., et al., *Angiotensin II–accelerated atherosclerosis and aneurysm formation is attenuated in osteopontin-deficient mice*. Journal of Clinical Investigation, 2003. **112**(9): p. 1318.
181. Golledge, J., et al., *Association between osteopontin and human abdominal aortic aneurysm*. Arteriosclerosis, thrombosis, and vascular biology, 2007. **27**(3): p. 655-660.